



UNIVERSITAT DE  
BARCELONA

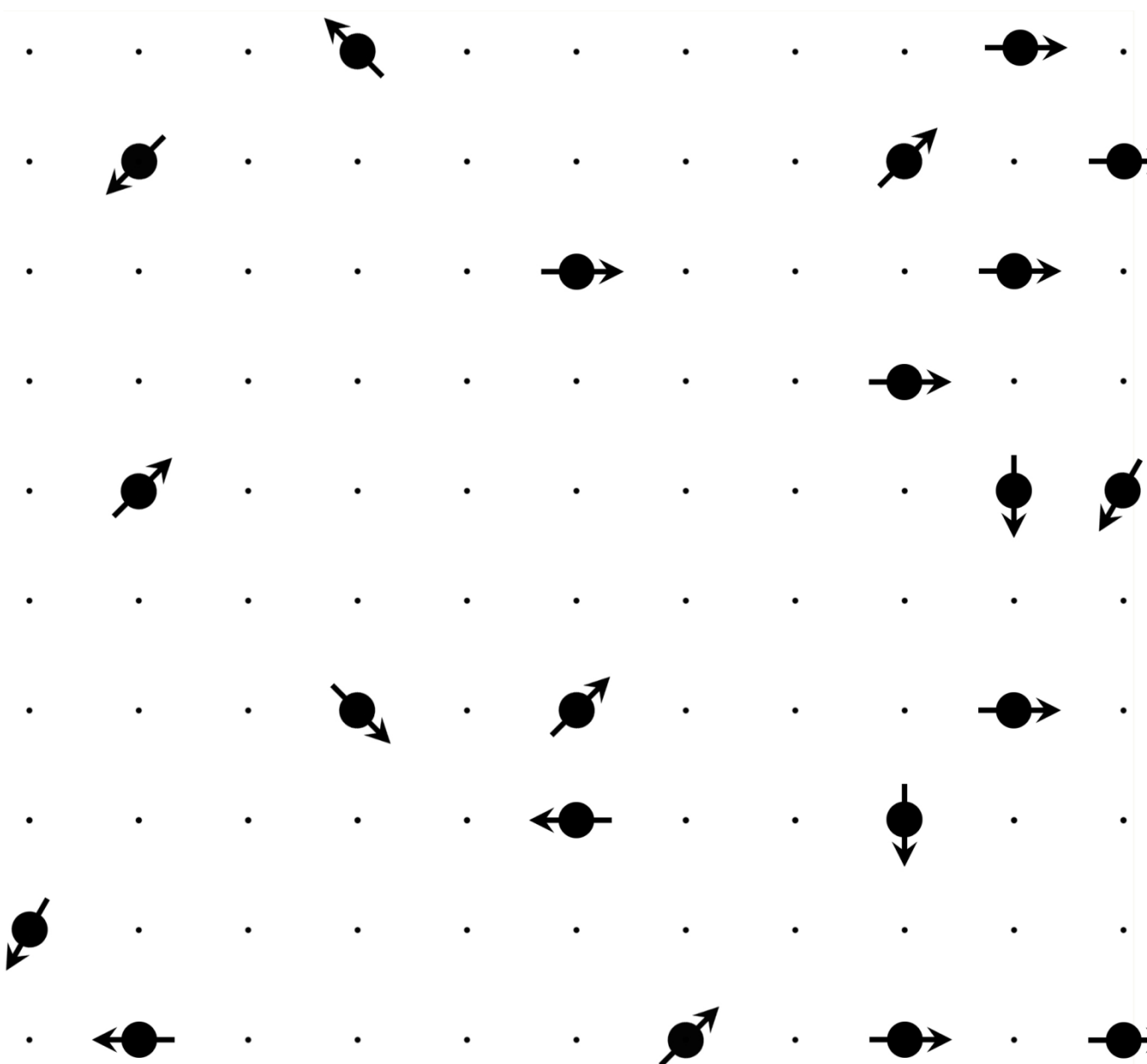
# The influence of selected genetic and environmental factors on white matter pathway structure measured with diffusion tensor imaging

Raquel Fenoll Sanguino

**ADVERTIMENT.** La consulta d'aquesta tesi queda condicionada a l'acceptació de les següents condicions d'ús: La difusió d'aquesta tesi per mitjà del servei TDX ([www.tdx.cat](http://www.tdx.cat)) i a través del Dipòsit Digital de la UB ([diposit.ub.edu](http://diposit.ub.edu)) ha estat autoritzada pels titulars dels drets de propietat intel·lectual únicament per a usos privats emmarcats en activitats d'investigació i docència. No s'autoritza la seva reproducció amb finalitats de lucre ni la seva difusió i posada a disposició des d'un lloc aliè al servei TDX ni al Dipòsit Digital de la UB. No s'autoritza la presentació del seu contingut en una finestra o marc aliè a TDX o al Dipòsit Digital de la UB (framing). Aquesta reserva de drets afecta tant al resum de presentació de la tesi com als seus continguts. En la utilització o cita de parts de la tesi és obligat indicar el nom de la persona autora.

**ADVERTENCIA.** La consulta de esta tesis queda condicionada a la aceptación de las siguientes condiciones de uso: La difusión de esta tesis por medio del servicio TDR ([www.tdx.cat](http://www.tdx.cat)) y a través del Repositorio Digital de la UB ([diposit.ub.edu](http://diposit.ub.edu)) ha sido autorizada por los titulares de los derechos de propiedad intelectual únicamente para usos privados enmarcados en actividades de investigación y docencia. No se autoriza su reproducción con finalidades de lucro ni su difusión y puesta a disposición desde un sitio ajeno al servicio TDR o al Repositorio Digital de la UB. No se autoriza la presentación de su contenido en una ventana o marco ajeno a TDR o al Repositorio Digital de la UB (framing). Esta reserva de derechos afecta tanto al resumen de presentación de la tesis como a sus contenidos. En la utilización o cita de partes de la tesis es obligado indicar el nombre de la persona autora.

**WARNING.** On having consulted this thesis you're accepting the following use conditions: Spreading this thesis by the TDX ([www.tdx.cat](http://www.tdx.cat)) service and by the UB Digital Repository ([diposit.ub.edu](http://diposit.ub.edu)) has been authorized by the titular of the intellectual property rights only for private uses placed in investigation and teaching activities. Reproduction with lucrative aims is not authorized nor its spreading and availability from a site foreign to the TDX service or to the UB Digital Repository. Introducing its content in a window or frame foreign to the TDX service or to the UB Digital Repository is not authorized (framing). Those rights affect to the presentation summary of the thesis as well as to its contents. In the using or citation of parts of the thesis it's obliged to indicate the name of the author.



the influence of selected **GENETIC** and  
**ENVIRONMENTAL** factors on  
**WHITE MATTER** pathway structure  
measured with **diffusion tensor imaging**

RAQUEL FENOLL SANGUINO



# THE INFLUENCE OF SELECTED GENETIC AND ENVIRONMENTAL FACTORS ON WHITE MATTER PATHWAY STRUCTURE MEASURED WITH DIFFUSION TENSOR IMAGING

Thesis presented by

**Raquel Fenoll Sanguino**

to obtain the grade of Doctor by the University of Barcelona  
in accordance with the requirements of the PhD Diploma

Supervised by

Dr. Jesús Pujol Nuez

Dr. Joan Deus Yela

Medicine and Traslational Research Doctorate Program  
School of Medicine, University of Barcelona





Dr. JESÚS PUJOL NUEZ and Dr. JOAN DEUS YELA

*CERTIFIE that they have supervised and guided the PhD thesis entitled “**THE INFLUENCE OF SELECTED GENETIC AND ENVIRONMENTAL FACTORS ON WHITE MATTER PATHWAY STRUCTURE MEASURED WITH DIFFUSION TENSOR IMAGING**”, presented by Raquel Fenoll Sanguino. They hereby assert that this thesis fulfils the requirements to be defended for the PhD degree.*

*Signature,*

*Signature,*

*Dr. Jesús Pujol Nuez*

*Dr. Joan Deus Yela*

*Barcelona, June 2017*

*This thesis has been carried out in the MRI Research Unit, Hospital del Mar, Barcelona.*

*The included studies have been financially supported by:*

- *European Research Council under the ERC (grant number 268479).  
The BREATHE project.*
- *Spanish Government (grants PSI2014-53524-P, PI11/00744 and PI/120219)*
- *Jérôme Lejeune Foundation, Paris.*

*To Jean  
and my 'children' Noah and Arya  
without whom this thesis would have  
been completed one year earlier.*





*Believe those who seek the truth,  
doubt those who have found it*  
- André Gide



# Contents

---

<i>Foreword</i> .....	XI
<i>Glossary of Abbreviations</i> .....	XIII
<i>Summary</i> .....	XV
<b>1. Introduction</b> .....	1
1.1 White Matter .....	3
1.2 White Matter Modulators .....	3
1.2.1 Environment .....	5
1.2.1.1 Pollutants .....	5
1.2.1.2 Video Games .....	6
1.2.2 Genetics .....	7
1.2.2.1 Down Syndrome .....	7
1.2.2.2 Prader-Willi Syndrome .....	8
1.3 White Matter Measurements .....	9
1.3.1 Diffusion Tensor Imaging .....	9
1.3.1.1 Fractional Anisotropy.....	9
<b>2 Approach, Objectives and Hypothesis</b> .....	11
2.1 <i>Study I: Airborne copper exposure in school environments associated with poorer motor performance and altered basal ganglia</i> .....	13
2.1.1 Objectives .....	13
2.1.2 Hypothesis .....	13
2.2 <i>Study II: Traffic pollution exposure is associated with altered brain connectivity in school children</i> .....	14
2.2.1 Objectives .....	14
2.2.2 Hypothesis .....	14
2.3 <i>Study III: Video gaming in school children: how much is enough?</i> .....	15
2.3.1 Objectives .....	15
2.3.2 Hypothesis .....	15
2.4 <i>Study IV: Anomalous white matter structure and the effect of age in Down syndrome patients</i> .....	16
2.4.1 Objectives .....	16
2.4.2 Hypothesis .....	16

2.5 <i>Study V: A longitudinal study of brain anatomy changes preceding dementia in Down syndrome</i> .....	17
2.5.1 Objectives .....	17
2.5.2 Hypothesis .....	17
2.6 <i>Study VI: Abnormal hypothalamus and related brain regions in Prader-Willi syndrome evaluated by diffusion tensor imaging</i> .....	18
2.6.1 Objectives .....	18
2.6.2 Hypothesis .....	18
<b>3. Methods</b> .....	19
3.1 Study Samples .....	21
3.2 Cognitive and Behavioral Assessment .....	22
3.3 Neuroimaging Approach .....	23
3.3.1 Diffusion Tensor Imaging .....	24
3.4 Statistical Analysis .....	25
<b>4. Results</b> .....	27
4.1 <i>Study I: Airborne copper exposure in school environments associated with poorer motor performance and altered basal ganglia</i> .....	39
4.2 <i>Study II: Traffic pollution exposure is associated with altered brain connectivity in school children</i> .....	47
4.3 <i>Study III: Video gaming in school children: how much is enough?</i> .....	69
4.4 <i>Study IV: Anomalous white matter structure and the effect of age in Down syndrome patients</i> .....	87
4.5 <i>Study V: A longitudinal study of brain anatomy changes preceding dementia in Down syndrome</i> .....	101
4.6 <i>Study VI: Preliminary results. Abnormal hypothalamus and related brain regions in Prader-Willi syndrome evaluated by diffusion tensor imaging</i> .....	113
<b>5. General Discussion</b> .....	117

<b>6. Conclusions</b> .....	127
<b>7. Resumen Abreviado en Castellano</b> .....	131
7.1 Introducción .....	133
7.2 Objetivos e Hipótesis .....	140
7.3 Metodología .....	145
7.4 Resultados .....	149
7.5 Discusión .....	155
7.6 Conclusiones .....	162
<b>8. References</b> .....	163
<b>9. Publications</b> .....	185



## **Foreword**

---

This thesis, presented to obtain the PhD degree by the University of Barcelona, is the result of five studies carried out at the MRI Research Unit of the Hospital del Mar, Barcelona.

The following papers have been published and/or accepted in international journals with mean impact factor (IF) of 5.2 (ISI of Knowledge, Journal Citations Reports inferred from 2016).

### *Study I:*

Pujol J, Fenoll R, Macià D, Martínez-Vilavella G, Álvarez-Pedrerol M, Rivas I, Forns J, Deus J, Blanco-Hinojo L, Querol X, Sunyer J. **Airborne copper exposure in school environments associated with poorer motor performance and altered basal ganglia.** *Brain and Behavior* 2016; 6(6): e00467.

**IF: 2.128**

### *Study II:*

Pujol J, Martínez-Vilavella G, Macià D, Fenoll R, Álvarez-Pedrerol M, Rivas I, Forns J, Blanco-Hinojo L, Capellades J, Querol X, Deus J, Sunyer J. **Traffic pollution exposure is associated with altered brain connectivity in school children.** *NeuroImage* 2016; 129: 175-184.

**IF: 5.463**

### *Study III:*

Pujol J, Fenoll R, Forns J, Harrison BJ, Martínez-Vilavella G, Macià D, Álvarez-Pedrerol M, Blanco-Hinojo L, González-Ortiz S, Deus J, Sunyer J. **Video gaming in school children: how much is enough?** *Annals of Neurology* 2016; 8(3): 424-433.

**IF: 9.638**

### *Study IV:*

Fenoll R, Pujol J, Esteba-Castillo S, De Sola D, Ribas-Vidal N, García-Alba J, Sánchez-Benavides G, Martínez-Vilavella G, Deus J, Dierssen M, Novell-Alsina R, De la Torre R. **Anomalous white matter structure and the effect of age in Down syndrome patients.** *Journal of Alzheimer's Disease* 2017; 57(1): 61-70.

**IF: 3.920**



*Study V:*

Pujol J, Fenoll R, Ribas-Vidal N, Martínez-Vilavella G, Blanco-Hinojo L, García-Alba J, Deus J, Novell R, Estaba-Castillo S. **A longitudinal study of brain anatomy changes preceding dementia in Down syndrome.** (*Submitted in Neurobiology of Aging 2017*)

**IF: 5.153**

## ***Glossary of Abbreviations***

---

<b>MRI</b>	Magnetic Resonance Imaging
<b>WM</b>	White Matter
<b>GM</b>	Gray Matter
<b>CSF</b>	Cerebrospinal Fluid
<b>DTI</b>	Diffusion Tensor Imaging
<b>FA</b>	Fractional Anisotropy
<b>MD</b>	Mean Diffusivity
<b>VBM</b>	Voxel-based Morphometry
<b>fMRI</b>	Functional Magnetic Resonance Imaging
<b>DS</b>	Down Syndrome
<b>PWS</b>	Prader-Willi Syndrome
<b>AD</b>	Alzheimer's Disease
<b>MCI</b>	Mild Cognitive Impairment
<b>DCL</b>	Deterioro Cognitivo Leve
<b>CU</b>	Copper
<b>TR</b>	Reaction Time
<b>NC</b>	Caudate Nucleus
<b>ACC</b>	Anterior Cingulate Cortex
<b>CC</b>	Corpus Callosum
<b>OFC</b>	Orbitofrontal Cortex
<b>DMN</b>	Default Mode Network
<b>ROI</b>	Region of Interest



## *Summary*

---

The present doctoral thesis is focused on describing the effects that different environmental and genetic modulators have on white matter pathways and its consequences measured with diffusion tensor imaging. We chose to focus on two examples of each type of modulators. Firstly, we selected as environment modulating factors: pollutants and video games. On one side, pollution as an external factor that enters passively the brain and may influence developmental trajectories. And on the other hand, we used video games as a good example of active behavior that can modify white matter tracts through practice. Secondly, Down syndrome and Prader-Willi syndrome were selected as representative genetic syndromes that may interfere on white matter growth because, although Down syndrome has higher incidence rate than Prader-Willi syndrome, both show behavioral and cognitive alterations, indicating an abnormal brain development. The results of this doctoral thesis lead to the conclusion that white matter pathways development is not an immutable process and it can be modified by diverse modulators. In the same way, diffusion tensor imaging is a good-quality technique to capture and identify those white matter changes through life.



# **1. INTRODUCTION**



# 1. Introduction

## 1.1 White Matter

Imagine if we could peek through the skull to see what makes one brain different than another. Or discover which anatomical traits might be driving a person's genetic disease. Currently, imaging techniques are helping to observe such evidence and it's revealing interesting findings: a large variety of genetic and environmental modulators may modify the maturation pathways of white matter tracts and generate different consequences through life.

Briefly, gray matter is where mental computation takes place and memories are stored. The cortex is the "topsoil" of the brain; it is composed of densely packed neuronal cell bodies. Underneath it, there's bedrock of "white matter" that fills approximately 45% of the human brain (Zhang et al., 2000; Liu et al., 2017). White matter is composed of millions of communication cables, each one containing an axon, coated with a white fatty substance called myelin. Like the trunk lines that connect telephones in different parts of a country, this white cabling connects neurons in one region of the brain with those in other regions.

To understand how white matter works, we must understand its growth process. White matter development follows the principles of general development: grows first and subsequently matures. Actually, the axon wrapping occurs at different ages. Myelin is prevalent only in a few brain regions at birth, expands in spurts and is not fully laid until age 25 or 30 in certain sites. Myelination generally proceeds in a wave from the back of the cerebral cortex to its front as we grow into adulthood. The frontal lobes are within the last places where myelination occurs (Figure 1). These regions are responsible for higher-level reasoning, planning and judgment - skills that only come with experience.

For decades neuroscientists exhibited little interest on white matter. They considered the myelin to be mere insulation and the axons inside it little more than passive passageways. But scientists are now realizing that we have underestimated the importance of white matter in the proper transfer of information among brain regions. New studies show that the extent of white matter varies in people who have been influenced by different experiences or who have certain dysfunctions or pathologies (Pujol et al., 2011; Via et al., 2014).

## 1.2 White Matter Modulators



With this new perspective about white matter, it is not hard to imagine how faulty transmission could lead to brain abnormalities (Soriano-Mas et al., 2011). After decades of searching gray matter for the causes of mental disabilities, neuroscientists now have evidence that white matter plays important role (Pujol et al., 2004).

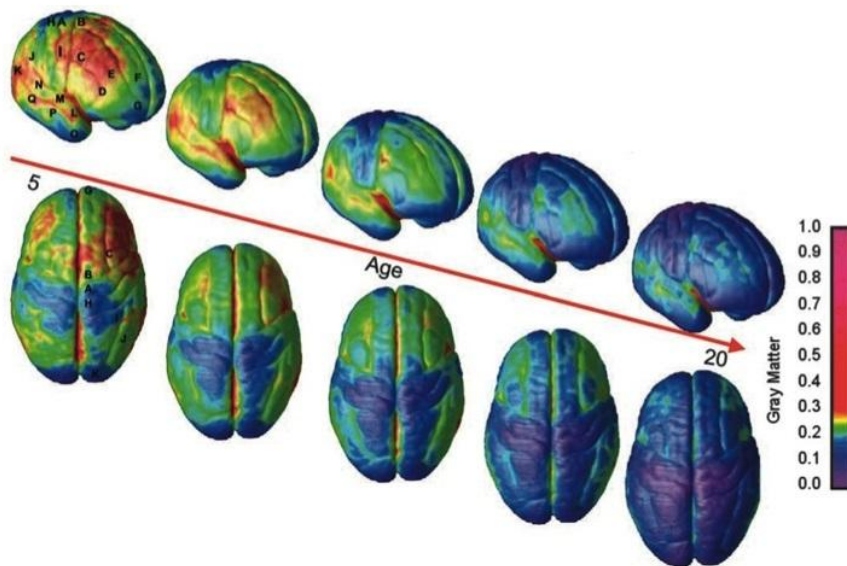


**Figure 1.** Gray matter maturation between ages 5 and 20. The side bar shows a color representation in units of gray matter volume (Gogtay et al., 2004). A few axons are covered with myelin at birth. More are insulated over time, from the back of the cerebral cortex to the front. The sequence here depicts the pruning of neurons and the relative increase in myelin. Basic functional areas such as vision (*back*) are completed before age 4, followed by language and, last self-control (*forehead*).

The development of white matter pathways is not immutable through life and it can be influenced by diverse modulators. In the following text we're going to focus on environmental and genetic factors according to the main goals of this thesis.

First, we're going to describe relevant findings to date about the effects of different ambient modulators have on white matter development and its consequences. We've chosen to focus on two examples of environment factors: pollutants and video games. On one side, pollution is an external factor that enters passively the brain and potentially may influence development

trajectories. And on the other hand, video gaming is a good example of active behavior that can modify brain development.

Secondly, we'll explain the effect of two genetic pathologies on white matter pathway development through life. We've chosen Down syndrome and Prader-Willi syndrome as representative genetic syndromes that may interfere on white matter growth because, although Down syndrome has an incidence rate higher than Prader-Willi syndrome, both show behavioral and cognitive alterations, indicating an abnormal brain growth and maturation.

### **1.2.1 Environment**

Although white matter development is a process determined by nature, it's not exempt to be modified in response to certain experiences and environmental exposures. Many findings suggest that some experiences influence myelin formation and that supports learning and improvement of skills (Bavelier et al., 2012). But, do all the experiences and environmental elements bring us benefits?

#### **1.2.1.1 Pollutants**

One of six children has a developmental disability and in most cases these disabilities affect the nervous system. The most common neurodevelopmental disorders include learning disabilities, sensory deficits and developmental delays (Boyle et al., 1994), processes closely related to the white matter.

The developing human brain is inherently much more susceptible to injury caused by toxic agents than is the brain of an adult (Dobbing et al., 1968). The susceptibility of infants and children to industrial chemicals is further enhanced by their increased exposures, augmented absorption rates and diminished ability to detoxify many exogenous compounds, relative to adults (Ginsberg et al., 2004).

Evidence has been accumulating over several decades that industrial chemicals can cause neurodevelopmental damage. The possibility of a link between chemicals and anatomical/functional brain abnormalities and widespread neurobehavioral changes was raised by research showing that lead was toxic to the developing brain across a wide range of exposures (Landrigan et al., 1975). That report was in accord with other reports indicating that other environmental pollutants were also toxic to early brain development (Grandjean et al., 2002) and could modify brain maturation trajectory. Many studies have classified air pollution as important developmental neurotoxicant (Grandjean et al., 2014). In children, exposure to traffic-related air pollutants during pregnancy or infancy,

when the brain rapidly develops, has been related to cognitive delays (Suglia et al., 2008; Perera et al., 2009; Guxens et al., 2012).

Children spend a large proportion of their day at school, including the period when daily traffic pollution peaks. Many schools are located in close proximity to busy roads, which increases the level of traffic-related air pollution in schools. There's currently very little evidence on the role of traffic-related pollution in schools on cognitive function (Wang et al., 2009). However, some studies have demonstrated that cognitive development is reduced in children exposed to higher levels of traffic-related air pollutants at school (Sunyer et al., 2015; Van Kempen et al., 2012; Clark et al., 2012).

### **1.2.1.2 Video Games**

Given the dramatic increase in the everyday use of technology over recent decades, interdisciplinary scholars have considered its impact on human cognition and development (Greenfield et al., 1984; Hunt et al., 2012). Over the last decades, effects of playing video games on human perception and cognition have been intensely studied and debated (Oei et al., 2014).

An overview of the existing literature of playing video games indicates benefits after action game play in many domains in reverse of what was thought about the topic. Video game players have also been documented to have better performance than non-gamers on several aspects of cognition such as visual short-term memory (Anderson et al. 2011; Boot et al. 2008), spatial cognition (Greenfield et al., 2009), multitasking (Green et al, 2006a), and some aspects of executive function (Anderson et al., 2011). But the most notable benefits are noted in reaction time and speed-accuracy trade-off, which corresponding brain regions are closely linked with white matter pathways that are essential for the acquisition of new skills through practice.

On the other hand, there's growing evidence of the prevalence and length of the problems of pathological video gaming. Several researchers have begun testing scientifically the concept of pathological video game use, commonly called video game "addiction" (Fisher et al., 1994). Most researchers have assumed that it would be similar to pathological gambling. The parallel seems justifiable, because both are assumed to be behavioral addictions that begin as entertainment that can stimulate emotional responses and dopamine release (Koepp et al., 1998). But playing is not pathological initially; it becomes pathological for some individuals when the activity turns dysfunctional, harming the individual's social, occupational, family, school, and psychological functioning.

In summary, although there is some evidence to suggest that video gaming can improve particular cognitive abilities in youth (Bavelier et al., 2012) other evidence links it with conduct-related problems and increased risk toward disorders of addiction (Anderson et al., 2010; Gentile et al., 2010).

## **1.2.2 Genetics**

Neurodevelopmental genetic disorders are a group of disorders in which the development of the central nervous system is disturbed. This can include atypical brain development which can manifest as neuropsychiatric problems, impaired motor function, learning and language disabilities or non-verbal communication problems. Some neurodevelopmental disorders alter the trajectory of white matter pathways and generate neuropsychiatric and cognitive consequences that may be more evident in adulthood. Studying the characteristic abnormalities of these disorders, many clues may emerge about biological mechanisms underlying neurodevelopmental disorders.

### **1.2.2.1 Down Syndrome**

Down syndrome, or trisomy 21, is a common chromosomal disorder and the most common cause of intellectual disability (Nadel et al., 1999). Research in Down syndrome has substantially progressed in the understanding of basic mechanisms via which gene over expression interferes in that brain development (Capone et al., 2001) but there's a lack of information about the general organization of the brain and its consequences (Pujol et al., 2014a). There are surprisingly a few brain imaging studies of Down syndrome in children, maybe because the main differences with healthy subjects are more evident in adulthood when the brain is completely developed. In fact, there're many studies focused on adults and the risk of developing Alzheimer's-like dementia (Stanton et al., 2004).

In adult Down syndrome patients, a large number of *in vivo* MRI studies have defined a different neuroanatomical pattern from healthy controls that parallel post-mortem reports of Down syndrome neuropathology (Schapiro et al., 1989; Weis et al., 1991; Kesslak et al., 1994; Raz et al., 1995; White et al., 2003; Teipel et al., 2004). Many of these studies have also reported hallmark pathologies of Alzheimer's disease; a finding which is consistent with the high rate of occurrence of dementia in Down syndrome individuals over the age of 40 (Wisniewski et al., 1985). Moreover, main findings show that adults with Down syndrome have lower white matter structure than healthy controls of the same age, particularly in the frontal lobes (Powell et al., 2014; Head et al., 2016) and

that can be associated with executive decline evident on neuropsychological testing (Hartley et al., 2014; Madden et al., 2009). These imaging studies have provided further insight into the potential cognitive repercussions of some structural alterations (Raz et al., 1995; Aylward et al., 1999; Ikeda et al., 2002; Krasuski et al., 2002).

Despite these findings, to detect early subclinical symptoms of dementia in Down syndrome patients is a challenge and it would be interesting to investigate whether involuntional changes in white matter pathways are detectable before dementia becomes clinically evident to get an effective diagnosis and design better interventions.

### **1.2.2.2 Prader-Willi Syndrome**

Prader-Willi syndrome is a complex genetic disorder associated with multiple clinical manifestations resulting from the failure of expression of paternal alleles in the 15q11.2-q13 region of chromosome 15 (Grugni et al., 2016).

The syndrome shows a characteristic phenotype which encompasses neonatal hypotonia and failure to thrive, progressive hyperphagia with early childhood-onset obesity (if uncontrolled), developmental impairment with learning disabilities, behavioral and psychiatric issues, dysmorphic features and endocrine abnormalities (Cassidy et al., 2012). Most patients have reduced growth hormone (GH) secretory capacity and hypogonadotropic hypogonadism, suggesting hypothalamic-pituitary dysfunction (Burman et al., 2001).

The brain imaging studies that have been performed in these patients showed that Prader-Willi syndrome is accompanied by abnormalities in specific areas of the brain (Yamada et al., 2006; Mantoulan et al., 2011; Ogura et al., 2011; Ogura et al., 2013). Some of the most important findings related to white matter are reported below.

Some studies have demonstrated that there're regional white matter abnormalities in Prader-Willi syndrome brain. Interestingly, the observed water diffusivity alterations which indicate developmental abnormalities in these areas are consistent with the clinical features of Prader-Willi syndrome. There's a significant reduction in white matter values in a number of brain regions in Prader-Willi syndrome than in controls based on a voxel-wise approach. A ROI-based analysis of fractional anisotropy showed changes in the following regions: the hypothalamus, right and left internal capsule, right and left cerebellum and all of the sub-region of corpus callosum. The corpus callosum, hypothalamus and right internal capsule have shown a significant reduction in fractional anisotropy

in Prader-Willi syndrome (Tant et al., 2009; Yamada et al., 2006). Thus, using diffusion tensor imaging, focal abnormalities of white matter between Prader-Willi syndrome and healthy subjects have been demonstrated. But, despite all the Prader-Willi syndrome knowledge we currently have, there're some aspects that remain poorly understood or inadequately managed, as the repercussion of white matter alterations on cognitive function, behavioral and psychiatric symptoms.

### **1.3 White Matter Measurements**

Despite there're many techniques to explore white matter characteristics, as specific regions of interest (ROI) or segmentation with voxel-based morphometry (VBM), the most used technique to explore white matter is diffusion tensor imaging (DTI). This technique allows us to visualize, at gross level, the rate of diffusion of water along axons. It can therefore be used to explore axonal pathways.

In DTI, the MRI signal decays when water is diffusing (Stejskal et al., 1965) and it's possible to design an MRI protocol whose signals are reduced by water diffusing in a particular direction. By measuring diffusion in a large set of different directions (at least 6) we can identify the primary directions of water diffusion in each voxel in the brain.

#### **1.3.1 Diffusion Tensor Imaging**

Diffusion tensor imaging is a noninvasive method that provides information about microstructural properties of white matter (Le Bihan et al., 1985; Le Bihan et al., 2001) by measuring the magnitude, direction and anisotropy of water molecules (Schmithorst et al., 2010). This method gives us many white matter measurements, but we're going to focus on fractional anisotropy because is the most informative one about maturation levels of white matter pathways.

##### **1.3.1.1 Fractional Anisotropy**

Random motion of water molecules, also known as Brownian motion, can be quantified and reflects intrinsic features of tissue microstructure *in vivo* (Pierpaoli et al., 1996). In pure water or cerebrospinal fluid, the diffusion of water molecules is unrestricted in all directions. This situation is referred as "isotropic" and often represented as a spherical tensor (Lerner et al., 2014) (Figure 2). But in brain tissue, water diffusion is substantially reduced by structures such as myelin sheaths, cell membranes and white matter tracts. In general, in white matter the diffusion of water molecules is less restricted along

the long-axis of a group of aligned tissue fibers than perpendicular to it (Dong et al., 2004). This condition of directionally-dependent diffusion is referred as “anisotropic” and may be represented by an elongated ellipsoid tensor (Lerner et al., 2014) (Figure 2). The most commonly used measure for diffusion anisotropy is fractional anisotropy (FA) that measures changes in ranges from 0 to 1 (Pfefferbaum et al., 2003; Assaf et al., 2008). As a result, DTI provides a great framework for the acquisition, analysis and quantification of white matter diffusion properties during development and the effects and consequences of different modulators through life.

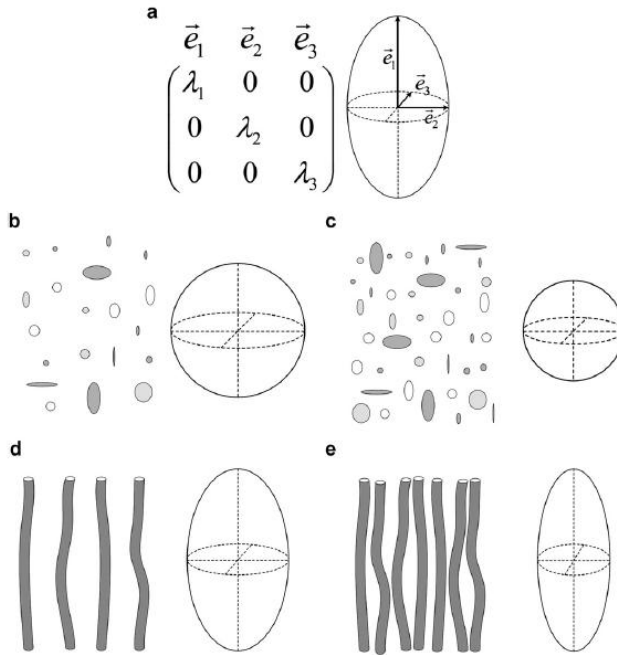


**Figure 2.** The diffusion tensor is generally characterized by a 3D ellipsoid (a), representing the diffusion isoprobability surface at the voxel level. The ellipsoid axes are oriented according to the tensor eigenvectors, and their length depends on the tensor eigenvalues. In an isotropic tissue (b) the ellipsoid is spherical, and the mean diffusivity depends on the tissue water content through the density of hindering structures (c). In white matter, fibers are oriented in bundles, diffusion is anisotropic (d), and the anisotropy increases with fiber density and decreasing membrane permeability (e).

# **2. APPROACH, OBJECTIVES AND HYPOTHESIS**





## **2. Approach, Objectives and Hypothesis**

### ***2.1 Study I: Airborne Copper exposure in School Environments Associated with Poorer Motor Performance and Altered Basal Ganglia***

#### **2.1.1 Objectives**

The development of white matter pathways is not immutable through life. There're life stages, like childhood, where white matter is more susceptible to be influenced by many environmental elements. A variety of air pollutants has been identified as factors causing neural damage at toxic concentrations. However, nowadays it's not totally clear that high levels of air pollutants are able to generate permanent alterations in a developing brain. One of the pollutants identified that may interfere with brain development is the copper. Although this element is necessary for molecular metabolism, abnormal levels can produce brain impairment.

Thus, the main goal of the present research was to investigate the neurotoxic effects of airborne copper exposure in white matter pathways.

The aims of our study were:

- I. To test the potential harmful effects of copper as an air pollutant in children aged from 8 to 12 years.
- II. Using a specific approach for white matter measurement (DTI), to explore potential repercussion on brain anatomy and architecture caused by copper exposure.
- III. Using specific motor testing, to examine the impact of copper in various motor skills, as speed and consistency of motor response.
- IV. To relate findings in DTI with alterations in motor skills.

#### **2.1.2 Hypothesis**

We hypothesized that children exposed to airborne copper will present poor motor performance and changes in the structure of the basal ganglia.

## ***2.2 Study II: Traffic Pollution Exposure is Associated with Altered Brain Connectivity in School Children***

### **2.2.1 Objectives**

Children are more vulnerable to the effects of environmental elements due to their active developmental processes. Exposure to urban pollution has been associated with alterations in children's cognition and supported by a set of studies showing significant association of pollutant exposure with inflammatory and degenerative brain pathology.

Thus, we aimed to assess the extent of such potential effects of urban pollution on white matter pathway maturation in children and its consequences in cognition.

In summary, the aims of this study were:

- I. To assess the impact of long-term exposure to urban pollution in a large children sample aged from 8 to 12.
- II. Using diffusion tensor imaging approach, to explore white matter tract architecture affected by long-term exposure to pollutants.
- III. Using a selected cognitive assessment, to determine what potential repercussions in cognition were detectable.
- IV. To relate findings in DTI technique with alterations in cognition.

### **2.2.2 Hypothesis**

Our hypothesis was the potential brain effects of air pollution will be evident on anatomical development during maturation processes and changes in water diffusion within white matter tracts would appear.

## ***2.3 Study III: Video Gaming in School Children: How Much is Enough?***

### **2.3.1 Objectives**

The benefits and risks of video gaming in young people remain unrated, particularly as regards an optimal level of use. Although there's some evidence to suggest that video gaming can improve particular cognitive abilities through practice, other evidence links it with conduct-related problems and increased risk of addiction.

Thus, the goal of this study was to clarify the consequences of video game playing on white matter architecture and its relationship with cognitive performance.

The main aims of our study were:

- I. Using a specific approach for detecting abnormalities on white matter pathways (DTI), to explore potential repercussion on brain anatomy of playing video games.
- II. Using specific motor testing, to examine the impact of video gaming on motor skills.
- III. To relate white matter findings with motor assessment outcomes.

### **2.3.2 Hypothesis**

- We predicted that video gaming in school children, considered as a training exercise based on repetitive use, would have a principal effect on speed of mental processing.
- In the brain, video gaming could notably reinforce neural connections, with a major effect on basal ganglia circuits, which are essential for the acquisition of new skills through practice.

## ***2.4 Study IV: Anomalous White Matter Structure and the Effect of Age in Down syndrome Patients***

### **2.4.1 Objectives**

Neural tissue abnormalities in Down syndrome are expressed at relatively late developmental stages. In addition, aging is accelerated with an early presence of neurodegenerative change. A large number of MRI studies have identified a variety of anatomical and functional alterations. But white matter changes and their functional significance have not been fully characterized yet. Nowadays, it's not evident whether the involuntional effect on white matter structure is detectable before dementia is expressed. If this were indeed the case, age-related FA changes could serve as early markers of neurodegeneration.

Thus, we wanted to characterize white matter abnormalities in adult Down syndrome patients using diffusion tensor imaging and to investigate whether involuntional changes in white matter structure could be used as markers for dementia.

The aims of this study:

- I. To characterize white matter abnormalities in the brain of adult non-demented Down syndrome patients using diffusion tensor imaging.
- II. To investigate whether involuntional changes in white matter structure are detectable before dementia becomes clinically evident.

### **2.4.2 Hypothesis**

We predicted that Down syndrome patients would exhibit both widespread FA reduction in white matter and an accelerated aging effect, and that the alteration would be associated with poorer cognitive performance.

## ***2.5 Study V: A Longitudinal Study of Brain Anatomy Changes preceding Dementia in Down syndrome***

### **2.5.1 Objectives**

Neuroimaging research is prominent in indicating that demented Down syndrome patients indeed show brain alterations in systems with typical degeneration in Alzheimer's disease (Emerson et al., 1995; Haier et al., 2008; Beacher et al. 2009; Powell et al., 2014). Nevertheless, studies are still not conclusive in distinguishing baseline Down syndrome dense brain pathology established during brain development from ongoing degenerative changes at time of progression to dementia.

Thus, the main goal of this research was to characterize Down syndrome patients at risk to develop dementia measuring changes in white matter structure and their relationship with cognitive deterioration.

In summary, the aims of this study were:

- I. To characterize white matter abnormalities in the brain of Down syndrome patients at risk of dementia using diffusion tensor imaging
- II. To match Down syndrome cognitive impairment progression with the well-established cognitive decline progression in Alzheimer's disease.
- III. To relate white matter changes identified by DTI with cognitive impairment progression.

### **2.5.2 Hypothesis**

We hypothesized that brain in older Down syndrome individuals displays many of the neuropathological features found in Alzheimer's disease and it could indicate a direct link between a genetic anomaly and neurodegeneration that may potentially contribute to elucidate the pathogenesis of Alzheimer's disease.

## ***2.6 Study VI: Abnormal Hypothalamus and related Brain Regions in Prader-Willi syndrome evaluated by Diffusion Tensor Imaging (DTI)***

### **2.6.1 Objectives**

Prader-Willi patients present several neuroendocrinological abnormalities, such as growth hormone deficiency, hypogonadotropic hypogonadism and hyperphagia, as the result of possible involvement of the hypothalamo-hypophyseal system. There's growing evidence suggesting abnormalities in white matter developmental trajectory. But few studies have explored this issue. There's only one research in Prader-Willi patients using DTI and it was not focused on the hypothalamo-hypophyseal region (Yamada et al., 2006). So, specific white matter alterations in Prader-Willi syndrome remain unknown.

Thus, the objective of the present study was to evaluate the hypothalamus and related brain regions in adult patients with Prader-Willi syndrome using DTI.

The main aims of our study were:

- I. Using a specific approach for detect abnormalities on white matter pathways (DTI); characterize white matter abnormalities in neuroendocrinological related areas.
- II. To relate white matter abnormalities with eating behavior related hormones in Prader-Willi syndrome patients.

### **2.6.2 Hypothesis**

We predicted the presence of structural abnormalities in white matter connecting the hypothalamus with related brain structures that may underlay clinical features of Prader-Willi syndrome patients.

# 3. METHODS





### 3. Methods

The present thesis consists of five studies and one set of preliminary results examining cognitive functions and structural and functional brain characteristics in normal and pathological brain development samples. To do so, we studied three different samples and we used different cognitive and MRI approaches. All the studies were approved by the ethics committee of the Hospital del Mar (Barcelona) and all the subjects or their family gave written informed consent prior to participation in the studies. A detailed description of the samples characteristics, methodological approaches, cognitive and/or behavioral test and MRI methods are detailed within each study.

#### 3.1 Study Samples

The healthy children in school age sample was developed in the context of a large-scale project designed to assess the effects of environmental factors on brain development children (BREATHE, European Commission FP7-ERC-2010-AdG, ID 268479). A totally of 2.897 children, from 39 schools in the city of Barcelona, were invited to participate in the MRI study via post, email or telephone. 810 of them gave initial positive response. The study sample was consecutively recruited from this group with the aim of including children from all participating schools. Parents of 491 children were directly contacted. Consent to participate was finally not obtained in 165 cases, 27 children were lost before the assessment and 21 children were not eligible because of dental braces. The finally selected group included 278 cases. A total of 263 children completed the imaging protocol (mean age  $9.7 \pm 0.9$ ; range 7.9-12.1). Additional cases were excluded on the basis of image quality criteria in each specific MRI analysis (*see chapter 4*).

The Down syndrome sample involved 68 Down syndrome participants (mean age  $36.3 \pm 10.9$ ; range 17-61). Candidates were recruited by Specialized Service in Mental Health and Intellectual Disability (SEMS-DI, Girona; TESDAD, Barcelona) from the community via parent organizations. Individuals with seizure or neurological disease (other than Down syndrome), psychiatric disorder (including autism spectrum disorder), non-stable medical conditions and current psychoactive medication were not eligible for the MRI assessment. Participants were selected from a large group of Down syndrome subjects on basis of having > 18 years, Down syndrome confirmed by karyotype, QI mild-moderate, no drug treatment that could bias the results obtained, capability to understand MRI instructions, follow the commands and remain still, as well as optimal attitude and the willingness (participants and parents) to participate. Maternal ethnicity

was Caucasian in all cases. No participant was taking psychotropic medication (*see chapter 4*).

The Prader-Willi syndrome sample involved 30 (mean age  $27.4 \pm 8.0$ ; range 18-47) adults with Prader-Willi syndrome from the Genetic, Pediatrics and Endocrinology Departments of Corporació Sanitària Parc Taulí of Sabadell, Barcelona, Spain (the clinical referral centre for Prader-Willi syndrome) and the Specialized Mental Health and Intellectual Disability Service, Parc Hospitalari Martí i Julià of Salt, Girona, Spain. The Catalan Association of Prader-Willi Syndrome of Barcelona and the Prader-Willi Syndrome Foundation of Madrid also assisted with recruitment. Patients younger than 18 years, those who had non-stable medical conditions and those considered unable to follow MRI instructions were not eligible to participate in the study. Genetic testing to confirm the chromosome 15 anomaly was repeated in all patients at the time of inclusion in the study. Blood samples were collected for genomic DNA extraction and for karyotype. In each case, Prader-Willi syndrome was confirmed by methylation-specific polymerase chain reaction (MS-PCR) with an absence of paternal allele at 15q11-q13, and the deletion status was established by fluorescence in situ hybridization (FISH) (*see chapter 4*).

### **3.2 Cognitive and Behavioral Assessment**

A cognitive assessment was performed in all studies.

In the first sample (healthy children), cognitive development was assessed through long-term change in working memory and attention. From January 2012 to March 2013, children were evaluated every 3 months over four repeated visits, using computerized tests in series lasting approximately 40 min in length. Working memory and attention functions were selected because they grow steadily during preadolescence (Anderson et al., 2002; Rueda et al., 2005). The computerized tests chosen (the N-back task on working memory (Anderson et al., 2002) and the Attentional Network Test [ANT]) (Rueda et al., 2004) have been validated with brain imaging (Thomason et al., 2009; Rueda et al., 2004) and in the general population. Groups of 10–20 children were assessed together, wearing ear protectors, and were supervised by one trained examiner per 3–4 children. For the N-back test, different N-back loads (up to 3-back) and stimuli (colors, numbers, letters, and words) were examined. For analysis here, we selected 2-back and 3-back loads for number and word stimuli as they showed a clear age-dependent slope in the four measurements and had little learning effect. Numbers and words activate different brain areas. The 2-back test predicts general mental abilities (working memory), while the 2-back test also predicts superior functions such as fluid intelligence (superior working memory) (Shelton

el al., 2010). All sets of N-back tests started with colors as a training phase to ensure the participant understands. The N-back parameter analyzed was  $d'$  prime ( $d'$ ), a measure of detection subtracting the normalized false alarm rate from the hit rate:  $(Z_{\text{hit rate}} - Z_{\text{false alarm rate}}) \times 100$ . A higher  $d'$  indicates more accurate test performance. Among the ANT measures, we chose hit reaction time standard error (HRT-SE) (standard error of reaction time for correct responses) (Conners et al., 2000)—a measure of response speed consistency throughout the test—since it showed very little learning effect and the clearest growth during the 1 year study period among all the ANT measurements. A higher HRT-SE indicates highly variable reactions related to inattentiveness.

The second sample (Down syndrome) received a comprehensive medical, psychiatric, neuropsychological and laboratory evaluation. Cognitive status was evaluated by Kaufman Brief Intelligent Test, Second Edition (K-BIT) (Kaufman, 2004). Candidates were assessed neuropsychologically by Wechsler Adult Intelligence Scale (WAIS), Neuropsychological Integrated Program for persons with Intellectual Disabilities (PIEN-ID) (Esteba-Castillo S. Neuropsicología del trastorno del desarrollo intelectual con y sin origen genético [Tesis Doctoral]. Bellaterra: Universidad Autónoma de Barcelona. Facultad de Medicina; 2015), Rey-Osterrieth Complex Figure (ROCF), Behavioral Rating Inventory of Executive Function (BRIEF), CAMDEX-DS, Tower of London (TOL), Color Trail Test (CTT), Aberrant Behavior Checklist (ABC Scale) and Adaptive Behavior Scale Residence Community-2 (ABS-RC2).

The third sample (Prader-Willi syndrome) received a selective testing to identify the presence and severity of characteristic symptoms related to obsessive-compulsive behavior in Prader-Willi syndrome, including the Compulsive Behavior Checklist (Gedye et al., 1992) which was used to confirm the presence of various compulsive symptoms grouped in several categories: ordering, completeness/incompleteness, cleaning/tidiness, checking/touching and deviant grooming. Additionally, the Yale-Brown Obsessive Compulsive Scale (Y-BOCS; Goodman et al., 1989) was used to provide a complementary assessment of the severity of target compulsions identified using the Compulsive Behavior Checklist. To target compulsive eating behavior we used the Hyperphagia Questionnaire (Dyken et al., 2007) a 13-item instrument specifically designed to measure food-related preoccupations and problems in Prader-Willi syndrome, as well as the severity of these concerns.

### 3.3 Neuroimaging Approach

Image acquisitions for all studies were performed in Neuroradiology Section, Radiology Service at the Hospital del Mar (Barcelona, Spain) according to the specific study protocol.

In summary, A 1.5 Tesla Signa Excite System (General Electric, Milwaukee, WI, USA) equipped with an eight-channel phased-array head coil and single shot echoplanar imaging (EPI) software was used. Diffusion-weighted scans were obtained using spin echo single-shot echo-planar sequences of 25 directions with a B-factor of 1000 s/mm<sup>2</sup>. Acquisition parameters were repetition time 8300ms; echo time 94 ms; thickness 5 mm, no gap; pulse angle 90°; field of view 26 cm; 128×128 acquisition matrix reconstructed into a 256×256 matrix, and scan duration was 3m52s. Twenty-six slices were prescribed parallel to the anterior-posterior commissure line covering the whole brain. Participants were instructed to relax, stay awake and lie still.

### **3.3.1 Diffusion Tensor Imaging (DTI)**

DTI was processed using Functional MRI of the Brain (FMRIB) Software Library 5.0 (FSL), developed by the Analysis Group at the Oxford Centre for FMRIB (Smith et al., 2004). Diffusion-weighted images were aligned to the B0 image using affine registration and corrected for motion and eddy current distortions (“Eddy Current Correction” option in the FMRIB Diffusion Toolbox [FDT] version 2.0 in FSL). A whole-brain mask generated with FSL Brain Extracting Tool was applied to DTI images. Subsequently, we estimated fractional anisotropy (FA) maps using FDT in FSL after local fitting of the diffusion tensor model at each voxel (“dtifit”). FA maps were then aligned to a common target (FMRIB58\_FA template) using Tract-Based Spatial Statistics (Smith et al., 2006), re-sliced to a 1mm × 1mm × 1 mm anatomical resolution and normalized to standard MNI space via the FMRIB58\_FA template using the FMRIB’s Non-linear Registration Tool (Figure 3).

To complement the analysis and assist interpretation of the FA results, we carried out a directional analysis of water diffusion along each (x, y, z) axis separately. We used the diffusion tensor estimated by FSL “dtifit” algorithm to determine diffusion strengths. Geometrically, the procedure involved determining the radius of the arbitrarily oriented ellipsoid along the spatially fixed x, y, and z axes using basic 3D quadratic geometry. As the eigenvectors and eigenvalues were previously normalized to MNI space in all subjects, we were able to carry out group-level voxel-wise analyses.

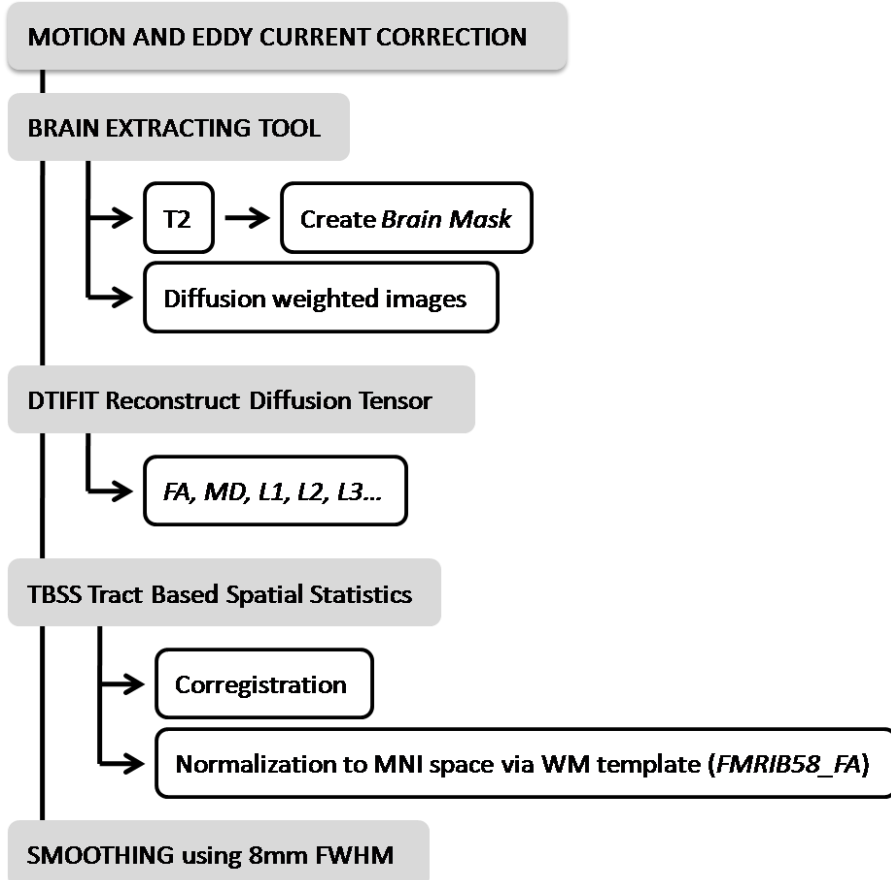


**Figure 3.** Diffusion tensor imaging (DTI) protocol applied in the studies.

### 3.4 Statistical Analysis

Subsequently, individual anatomical, diffusion tensor imaging and functional connectivity maps were included in second-level (group) analyses. Results were considered significant with clusters of 1.032 mL (e.g, 1,032 voxels with a resolution of 1 x 1 x 1 mm) and height threshold of  $P < 0.005$ , which satisfied the FWE (family-wise error) rate correction of  $P_{FWE} < 0.05$  estimated using Monte Carlo simulation (Pujol et al., 2014c).



# 4. RESULTS





## 4. Results

### 4.1 Study I:

#### *Airborne Copper exposure in School Environments Associated with Poorer Motor Performance and Altered Basal Ganglia*

Jesús Pujol<sup>1,2</sup>, Raquel Fenoll<sup>1</sup>, Dídac Macià<sup>1</sup>, Gerard Martínez-Vilavella<sup>1</sup>, Mar Álvarez-Pedrerol<sup>3,4,5</sup>, Ioar Rivas<sup>3,4,5,6</sup>, Joan Fornés<sup>3,4,5</sup>, Joan Deus<sup>1,7</sup>, Laura Blanco-Hinojo<sup>1</sup>, Xavier Querol<sup>6</sup> & Jordi Sunyer<sup>3,4,5,8</sup>

<sup>1</sup> MRI Research Unit, Hospital del Mar, Barcelona, Spain

<sup>2</sup> Centro Investigación Biomédica en Red de Salud Mental, CIBERSAM G21, Barcelona, Spain

<sup>3</sup> Centre for Research in Environmental Epidemiology (CREAL), Barcelona, Catalonia, Spain

<sup>4</sup> Pompeu Fabra University, Barcelona, Catalonia, Spain

<sup>5</sup> Ciber on Epidemiology and Public Health (CIBERESP), Barcelona, Spain

<sup>6</sup> Institute of Environmental Assessment and Water Research (IDAEA-CSIC), Barcelona, Catalonia, Spain

<sup>7</sup> Department of Clinical and Health Psychology, Autonomous University of Barcelona, Barcelona, Spain

<sup>8</sup> IMIM (Hospital del Mar Medical Research Institute), Barcelona, Catalonia, Spain

### **Abstract**

**Introduction:** Children are more vulnerable to the effects of environmental elements. A variety of air pollutants are among the identified factors causing neural damage at toxic concentrations. It is not obvious, however, to what extent the tolerated high levels of air pollutants are able to alter brain development. We have specifically investigated the neurotoxic effects of airborne copper exposure in school environments. **Methods:** Speed and consistency of motor response were assessed in 2836 children aged from 8 to 12 years. Anatomical MRI, diffusion tensor imaging, and functional MRI were used to directly test the brain repercussions in a subgroup of 263 children. **Results:** Higher copper exposure was associated with poorer motor performance and altered structure of the basal ganglia. Specifically, the architecture of the caudate nucleus region was less complete in terms of both tissue composition and neural track water diffusion. Functional MRI consistently showed a reciprocal connectivity reduction between the caudate nucleus and the frontal cortex. **Conclusions:** The results establish an association between environmental copper exposure in children and alterations of basal ganglia structure and function.

**Keywords:** Air pollution, brain development, copper, diffusion tensor imaging, fMRI, neurodegenerative disorders

### 4.1.1 Introduction

Brain development is extraordinarily complex and extends into adulthood to achieve maximum effectiveness in cognition and skills (Pujol et al., 1993; Paus et al., 2005). Nonetheless, both the complexity and duration of such a process expose developing children to the potentially harmful effects of environmental elements. A variety of air pollutants are among the identified factors causing neural damage at toxic concentrations (Grandjean et al., 2014). It is not obvious, however, to what extent the tolerated high levels of urban air pollutants are able to generate subtle, subclinical alterations in the developing brain in school-age children.

Copper is an air pollutant that may potentially interfere with brain development. Although this element is necessary for cellular metabolism, abnormal copper levels lead to relevant brain impairment (Scheiber et al., 2014). The deleterious effect of an excess of copper is well-known from Wilson's disease, an inherited metabolic disorder affecting the basal ganglia with symptoms usually evident from preadolescence onward and mainly in the form of deficient motor control (Bandmann et al., 2015). We have tested the potential harmful effects of copper as an air pollutant in children aged from 8 to 12 years using specific motor testing and brain structural and functional imaging. Exposure to airborne copper at school was estimated for 2836 children in the city of Barcelona. Both the speed and consistency of motor response were measured to test the integrity of motor function in the whole sample. High-resolution 3D MRI, DTI (diffusion tensor imaging), and functional MRI were used to directly test the potential repercussion on brain anatomy, architecture, and function in a subgroup of 263 children.

### 4.1.2 Methods

#### *Participants*

This study was developed in the context of the BREATHE project (The European Commission: FP7-ERC-2010-AdG, ID 268479) aimed at assessing the impact of long-term exposure to traffic-related air pollutants on school children. A total of 2897 children participated in the whole survey from 39 representative schools of the city of Barcelona (Sunyer et al. 2015). A group of 2836 children completed the behavioral testing (mean age at the study end, 9.4 years; SD 0.9; and range 7.9–

12.1 years) and served to test the effect of copper on motor function. From this sample, 1564 families were invited to participate in the MRI study via post, e-mail, or telephone, and 810 of them gave an initial positive response. The recruitment of this group was consecutive with the aim of including children from all participating schools. Parents of 491 children were directly contacted. Consent to participate was finally not obtained in 165 cases, 27 children were lost before the assessment and 21 children were not eligible because of dental braces. The finally selected MRI group included 278 participants, 263 of whom completed the imaging protocol (mean age of 9.7 years, SD 0.9 and range, 8.0–12.1 years) and served to test direct effects of copper on brain. Study design and participant selection is fully described in Sunyer et al. (2015). Table 1 reports the characteristics of the study samples. All parents or tutors signed the informed consent form approved by the Research Ethical Committee (No. 2010/ 41221/I) of the IMIM-Parc de Salut MAR, Barcelona, Spain, and the FP7-ERC-2010-AdG Ethics Review Committee (268479-22022011).

### *Copper Exposure*

Each school was measured twice during 1-week periods separated by 6 months, in the warm (year 2012) and cold (year 2012/2013) periods. Indoor air in a single classroom and outdoor air in the courtyard were measured simultaneously. Several pollutants were measured during class time (Amato et al., 2014; Rivas et al., 2014; Sunyer et al., 2015). Copper specifically was measured during 8 h (09:00–17:00 h) in particulate matter with an aerodynamic diameter <2.5  $\mu\text{m}$  (PM<sub>2.5</sub>) collected on filters with high-volume samplers (MCV SA, Spain). After acid digestion of the filter, copper concentrations were determined via ICP-MS (inductively coupled plasma mass spectrometry). Yearly school air pollution levels were obtained by averaging the two 1-week measurements. This study was focused on outdoor (courtyard) copper measurements, as they are more directly related to urban pollution, which is the primary interest of this project. All children had been in the school for more than 18 months (and 98% more than 2 years) at imaging assessment, which was carried out after the pollution measurement campaigns.

### *Behavioral Measurements*

Behavioral assessment was focused on testing speed and consistency of motor responses. We used the computerized “Attentional Network Test,” child version (Child ANT) (Rueda et al., 2004), which was developed to specifically assess children’s motor speed during attentional challenge. Among the ANT measurements, we used the overall “reaction time” to measure speed and “reaction time standard deviation” to measure trial-to-trial consistency of motor responses. A higher reaction time standard deviation indicates higher reaction

time variability, which increases with reduced executive and attentional resources depending on the integrity of frontal-basal ganglia circuits (Bellgrove et al., 2004; MacDonald et al., 2006; Langner et al., 2013). Normal children become efficient in sustained motor responses during the preadolescent age period contemplated in our study (MacDonald et al., 2006).

The procedure used to administer the task is fully described in a previous report (Forns et al., 2014). The Child ANT takes approximately 20 min to complete. Groups of 10–20 children were assessed together wearing ear protectors and were supervised by one trained examiner per 3–4 children. The task required to respond to a target (yellow-colored fishes) presented on a computer screen by pressing a key. The whole task contains cues to test different attentional aspects, but outcome measurements for the current study were limited to median reaction time and standard deviation expressed in milliseconds from the correct responses obtained across the 128 trials of the task (four separate blocks of 32 trials each). Commission and omission errors were also registered. Cases with more than 30% commission or omission errors were excluded from further analyses (total nine cases in the whole sample and two cases in the MRI sample).

**Table 1.** Characteristic of Study Samples

	<b>Whole Sample (n=2836)</b>	<b>MRI Sample (n=263)</b>
Gender	49.5% girls 50.5% boys	48.3% girls 51.5% boys
Age, years, mean ±SD (range)	9.4 ± 0.9 (7.9-12.1)	9.7±0.9 (8.0-12.1)
Overall school achievement, 5-point scale	3.5 ± 1.1 (1-5)	3.7 ± 1.0 (1-5)
Difficulties score (SDQ), range 0-40	8.4 ± 5.2 (0-32)	8.8 ± 5.3 (0-25)
Obesity:		
Normal	72.1%	71.4%
Overweight, BMI ≥25-29.9 kg/m <sup>2</sup>	18.5%	18.4%
Obesity, BMI ≥ 39 kg/m <sup>2</sup>	9.4%	10.2%
Mother education (5-point scale, 5=University)	4.4 ± 0.8 (1-5)	4.5 ± 0.8 (1-5)
Father education (5-point scale, 5=University)	4.4 ± 0.8 (1-5)	4.4 ± 0.8 (1.5)
Vulnerability index <sup>1</sup> - Home	0.45 ± 0.21 (0.06-1.0)	0.43 ± 0.21 (0.06-0.90)
Vulnerability index <sup>1</sup> - School	0.42 ± 0.21 (0.13-0.84)	0.43 ± 0.22 (0.13-0.84)
Public/Non public school	36% vs. 64%	43% vs. 57%
Task performance:		
Reaction time (mean of medians, msec)	671.5 ±124.6 (389-1277)	650.6 ± 119.9 (431-1091)
Reaction time standard deviation (msec)	235.7 ± 91.1 (60.6-598.6)	222.9 ± 91.2 (77.5-571.6)
Commission errors (number)	4.0 (3.1%) ± 4.2 (0-50)	4.3 (3.4%) ± 5.0 (0-49)
Omission errors (number)	1.4 (1.1%) ± 3.6 (0-94)	1.6 (1.3) ± 3.9 (0-44)

BMI, body mass index; SDQ, Strengths and Difficulties Questionnaire

<sup>1</sup> Neighborhood socioeconomic status vulnerability index based on the level of education, unemployment and occupation at census tract (Atlas de vulnerabilidad de urbana de España, 2012).

## *Contextual Behavioral Assessment*

Sociodemographic factors were measured using a neighborhood socioeconomic status vulnerability index (based on the level of education, unemployment, and occupation at the census tract) (Atlas de Vulnerabilidad Urbana de España, 2012; <http://www.fomento.gob.es/. . ./AtlasVulnerabilidadUrbana/>) according to both school and home address. Parental education was registered for both parents using a 5-point scale (1 illiterate/2 less than/3 primary/ 4 secondary/5 university). Standard measurements of height and weight were performed to define overweight and obesity (de Onis et al. 2009). Parents completed the SDQ (Strengths and Difficulties Questionnaire) on child behavioral problems (Goodman et al., 2001). A “difficulties” score ranging from 0 to 40 was generated. Overall school achievement was rated by teachers using a 5-point scale (from the worse = 1 to the best = 5).

## *MRI Acquisition*

A 1.5-Tesla Signa Excite system (General Electric, Milwaukee, WI) equipped with an eight-channel phased array head coil and single-shot EPI (echoplanar imaging) software was used. The imaging protocol included high resolution T1-weighted 3D anatomical images, DTI, and a functional MRI sequence acquired in the resting state.

High-resolution 3D anatomical images were obtained using an axial T1-weighted three-dimensional fast spoiled gradient inversion recovery prepared sequence. A total of 134 contiguous slices were acquired with repetition time 11.9 msec, echo time 4.2 msec, flip angle 15°, field of view 30 cm, 256 x 256 pixel matrix, and slice thickness 1.2 mm.

Diffusion tensor imaging was obtained using spin-echo single-shot echo-planar sequences of 25 directions with a B-factor of 1000 sec/mm<sup>2</sup>. Twenty-six slices were acquired with repetition time 8300 msec, echo time 94 msec, thickness 5 mm, no gap, pulse angle 90°, field of view 26 cm, and 128 x 128 acquisition matrix reconstructed into a 256 x 256 matrix. The functional MRI sequence consisted of gradient recalled acquisition in the steady state with repetition time 2000 msec, echo time 50 msec, pulse angle 90°, field of view 24 cm, 64 x 64-pixel matrix, and slice thickness 4 mm (interslice gap, 1.5 mm). Twenty-two interleaved slices were prescribed parallel to the anterior–posterior commissure line covering the whole brain. A 6-minute continuous resting-state scan was acquired for each participant. Children were instructed to relax, stay awake, and lie still without moving, while keeping their eyes closed throughout. This scan generated 180 whole-brain EPI volumes. The first four (additional) images in each run were discarded to allow magnetization to reach equilibrium.

## *Image Preprocessing*

### Anatomical 3D

All the anatomical images were visually inspected before analysis by a trained operator to detect any motion effect. A total of 10 children were discarded as a result of poor quality images and thus the final sample for the 3D anatomical analysis included 253 children. Anatomical 3D data were processed in two separate analyses assessing different anatomical characteristics.

Gray and white matter tissue concentration and volume at a voxel level were measured using Statistical Parametric Mapping (SPM8) (<http://www.fil.ion.ucl.ac.uk/spm>, Wellcome Department of Cognitive Neurology, London, UK, 2008). SPM VBM (voxel-based morphometry) algorithms with DARTEL registration were used with the following processing steps: segmentation of anatomical images into gray and white matter tissue probability maps in their native space; estimation of the deformations that best align the images together by iteratively registering the segmented images with their average; finally, generating spatially normalized and smoothed segmentations (5 x 5 x 5 FWHM) using the deformations estimated in the previous step. The analyses were performed with scaling by Jacobian determinants (estimates of volume change during the normalization) to consider tissue volume and without Jacobian scaling to assess the relative concentration of gray matter and white matter. Normalized images were finally transformed to the standard SPM template, resliced to 1.5 mm resolution in MNI (Montreal Neurological Institute) space.

Cortical thickness measurements across the whole cortex were obtained using FREESURFER tools (<http://surfer.nmr.mgh.harvard.edu/>). Processing steps included removal of non-brain tissue, segmentation of the subcortical white matter and deep gray matter volumetric structures, tessellation of the gray and white matter boundary, registration to a spherical atlas which is based on the individual cortical folding patterns to match cortical geometry across subjects, and creation of a variety of surface-based data. Cortical thickness is calculated as the closest distance from the gray/white boundary to the gray/CSF boundary at each vertex on the tessellated surface (Fischl et al., 1999).

### Diffusion Tensor Imaging

Diffusion tensor imaging was processed using FMRIB (functional MRI of the brain) Software Library 5.0 (FSL), developed by the Analysis Group at the Oxford Centre for FMRIB (Smith et al., 2004). Diffusion-weighted images were corrected for motion and eddy current distortions (“Eddy Current Correction” option in the FMRIB Diffusion Toolbox [FDT] version 2.0 in FSL), and a whole brain mask was applied using the FSL Brain Extracting Tool. A further rigorous image quality

control was carried out to identify potential residual effects of head motion, which involved the visual inspection of each DTI slice for all 25 DTI volumes in all participants. Volumes with slices with signal loss (greater than  $\sim 10\%$ ) or residual artifacts were identified by an expert researcher. DTI full examinations showing one or more degraded images in more than five volumes were discarded. A total of 76 children were removed from the DTI analysis on the basis of this criterion (in addition to 10 cases showing gross image degradation). The final DTI sample involved 177 children showing a mean  $\pm$  SD of 23.5 (94%)  $\pm$  1.9 optimal quality volumes. Subsequently, we estimated FA (fractional anisotropy) maps using FDT in FSL after local fitting of the diffusion tensor model at each voxel (“dtifit”). Next, diffusion data were processed using tract-based spatial statistics (Smith et al., 2006). Each FA dataset was re-sliced to a 1mm x 1mm x 1mm anatomical resolution and normalized to standard MNI space via the FMRIB58\_FA template using the FMRIB’s nonlinear registration tool.

To complement the analysis and assist interpretation of the FA results, we carried out a directional analysis of water diffusion along each (x, y, z) axis separately. We used the diffusion tensor estimated by FSL “dtifit” algorithm to determine diffusion strengths. Geometrically, the procedure involved determining the radius of the arbitrarily oriented ellipsoid along the spatially fixed x, y, and z axes using basic 3D quadratic geometry. As the eigenvectors and eigenvalues were previously normalized to MNI space in all subjects, we were able to carry out group-level voxel-wise analyses.

## Functional MRI

Preprocessing was carried out using SPM8 and involved motion correction, spatial normalization, and smoothing using a Gaussian filter (full-width half-maximum, 8 mm). Data were normalized to the standard SPM-EPI template and re-sliced to 2-mm isotropic resolution in MNI space.

The following procedures were adopted to control for potential head motion effects: (1) Conventional SPM time-series alignment to the first image volume in each subject. (2) Exclusion of 24 children with large head motion (boxplot-defined outliers) (Pujol et al. 2014b).

The finally analyzed sample therefore included 239 children. (3) Both motion-related regressors and estimates of global brain signal fluctuations were included as confounding variables in first-level (single-subject) analyses. (4) Within-subject, censoring-based MRI signal artifact removal (Power et al., 2014) (scrubbing) was used to discard motion-affected volumes. For each subject, interframe motion measurements (Pujol et al., 2014b) served as an index of data quality to flag volumes of suspect quality across the run. At points with interframe motion  $>0.2$  mm, that corresponding volume, the immediately preceding and the succeeding two volumes were discarded. Using this procedure, a mean  $\pm$  SD of 11.2 (6.2%)  $\pm$  13.8 volumes of the 180 fMRI sequence volumes



were removed in the analyzed sample. (5) Potential motion effects were further removed using a summary measurement for each participant (mean interframe motion across the fMRI run) as a regressor in the second-level (group) analyses in SPM (Pujol et al., 2014b).

Functional connectivity maps were generated using procedures detailed in previous reports (Harrison et al., 2013; Pujol et al., 2014a). Maps representative of frontal lobe functional connectivity were obtained by locating seed regions at the medial-dorsal, lateral (right and left), and medial-anterior aspects of the frontal cortex using coordinates taken from previous literature (Fox et al., 2005) converted to MNI: medial-dorsal ( $x = -2, y = -2, z = 55$ ), right lateral ( $x = 45, y = 3, z = 15$ ), left lateral ( $x = -45, y = 5, z = 9$ ), and medial-anterior ( $x = 1, y = 54, z = 26$ ). Additional maps were generated from the results obtained in the structural (anatomical and DTI) analyses. The seed regions were centered at the left caudate nucleus at three anterior-posterior levels covering the part of the head of the caudate nucleus showing significant copper effects on its structure (MNI coordinates [ $x = -12, y = 20, z = 4$ ], [ $x = -12, y = 14, z = 9$ ], and [ $x = -12, y = 8, z = 12$ ]). For each of the striatal locations, the seed region was defined as a 3.5-mm radial sphere (sampling  $\sim 25$  voxels in 2 mm isotropic space). This was performed using MarsBaR ROI (region of interest) toolbox in MNI stereotaxic space (Brett et al. 2003). Signals of interest were then extracted for each seed region, respectively, by calculating the mean ROI value at each time point across the time series. To generate the seed maps, the signal time course of a selected seed region was used as a regressor to be correlated with the signal time course of every voxel in the brain in order to generate first-level (single-subject) voxel-wise statistical parametric maps (contrast images). The maps were estimated for each seed separately. A high-pass filter set at 128 sec was used to remove low-frequency drifts below  $\sim 0.008$  Hz. In addition, we derived estimates of white matter, CSF, and global brain signal fluctuations to include in the regression analyses as nuisance variables.

### *Statistical Analysis*

A multiple linear regression was used to estimate the source of copper and the relative contributions were given as standardized b values. A linear regression was used to estimate the association of copper measurements with motor performance. b values are reported as time increments (msec) for each copper measurement unit ( $\text{ng}/\text{m}^3$ ). Imaging data were analyzed using SPM. Individual anatomical (Jacobian-modulated and non-modulated white and gray matter and cortical thickness), DTI, and functional connectivity maps were included in second-level (group) analyses to map voxel-wise the correlation across-subjects between individual brain measurements and individual copper exposure (the measurements obtained in the school of each participant). Results were considered significant with clusters of 1.032 mL (e.g., 129 voxels with a

resolution of 2 x 2 x 2 mm) at a height threshold of  $P < 0.005$ , which satisfied the FWE (family wise error) rate correction of  $P_{\text{FWE}} < 0.05$  according to recent Monte Carlo simulations (Pujol et al., 2014c). Maps in figures are displayed at  $t > 2.3$ .

### 4.1.3 Results

#### *Copper as an Air Pollutant*

Copper measured in fine particles ( $\text{PM}_{2.5}$ ) from school playgrounds showed a mean of 8.7 ng/m<sup>3</sup> (SD, 3.0; range 3.7–13.8). According to the correlation with specific tracers, the main source of copper was road traffic, but a significant contribution was the result of industrial activity. An additional third source was identified in relation to the close proximity (mean  $\pm$  SD, 90  $\pm$  58 m) of seven schools to busy overhead-wire railway lines. For instance, a multiple regression accounted for 70% variance of copper measurements including elemental carbon as a single road traffic tracer (Amato et al. 2014) (standardized  $\beta = 0.66$ ,  $P < 0.00001$ ), zinc as a single industry tracer (Amato et al. 2014) (standardized  $\beta = 0.31$ ,  $P = 0.002$ ), and train proximity (standardized  $\beta = 0.20$ ,  $P = 0.037$ ).

#### *Relationship of Copper Exposure with Children's Performance*

Higher copper exposure was associated with poorer motor performance in children. Although in terms of the whole sample ( $n = 2827$  after nine exclusions), the association was significant for motor response speed (reaction time,  $\beta = 2.2$  and  $P = 0.006$ ), the effect was more robust on motor response consistency (reaction time standard deviation,  $\beta = 2.9$  and  $P < 0.00001$ ). Such a negative relationship with reaction time variability was significant in the group of children receiving MRI ( $n = 261$  after two exclusions;  $\beta = 4.2$  and  $P = 0.026$ ). Table 1 shows descriptive statistics.

#### *Neuroimaging Results*

Three-dimensional anatomical (T1-weighted) MRI and DTI were used to assess the potential association of copper exposure with alteration in the fine brain structure. Copper was associated with higher gray matter concentration (i.e., a higher proportion of gray matter in the tissue) in the striatum, specifically in the caudate nucleus (Fig. 4 and Table 2), with no effect on tissue volume. This finding potentially expresses a relative reduction of striatum white matter (i.e., of white matter “striae” that actually give the corpus striatum its anatomical name). No other significant alterations were identified with 3D anatomical MRI with the exception of an area of increased cortical thickness in the supplementary motor area of the left hemisphere (data not shown).

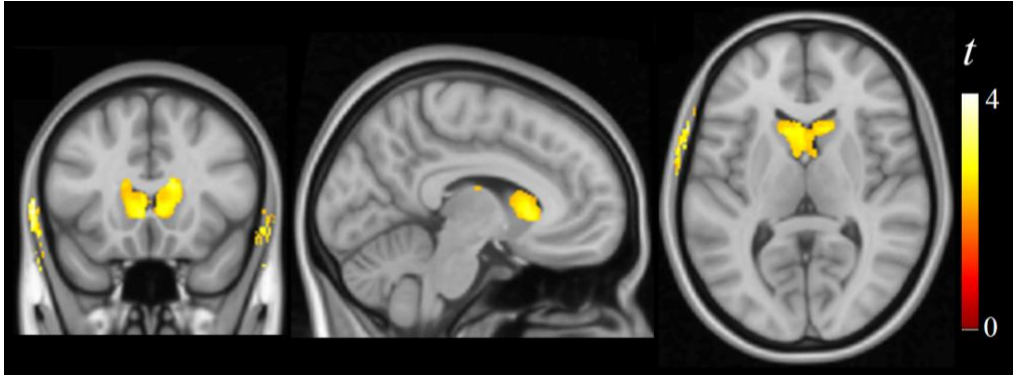


**Figure 4.** Correlation of copper measurements with brain tissue composition. Higher gray matter (presumably expressing lower white matter) concentration in the caudate nucleus bilaterally. The right hemisphere corresponds to the right side of axial and coronal views.

Results from the DTI analysis were highly consistent with the anatomical results (Fig. 5, Table 2). Copper was associated with an increase of neural tissue FA. This DTI measurement may express the extent to which an anatomical structure is composed of white matter tracts showing one dominant direction. In brain regions containing tracts with a single direction, FA increases as a result of brain maturation. Nevertheless, in complex structures with tracts crossing in different directions, higher FA may denote less mature or less structured tissue (Douaud et al., 2011; Jones et al., 2013). In our analysis, higher copper levels were associated with higher FA in white matter close to the caudate nucleus and in the caudate nucleus itself. This region is anatomically characterized as showing superior–inferior, posterior–anterior, and lateral–medial crossing white matter tracts (see Fig. 6 and Kotz et al., 2013). Within this scenario, a less mature structure will show higher FA (the effect of copper in our study).

A voxel-wise correlation analysis with behavior measurements helped to establish the nature of the identified changes associated with copper exposure. Reaction time and, mostly, reaction time variability showed significant positive correlation with FA of white matter adjacent to the caudate nucleus (Fig. 5). Thus, in the direction of copper exposure findings, slower children and the children with less consistent motor response exhibited higher FA in this region.

To investigate copper effects on the neural track architecture in the caudate nucleus region, we analyzed tissue diffusion along the three orthogonal ( $x$ ,  $y$ ,  $z$ ) directions separately. Higher copper exposure was associated with a complex combination of diffusion changes in the caudate nucleus region, with distinct sectors showing reduced diffusion in one or more directions (Fig. 7). In other words, copper was related to changes in the complex architecture of neural tissue diffusion, further supporting the notion that white matter pathways in the caudate nucleus region may be affected by copper exposure.

**Table 2.** MRI correlations results.

	<i>Cluster size, ml</i>	<i>x, y, z</i>	<i>t</i>
<b>Copper vs. Gray matter concentration</b>			
R Caudate nucleus – positive correlation	4.09	8, 19, 3	3.12
L Caudate nucleus – positive correlation	4.09*	-3, 16, 6	3.12
<b>Copper vs. Fractional anisotropy</b>			
R Caudate nucleus – positive correlation	1.40	11, 9, 9	3.8
L Caudate nucleus – positive correlation	9.23	-8, 9, 10	3.9
R Supracaudate white matter – positive correlation	9.23*	-17, 20, 25	3.6
L Suprathalamic white matter – positive correlation	9.23*	-20, -17, 28	3.4
R Corpus callosum – positive correlation	1.90	17, -40, 13	3.8
<b>Reaction time vs. Fractional anisotropy</b>			
L Supracaudate white matter – positive correlation	1.46	-15, 11, 21	3.6
<b>Reaction time SD vs. Fractional anisotropy</b>			
L Supracaudate white matter – positive correlation	4.29	-17, 10, 19	3.9
R Supracaudate white matter – positive correlation	3.60	19, 15, 20	4.1
<i>Copper vs. Functional connectivity</i>			
<b>Left caudate nucleus seed map</b>			
R Frontal operculum – negative correlation	5.85	48, 2, 16	4.2
L Frontal operculum – negative correlation	3.30	-38, 12, 12	3.9
<b>Right frontal operculum seed map</b>			
L Caudate nucleus – negative correlation	2.35	-14, 22, 8	3.9
R Caudate nucleus – negative correlation	1.39	16, 22, 10	3.1
<b>Left frontal operculum seed map</b>			
L Caudate nucleus – negative correlation	1.30	-16, 24, 6	4.4
<b>Frontal medial seed map</b>			
L Frontal operculum – positive correlation	3.29	-44, 32, -2	3.2
L Auditory cortex – positive correlation	1.72	-50, -18, 2	3.5
L Medial frontal cortex – positive correlation	1.42	-12, 22, 44	3.9
R Visual cortex – negative correlation	12.81	14, -54, 2	3.8
<b>Supplementary motor area seed map</b>			
L Supramarginal gyrus – positive correlation	1.08	-56, -34, 24	3.6

SD, standard deviation; \* same cluster.

*x, y, z* coordinates given in MNI (Montreal Neurological Institute) space. Statistics at corrected threshold  $P_{FWE} < 0.05$  estimated using Monte Carlo simulations.

The functional significance of the identified basal ganglia changes was further investigated by assessing functional connectivity in the basal ganglia network. Functional connectivity MRI maps representative of frontal-basal ganglia circuits were generated using coordinates taken from previous works and from the current anatomical and DTI results centered at the caudate nucleus (see Methods). The most relevant finding was the association of higher copper exposure to a reciprocal reduction of functional connectivity between the caudate nucleus and the frontal lobe operculum bilaterally (Fig. 8). This association was consistent with the anatomical and DTI results and notably specific in terms of functional anatomy. Remarkably, reduced caudate-to-frontal operculum connectivity was the only significant finding in three functional connectivity maps (see Table 2).

The effect of potential confounders was tested for each significant finding including age, sex, academic achievement, academic difficulties score, obesity, parental education, home and school vulnerability index, and public/nonpublic school category as covariates. No single confounder or combination showed a significant effect. That is, decreases in  $\beta$  estimates after the inclusion of confounders in a regression model were very small with no variables affecting the primary results with  $\beta$  reductions  $>10\%$ . Finally, potential alterations associated with Mn (manganese) were also investigated, as this element may be associated with basal ganglia alterations. We did not, however, find any significant finding associated with manganese. Moreover, the effect of copper had a tendency to be more robust when adjusted by Mn (e.g., the primary correlation between copper and motor response consistency showing  $\beta = 2.9$  in the whole sample, showed  $\beta = 3.3$  after entering Mn measurements as a covariate). Similarly, the effect of copper remained (no  $\beta$  decrease  $> 10\%$ ) after additionally adjusting by other representative elements (Table 3, i.e., C, Pb, Fe, and Sb).

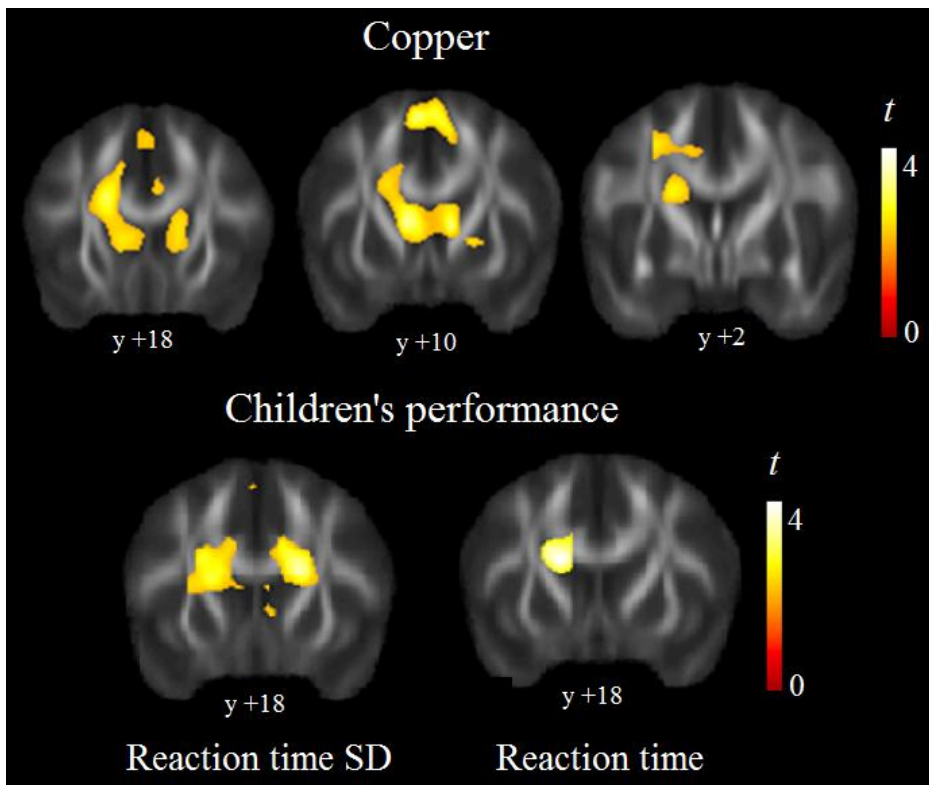


**Figure 5.** Diffusion tensor imaging results. Higher copper levels correlated with higher FA (fractional anisotropy) predominantly in caudate nucleus (top panel). The correlation with motor performance (bottom panel) showed both slower reaction time and larger reaction time standard

deviation associated with higher FA in white matter adjacent to the caudate nucleus. The right hemisphere corresponds to the right side. Y denotes “y” MNI coordinates.

#### 4.1.4 Discussion

Airborne copper was significantly associated with poorer motor performance and detectable brain damage in developing children. The alterations are highly consistent with the known consequences of copper excess on the brain with basal ganglia as the main target. The associations were demonstrated with copper levels common in urban environments, thus suggesting a risk to large populations with potentially significant implications for public health. Children may be particularly vulnerable to copper as an agent capable of interfering with brain development during critical developmental stages. Consistent with our results, a recent study has reported a significant association between high copper levels in blood and poorer cognitive performance in normal school children (Zhou et al., 2015).

The  $\beta$  weights reported in Table 4 may help in determining the biological relevance of behavior and imaging changes associated with air copper in our study. While the change related to reaction time was small, the effect on motor response consistency (measured as reaction time standard deviation) was more important. For instance, the increase in one unit ( $\text{ng}/\text{m}^3$ ) of air copper predicts an increase of 2.9 msec in reaction time standard deviation. Therefore, if the range of copper measurements is 10 units, from the least ( $3.7 \text{ ng}/\text{m}^3$ ) to the most polluted school ( $13.8 \text{ ng}/\text{m}^3$ ), the potential variation predicted is 29 msec, which is approximately one third of the standard deviation of this motor performance measurement (SD, 91 msec). The magnitude of the effect on the caudate nucleus structure and function was of the same order. Overall, our conclusion is that the effect of copper is subtle, but biologically meaningful.

In the current study, we have identified copper as one road traffic-related pollutant. Traffic-related copper is thought to be mostly released from brake pads (Hulskotte et al., 2007) and it was the main source in our study. A significant proportion of copper, however, comes from industrial activity and a third source seems to be the result of railway traffic. This is consistent with reports indicating that the air in busy train stations contains large amounts of copper generated by overhead train wire supplying electrical power (Kim et al., 2010; Loxham et al., 2013). Although a normal oral diet contains a considerable amount ( $\sim 1 \text{ mg}$ ) of copper (Morris et al., 2006), our data suggest that relatively lower levels are neurotoxic in chronic airborne exposures. Ingested copper is mostly incorporated into ceruloplasmin (safe copper) and any excess is removed by excretion into the bile (Madsen et al., 2007). There is evidence indicating that the “toxic copper” is actually the circulating free (i.e., nonceruloplasmin bound)

copper (Squitti et al., 2014c; Pal et al., 2015), which is the only fraction capable of penetrating the brain parenchyma (Zheng et al., 2012). Inhaled copper may notably circumvent the liver regulation and safe binding to ceruloplasmin. So, nonceruloplasmin-bound copper absorbed in the respiratory tract can more easily enter the brain and achieve higher tissue concentrations.

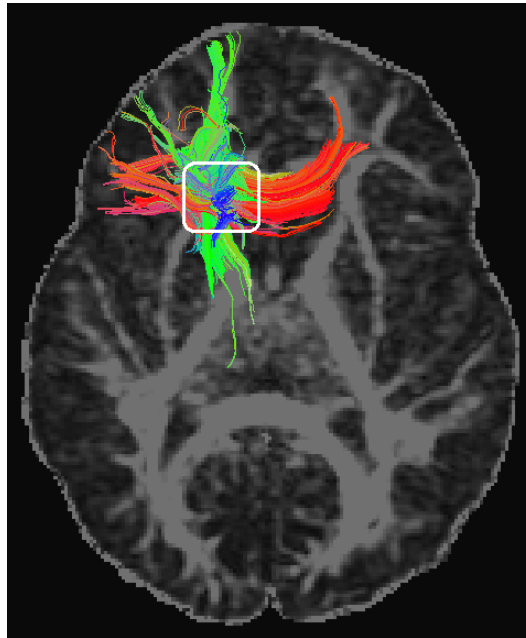


**Figure 6.** Diffusion tensor imaging tractographic display of representative participant. The colors are coded to show diffusion defined left-right tracts in red, anterior-posterior tracts in green and superior-inferior tracts in blue. Note convergence of the three directions in our region of interest (white rectangle).

Environmental copper has been proposed as a risk factor for neurodegenerative disease (Morris et al. 2006; Caudle 2015; Pal and Prasad 2015). The highest exposures occur through the inhalation of fumes generated from welding, as well as metal mining and smelting activities. Long-term (20 years) occupational copper exposure has been shown associated with 2.5-fold increase in risk for Parkinson's disease (Gorell et al., 2004; Caudle et al., 2015) and with a younger age at onset (46 years) (Racette et al., 2001). However, manifest neurological disease seems not to be a necessary outcome in occupational copper exposure, which suggests different susceptibilities among individuals and the potential interaction between a genetic predisposition and copper availability. This is obvious in the paradigmatic Wilson disease where a similar genetic alteration may correspond to a range of clinical severity and, on the other hand, the

neurological disorder may be not expressed if copper intake is properly controlled (Bandmann et al. 2015). Also, there is a possibility that the toxic capacity of environmental copper excess saturates at relatively lower copper levels (i.e., high environmental copper concentrations and very high concentrations could generate similar brain damage if the assumption is correct).

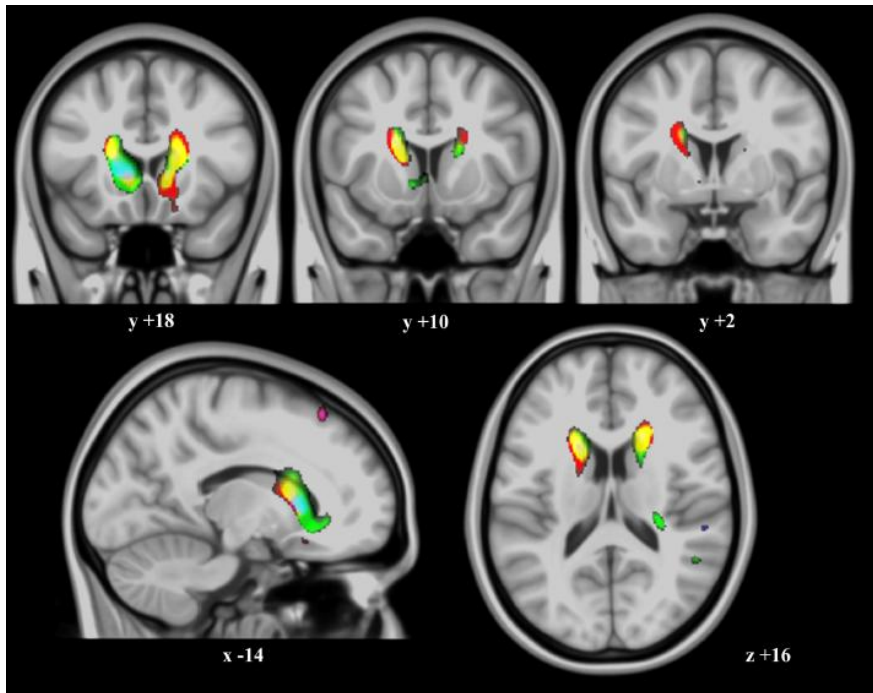


**Figure 7.** Water diffusion direction changes related to copper. Correlation of copper measurements with water diffusion along the three ( $x$ ,  $y$ ,  $z$ ) axes separately and superimposed in a single RGB color display (thresholded at  $P=0.001$  in MRIcron). Color regions express sites where higher copper levels were associated with diffusion for one or more directions. The most evident changes were along the right-left (red), anterior-posterior (green) directions or both (yellow) (note that regions with mixed effects show RGB composite colors). The right hemisphere corresponds to the right side of axial and coronal views.  $x$ ,  $y$ ,  $z$ , denote MNI coordinates.

The neurotoxic action of copper via oxidative stress and mitochondrial injury (Eskici et al., 2012; Bandmann et al., 2015) may also depend on tissue energy consumption rates. In children, the highly energetic basal ganglia appear to be the main target. This occurs in our study and in Wilson's disease, in which the lenticular nucleus (putamen and globus pallidus) was originally described with the most dramatic pathological changes (Compston et al., 2009), although the caudate nucleus may show the most severe reduction in glucose consumption (Hermann et al., 2014). By contrast, a more persistent subtle excess of copper throughout life could be responsible for protracted but widespread brain



damage. In this context, an increasing amount of evidence indicates that copper may play a causal role in late-onset neurodegenerative disorders (Bush et al., 2003; Bandmann et al., 2015). For example, nonceruloplasmin-bound copper levels are higher than normal reference values in up to 60% of Alzheimer’s disease patients (Squitti et al., 2014c; Squitti et al., 2014b). Also, high-nonceruloplasmin-bound copper concentrations were associated with an increased rate of mild cognitive impairment conversion to full Alzheimer’s disease (Squitti et al., 2014a). A prospective study revealed an association between a diet simultaneously high in copper and saturated fats and cognitive decline (Morris et al., 2006). In a variety of experimental animal studies, oral copper intake resulted in significant amyloid  $\beta$  deposition and performance decline (Alzheimer’s disease-like pathology), even at low concentrations (Pal et al., 2015).

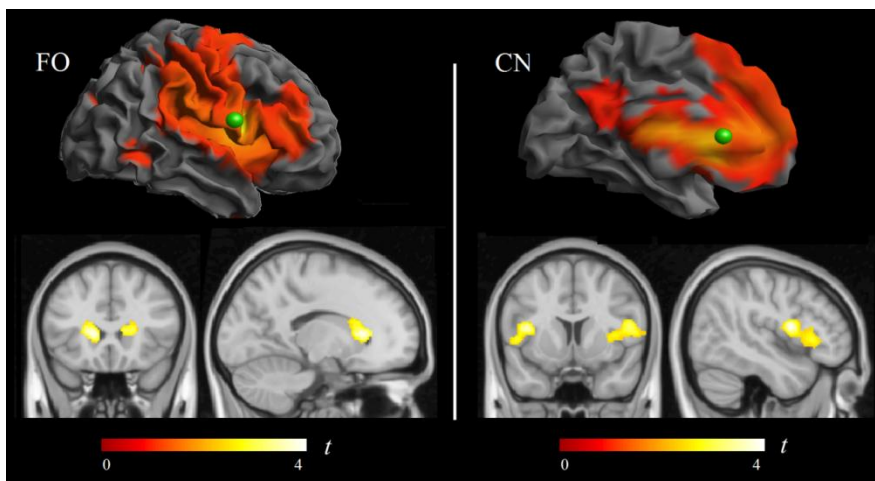


**Figure 8.** Correlation of copper measurements with functional connectivity MRI. Within the frontal operculum functional connectivity map (left panel), copper was associated with a connectivity reduction between the frontal (seed) region of interest (green sphere) and the caudate nucleus. Reciprocally, within the caudate nucleus functional connectivity map (right panel), copper was associated with a connectivity reduction between the caudate nucleus seed region (green sphere) and the frontal operculum.

**Table 3.** Potentially relevant airborne elements and their correlation with Cu.

<i>Measures from 39 schools</i>	<i>Mean ± SD</i>	<i>Range</i>	<i>Corr, with Cu r values</i>	<i>Shared variance (adjusted r<sup>2</sup> x 100)</i>
Carbon (C), µg/m <sup>3</sup>	1.5 ± 0.7	0.6-3.9	0.41	15%
Manganese (Mn), ng/m <sup>3</sup>	15.3 ± 13.8	3.7-64.8	0.22	2%
Lead (Ob), ng/m <sup>3</sup>	8.1 ± 2.8	4.3-16.8	0.46	19%
Iron (Fe) µg/m <sup>3</sup>	0.6 ± 0.6	0.1-3.0	0.15	0.4%
Antimony (Sb), ng/m <sup>3</sup>	1.1 ± 0.4	0.4-2.4	0.75	55%

Cu, copper; SD, standard deviation.

In the broader context of traffic-related pollution, the effect of air pollutants may be more dramatic when the exposure involves earlier developmental periods. Indeed, Peterson et al. (2015) have provided evidence of brain structural alterations in later childhood associated with prenatal pollutant exposure affecting large areas of the left hemisphere white matter, and a less severe effect associated with postnatal exposures at age 5 years. On the other hand, recent studies have revealed that long-term ambient air pollution exposure may ultimately affect brain tissue volume in older people (Chen et al., 2015; Wilker et al., 2015).

A general limitation when assessing children with MRI is the potential effect of head movements on image quality, particularly on functional MRI and DTI acquisitions. We have considered this issue carefully and adopted several means to rigorously control the effects of motion on functional MRI (see Methods). In the case of DTI, we decided to exclude cases with detectable image degradation, as no correction procedure is wholly efficient. A post hoc analysis on DTI using less rigorous exclusion criteria ( $n = 242$ ) showed similar but weakened DTI results, indicating that the data obtained in the more selective sample ( $n = 177$ ) were most probably not the result of motion effects. Also, a higher MRI signal may be obtained using a higher magnetic field (i.e., 3-Tesla magnets). Although we did have the 3-Tesla option, the present study was developed using a 1.5-Tesla magnet following the recommendations of the FP7- ERC Ethics Review Committee to limit magnetic field strength in children.

#### **4.1.5 Conclusions**

Our study has revealed that apparently safe school environments may indeed to expose developing children to the harmful effects of air pollutants. Tolerated amounts of airborne copper were associated with poorer motor performance in children in the city of Barcelona. The effect on motor performance was directly associated with changes in the structure and function of the basal ganglia, suggesting underdevelopment of the caudate nucleus complex neural connections.

#### **Acknowledgments**

This work was supported by the European Research Council under the ERC (grant number 268479) -the BREATHE project. The Agency of University and Research funding management of the Catalonia Government participated in the context of Research Group SGR2014-1673. We acknowledge C. Persavento, J. González, M. López and P. Figueras their contribution to the field work. We also acknowledge all the families and schools participating in the study.

**Table 4.** Behaviour and imaging changes associated with air copper (copper range, 3.7-13.8 ng/m<sup>3</sup>)

Whole Sample	Mean ± SD	$\beta$ Coefficient (adjusted $\beta$ ) <sup>2</sup>	95% CI (adjusted 95% CI)	t	P
Motor speed (reaction time)	671 ± 124 msec	2.2 (4.7) ms/(ng/m <sup>3</sup> )	0.6 to 3.7 (1.8 to 7.5) ms/(ng/m <sup>3</sup> )	2.7	0.006
Motor response consistency (reaction time SD)	235 ± 91 msec	2.9 (4.7) ms/(ng/m <sup>3</sup> )	1.7 to 7.9 (1.7 to 17.6) ms/(ng/m <sup>3</sup> )	4.9	8e-7
MRI sample (n=261) <sup>1</sup>					
Motor response consistency (reaction time SD)	224 ± 91 msec	4.2 (9.6) ms/(ng/m <sup>3</sup> )	0.5 to 7.9 (1.7 to 17.6) ms/(ng/m <sup>3</sup> )	2.2	0.026
Gray matter concentration L caudate nucleus	14.2 ± 3.9 GMc	0.3 (0.3) GMc/(ng/m <sup>3</sup> )	0.1 to 0.4 (0.1 to 0.5) GMc/(ng/m <sup>3</sup> )	3.1	0.001
Fractional anisotropy DTI L caudate nucleus	16 ± 1 FAI	0.1 (0.1) FAI/(ng/m <sup>3</sup> )	0.06 to 0.2 (0.05 to 0.2) FAI/(ng/m <sup>3</sup> )	3.9	0.0001
Functional connectivity L frontal cortex to L caudate	0.3 ± 1.1 FCI	-0.1 (-0.1) FCI/(ng/m <sup>3</sup> )	-0.14 to -0.05 (-0.2 to -0.1) FCI/(ng/m <sup>3</sup> )	-4.4	0.00001

SD, standard deviation;  $\beta$ ,  $\beta$  coefficients from the regression with copper as the predictor factor; GMc, percentage of gray matter concentration; FAI, anisotropy index expressed in range of 0-100 units; FCI, strength of functional connectivity expressed in arbitrary units.

<sup>1</sup> n varied in each imaging modality (see Methods section).

<sup>2</sup> Socioeconomic status, a general indicator of traffic pollution (elemental carbon) and other potentially toxic agents (Pb, Mn, Sb and Fe) were used in the adjusted model.

## 4.2 Study II:

### ***Traffic Pollution Exposure in Associated with Altered Brain Connectivity in School Children***

Jesús Pujol<sup>1,2</sup>, Gerard Martínez-Vilavella<sup>1</sup>, Dídac Macià<sup>1</sup>, Raquel Fenoll<sup>1</sup>, Mar Álvarez-Pedrerol<sup>3,4,5</sup>, Ioar Rivas<sup>3,4,5,6</sup>, Joan Fornas<sup>3,4,5</sup>, Laura Blanco-Hinojo<sup>1</sup>, Jaume Capellades<sup>7</sup>, Xavier Querol<sup>6</sup>, Joan Deus<sup>1,8,9</sup>, Jordi Sunyer<sup>3,4,5,10</sup>

<sup>1</sup> MRI Research Unit, Hospital del Mar, Barcelona, Spain

<sup>2</sup> Centro Investigación Biomédica en Red de Salud Mental, CIBERSAM G21, Barcelona, Spain

<sup>3</sup> Centre for Research in Environmental Epidemiology (CREAL), Barcelona, Catalonia, Spain

<sup>4</sup> Pompeu Fabra University, Barcelona, Catalonia, Spain

<sup>5</sup> Ciber on Epidemiology and Public Health (CIBERESP), Spain

<sup>6</sup> Institute of Environmental Assessment and Water Research (IDAEA-CSIC), Barcelona, Catalonia, Spain

<sup>7</sup> Radiology Department, Hospital del Mar, Barcelona, Spain

<sup>8</sup> Department of Clinical and Health Psychology, Autonomous University of Barcelona, Spain

<sup>9</sup> Instituto Universitario de Neurorehabilitación Guttmann, Badalona, Spain

<sup>10</sup> IMIM (Hospital del Mar Medical Research Institute), Barcelona, Catalonia, Spain

#### ***Abstract***

*Children are more vulnerable to the effects of environmental elements due to their active developmental processes. Exposure to urban air pollution has been associated with poorer cognitive performance, which is thought to be a result of direct interference with brain maturation. We aimed to assess the extent of such potential effects of urban pollution on child brain maturation using general indicators of vehicle exhaust measured in the school environment and a comprehensive imaging evaluation. A group of 263 children, aged 8 to 12 years, underwent MRI to quantify regional brain volumes, tissue composition, myelination, cortical thickness, neural tract architecture, membrane metabolites, functional connectivity in major neural networks and activation/deactivation dynamics during a sensory task. A combined measurement of elemental carbon and NO<sub>2</sub> was used as a putative marker of vehicle exhaust. Air pollution exposure was associated with brain changes of a functional nature, with no evident effect on brain anatomy, structure or membrane metabolites. Specifically, a higher content of pollutants was associated with lower functional integration and segregation in key brain networks relevant to both inner mental processes (the default mode network) and stimulus-driven mental operations. Age and performance (motor response speed) both showed the opposite effect to that of pollution, thus indicating that higher exposure is associated with slower brain maturation. In*

*conclusion, urban air pollution appears to adversely affect brain maturation in a critical age with changes specifically concerning the functional domain.*

**Keywords:** *Brain development, air pollution, functional MRI, functional connectivity*

### **4.2.1 Introduction**

Common to living beings, the brain development cycle is characterized by primary growth and subsequent maturation. Maturation changes implicate structure and function with anatomical shaping, progressive myelination of neural tracks and fine-tuning of functional brain networks (Menon et al., 2013; Pujol et al., 2006; Toga et al., 2006). The highest-order events procure the integration of brain areas into functional systems and the segregation of distinct but interconnected large-scale networks (Uddin et al., 2010; Vogel et al., 2010; Dwyer et al., 2014; Di Martino et al., 2014).

Developing children are at risk due to the potentially hazardous effects of environmental factors (Paus, 2010). Long-term exposure to traffic-related air pollution has been associated with alterations in children's cognition (Perera et al., 2009; Suglia et al., 2008; Wang et al., 2009). We have recently identified a significant association between general markers of road traffic pollution and slower cognitive growth in a large group of children (Sunyer et al., 2015).

Epidemiological studies, therefore, indicate that high levels of urban air pollution may be dangerous to children, as they presumably interfere with brain maturation processes. This hypothesis is largely supported by a set of studies in both animals and humans showing significant associations of pollutant exposure with inflammatory and degenerative brain pathology (Block et al., 2009; Calderón-Garcidueñas et al., 2012). However, such an interference effect on brain development has not been thoroughly investigated. We aimed to assess the extent of potential repercussions of traffic pollution exposure on child brain maturation using a variety of imaging measurements ranging from basic anatomy to high-order functional integration. A group of 263 children, aged 8 to 12 years, recruited from a large study assessing the impact of long-term exposure to urban pollution in Barcelona city school environments (Sunyer et al., 2015) completed the protocol.

Our hypothesis was that the potential brain effects of air pollution will be more evident on the more detectable anatomical and functional maturation processes. Whereas developmental changes in gray matter volume are less evident in this age period, active myelination implicates increases of relative white matter volumes, elevated choline compounds and water diffusion changes within white matter tracts (Blüml et al., 2013; Toga et al., 2006; Yoshida et al., 2013). At the functional domain, preadolescence is critical to the optimal assembling of large-scale functional networks (Menon et al., 2013). Accordingly, the imaging protocol included a high resolution 3D anatomical acquisition to measure regional

volumes, brain tissue composition, myelination levels and cortical thickness. Diffusion tensor imaging (DTI) measurements of fractional anisotropy served to explore white matter tract architecture.

In vivo spectroscopy was used to grossly estimate precursors of membrane components in white matter. Finally, functional MRI was used to test the integrity of relevant networks using both resting-state functional connectivity and a task activation/deactivation paradigm.

Selected cognitive assessment was also conducted to determine to what extent potential repercussions were also detectable on children's performance in the current study sample.

## **4.2.2 Methods**

### *Participant Selection*

This study was developed in the context of the BREATHE project (The European Commission: FP7-ERC-2010-AdG, ID 268479). The general project design is fully described in Sunyer et al. (2015). A total of 1564 families, from 39 schools in the city of Barcelona, were invited to participate in the MRI study via post, email or telephone, and 810 of them gave an initial positive response. The study sample was consecutively recruited from this group with the aim of including children from all participating schools. Parents of 491 children were directly contacted. Consent to participate was finally not obtained in 165 cases, 27 children were lost before the assessment and 21 children were not eligible because of dental braces. The finally selected study group included 278 cases. A total of 263 children completed the imaging protocol (mean age of 9.7 years, SD 0.9 and range, 8.0 to 12.1 years). Table 5 reports the characteristics of these participants. Additional cases were excluded on the basis of image quality criteria in each specific MRI analysis (see further).

All parents or tutors signed the informed consent form approved by the Research Ethical Committee (No. 2010/41221/I) of the IMIM-Parc de Salut Mar., Barcelona, Spain and the FP7-ERC-2010-AdG Ethics Review Committee (268479-22022011).

### *Pollutant Exposure*

Each school was measured twice during one-week periods separated by 6 months, in the warm (year 2012) and cold (year 2012/2013) seasons. Indoor air in a single classroom and outdoor air in the playground were measured simultaneously. Pollutants were measured during class-time using methods previously described (Amato et al., 2014; Rivas et al., 2014; Sunyer et al., 2015).

Elemental carbon was measured during 8 h (09:00 to 17:00 h) in particulate matter with an aerodynamic diameter < 2.5 µm (PM2.5) collected on filters with High-Volume samplers (MCV SA, Spain) using a Thermo Optical Transmission method (Sunset Laboratories Inc.). We carefully followed the EUSAAR-2 protocol, TOT Sunset Laboratories measurements, with a detection limit of 0.1 µg/m<sup>3</sup> and an uncertainty of ± 5%. The air cleaning effect of High-Volume samplers may underestimate absolute measurements of elemental carbon in poorly ventilated indoors. In our study, however, elemental carbon penetration was almost 1 (indoor/outdoor ratio 94.1% [95% CI 85.7%–102.4%]), which suggests a permanent ventilation of the measured classrooms. Elemental carbon was additionally measured in each classroom using the MicroAeth AE51 (AethLabs). The correlation between elemental carbon measured through High-Volume samplers and with the aethalometer was 0.95, supporting that High-Volume sampler measurements may be adequate estimations of classroom elemental carbon.

**Table 5.** Characteristic of the study sample (n=263)

Gender	48.3% girls 51.7% boys
Age, years, mean ± SD (range)	9.7 ± 0.9 (8.0-12.1)
Overall school achievement – 5 point scale	3.7 ± 1.0 (1-5)
Difficulties score (SDQ), range 0-40	8.8 ± 5.3 (0-25)
Obesity:	
Normal	71.4%
Overweight, BMI 85-94	18.4%
Obesity, BMI > 94	10.2%
Mother education (5–point scale, 5=University)	4.5 ± 0.8 (1-5)
Father education (5–point scale, 5=University)	4.4 ± 0.8 (1-5)
Vulnerability index <sup>1</sup> - home	0.43 ± 0.21 (0.06-0.90)
Vulnerability index <sup>1</sup> - school	0.43 ± 0.22 (0.13-0.84)
Public/Non-public school	43% vs. 57%
Task performance, N-Back:	
Working memory, 2-Back (detectability)	2.5 ± 1.3 (-0.6-3.9)
Working memory, 3-Back (detectability)	1.5 ± 1.1 (-1.4-3.9)
Task performance, Attentional network test:	
Reaction time (ms)	650.6 ± 119.9 (431-1091)
Reaction time standard deviation (ms)	222.9 ± 91.2 (77.5-571.6)
Commission errors (number)	4.3 (3.4%) ± 5.0 (0-49)
Omission errors (number)	1.6 (1.3%) ± 3.9 (0-44)
Alerting (ms)	53.1 ± 55.5 (-138-270)
Orienting (ms)	24.4 ± 53.8 (-204-191)
Intereference (ms)	39.4 ± 35.5 (-91-170)
Air pollution measurements <sup>2</sup> :	
Outdoor elemental carbon (EC) year average (µg/m <sup>3</sup> )	1.4 ± 0.6 (0.6-3.99)
Outdoor NO <sub>2</sub> year average (µg/m <sup>3</sup> )	46.8 ± 12.0 (25.9-84.6)
Indoor elemental carbon (EC) year average (µg/m <sup>3</sup> )	1.2 ± 0.5 (0.4-2.7)
Indoor NO <sub>2</sub> year average (µg/m <sup>3</sup> )	29.4 ± 11.7 (11.5-65.6)
Overall air pollution indicator (EC + NO <sub>2</sub> weighted average)	0.92 ± 0.30 (0.42-1.92)

BMI, body mass index; SDQ, Strengths and Difficulties Questionnaire.

<sup>1</sup> Neighborhood socioeconomic status vulnerability index based on level of education, unemployment and occupation at the census tract (Atlas de vulnerabilidad urbana de España, 2012).

<sup>2</sup> After excluding 3 children with outlier measurements.

Nitrogen dioxide (NO<sub>2</sub>) was measured with passive dosimeters (Gradko). The dosimeter was exposed during a period of 96 h (4 days) from Monday to Thursday in each school in both the warm and cold campaigns. Weekly data from both seasons were averaged to obtain a single measurement. Prior to the campaigns, we tested Gradko NO<sub>2</sub> passive dosimeters in our urban background monitoring station Palau Reial (with relatively low NO<sub>2</sub> concentrations) by measuring during 4 days and comparing the results with simultaneous chemiluminescence NO<sub>2</sub> online data. The results showed that sampling periods of 4 days were enough for ensuring a good precision. Also, during the whole sampling campaign, NO<sub>2</sub> was measured each week (from Monday to Thursday) with both the Gradko passive dosimeter and conventional chemiluminescence analyzers in this reference station. We obtained a correlation of Gradko = 0.85 × chemiluminescence + 3.6 (R<sup>2</sup>=0.7) for a mean of 37 µg NO<sub>2</sub>/m<sup>3</sup>, and an uncertainty of ±17%.

We operationally selected elemental carbon and NO<sub>2</sub> to compute a general traffic pollution indicator given their relation to vehicle exhaust emissions in the city of Barcelona (Amato et al., 2014). Our interest here was not to identify specific neurotoxic agents directly responsible for neuronal damage, but it was merely to use a measurement globally representing exposure to this sort of air contamination. NO<sub>2</sub> is highly correlated with elemental carbon in Barcelona and shows the two typical rush hour peaks (Reche et al., 2011). Barcelona has a diesel dominated vehicle fleet (with very high NO<sub>x</sub> emissions and a high NO<sub>2</sub>/NO<sub>x</sub>rate) with a primary NO<sub>2</sub> driven daily pattern (Reche et al., 2011). In Barcelona, 80% of the NO<sub>x</sub> emissions arise from road traffic (Catalonian Government Emission Inventory, 2011–2015 Air Quality. [http://airuse.eu/wp-content/uploads/2012/10/Kick-off\\_Generalitat.pdf](http://airuse.eu/wp-content/uploads/2012/10/Kick-off_Generalitat.pdf)), and even if a fraction of NO<sub>2</sub> is secondary, this is arising in a large proportion from

NO<sub>2</sub> emitted from road traffic as well (Grice et al., 2009). We did not use in this study levels of ultrafine particles, which may be more directly related to the potential neural damage, because in high cities such as Barcelona, levels of ultrafine particles are highly influenced by photochemical nucleation usually occurring at midday. This effect prevents a high correlation of ultrafine particle levels with other traffic tracers (Brines et al., 2015; Reche et al., 2011).

To obtain more representative measurements, elemental carbon and NO<sub>2</sub> were adjusted for temporal variability using whole-year data from a background monitoring station in Barcelona (Sunyer et al., 2015). A single traffic-related pollutant indicator was computed using the weighted average of elemental carbon and NO<sub>2</sub> [(EC/group median) + (NO<sub>2</sub>/group median) / 2] of pooled indoor and outdoor measurements from both cold and warm seasons. All children had been in the school for more than 18 months (and 98% more than two years) at imaging assessment, which was carried out after the pollution measurement campaigns.



## *Cognitive Performance Measurements*

General cognitive assessment included working memory, motor response speed and attention. Working memory was assessed using a computerized version of the N-Back task (Anderson et al., 2002). Children's correct detections on 2-back and 3-back loads for number items were used. Specifically, the n-back parameter analyzed was “detectability”, a measure of detection subtracting the normalized false alarm rate from the hit rate ( $Z$  hit rate  $- Z$  false alarm rate). A higher detectability indicates more accurate test performance. Attention and speed of motor responses were assessed using the computerized “Attentional Network Test”, child version (Child ANT) (Rueda et al., 2004). We used the overall “reaction time” to measure speed of motor responses and reaction time standard deviation to measure trial-to-trial variability. A higher reaction time standard deviation indicates lower executive and general attentional resources (Langner et al., 2013). The ANT task also uses a set of cued and congruent/incongruent conditions to measure specific attention features such as “alerting”, “orienting” and “interference”. Details for administering both ANT and N-Back tasks are fully described in a previous report (Forns et al., 2014).

## *Additional Contextual Assessments*

Socio-demographic factors were measured using a neighborhood socioeconomic status vulnerability index (based on level of education, unemployment and occupation at the census tract) (Atlas de Vulnerabilidad Urbana de España, 2012. [http://www.fomento.gob.es/.../Atlas Vulnerabilidad Urbana/](http://www.fomento.gob.es/.../Atlas_Vulnerabilidad_Urbana/)) according to both school and home address. Distance from home to school was estimated based at the geocoded postal address of each participant and school. Parental education was registered for both parents using a 5-point scale (1 illiterate/2 less than/3 primary/4 secondary/5 university). Standard measurements of height and weight were performed to define overweight and obesity (de Onis et al., 2009). Parents completed the Strengths and Difficulties Questionnaire (SDQ) on child behavioral problems (Goodman et al., 2001). A “difficulties” score ranging from 0 to 40 was generated. Overall school achievement was rated by teachers using a 5-point scale (from the worse= 1 to the best = 5).

## *MRI and MR Spectroscopy Acquisition*

A 1.5 Tesla Signa Excite system (General Electric, Milwaukee, WI, USA) equipped with an eight-channel phased-array head coil and single-shot echoplanar imaging (EPI) software was used. The imaging protocol involved an anatomical T1-weighted 3D sequence, diffusion tensor imaging (DTI), MR proton spectroscopy and functional MRI.

### *High-resolution 3D Anatomical Images*

High-resolution 3D anatomical images were obtained using an axial T1-weighted three-dimensional fast spoiled gradient inversion recovery-prepared sequence. A total of 134 contiguous slices were acquired with inversion time 400 ms; repetition time 11.9 ms; echo time 4.2ms; flip angle 15°; field of view 30 cm; 256 × 256 pixel matrix; slice thickness 1.2 mm.

### *Diffusion Tensor Imaging (DTI)*

Diffusion tensor imaging (DTI) was obtained using spin-echo single-shot echo-planar sequences of 25 directions with a B-factor of 1000 s/mm<sup>2</sup>. Twenty-six slices were acquired with repetition time 8300 ms; echo time 94 ms; thickness 5 mm, no gap; pulse angle 90°; field of view 26 cm; 128 × 128 acquisition matrix reconstructed into a 256 × 256 matrix.

### *Magnetic Resonance Spectroscopy*

Proton (1 H) spectroscopy was performed using the fully automated Proton Brain Exam-Single Voxel (PROBE-SV) software package (GE Medical Systems, Milwaukee, WI) and a Stimulated Echo Acquisition Mode (STEAM) pulse sequence with TR/TE=2000/30 ms and 128 signal averages. Total acquisition time was 5m 4 s. The voxel showed a dimension of 23 × 14 × 14 mm and was always placed in the left frontal white matter with the aid of high-resolution 3-D images. Orthogonal projections in the three planes assisted the placement of the voxel. The major axis (23mm) was aligned along the anterior-posterior direction in the frontal white matter. Care was taken to minimally include gray matter and to place the voxel just above the caudate nucleus between the cingulate cortex and the frontal cortex at the level of the precentral sulcus.

### *The Functional MRI Sequences*

The functional MRI sequences consisted of gradient recalled acquisition in the steady state with repetition time 2000 ms; echo time 50 ms; pulse angle 90°; field of view 24 cm; 64 × 64-pixel matrix; slice thickness 4mm(inter-slice gap, 1.5mm). Twenty-two interleaved slices were prescribed parallel to the anterior-posterior commissure line covering the brain. Two fMRI sequences were acquired for each participant including a 6-min continuous resting-state scan generating 180 whole-brain EPI volumes, and a 4-min sensory task generating 120 whole-brain EPI volumes. The first four (additional) images in each fMRI run were discarded to allow magnetization to reach equilibrium.

During the resting-state functional MRI, children were instructed to relax, stay awake and lie still without moving, while keeping their eyes closed throughout. The task-activation paradigm involved an ABABABAB block design alternating four 30-s periods of rest (visual fixation to a cross) with four 30-s periods of visual–auditory stimulation delivered using MRI compatible goggles and headphones (VisuaStim Digital, Resonance Technology, USA). Subjects were passively confronted with a set of facial images expressing happiness and with music showing a rapid tempo (Beethoven Symphony No. 6 “Pastorale”).

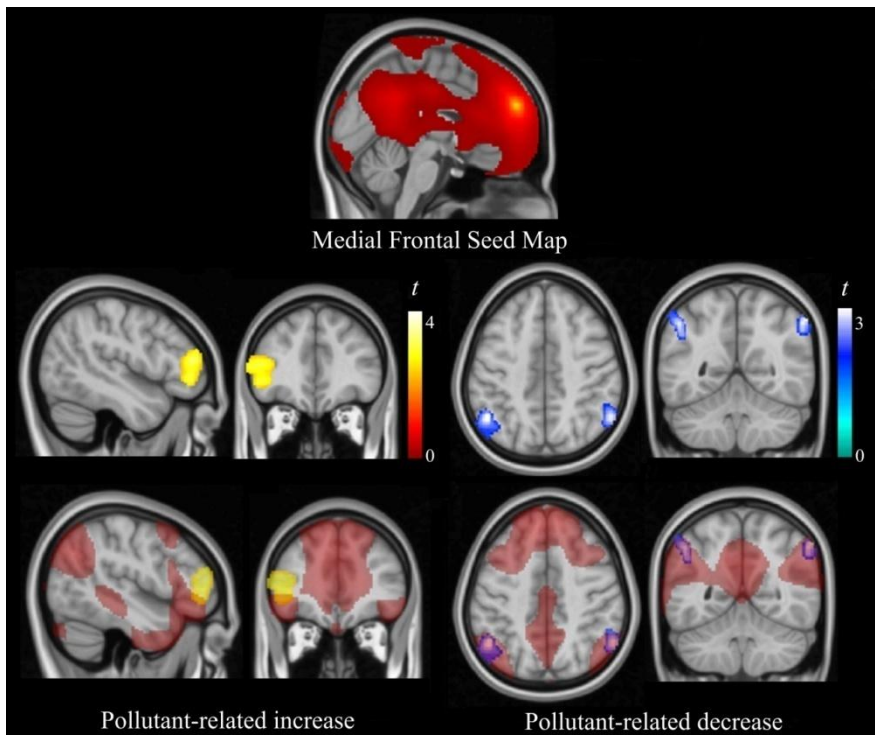


**Figure 9.** Correlations of urban pollution with functional connectivity in the medial frontal seed map. Higher pollution levels were associated with higher functional connectivity between the medial frontal (seed) region and the lateral frontal cortex (left panels), and lower functional connectivity between the seed and both angular gyri (right panels). The right hemisphere corresponds to the right side of axial and coronal views.

## *Image/Spectra Processing*

### 3D Anatomical Images

All the anatomical images were visually inspected before analysis by a trained operator to detect any motion effect. A total of 10 children were discarded as a result of poor quality images and thus the final sample for the 3D anatomical analysis included 253 children. Anatomical 3D data were processed in two separate analyses assessing different anatomical characteristics:

Gray and white matter tissue concentration and volume at a voxel level was measured using Statistical Parametric Mapping (SPM8) (<http://www.fil.ion.ucl.ac.uk/spm>, Wellcome Department of Cognitive Neurology, London, UK, 2008). SPM voxel-based morphometry (VBM) algorithms with DARTEL registration were used with the following processing steps: segmentation of anatomical images into gray and white matter tissue probability maps in their native space; estimation of the deformations that best align the images together by iteratively registering the segmented images with their average; finally, generating spatially normalized and smoothed segmentations ( $5 \times 5 \times 5$  FWHM) using the deformations estimated in the previous step. The analyses were performed with scaling by Jacobian determinants (estimates of volume change during the normalization) to consider tissue volume and without Jacobian scaling to assess the relative concentration of gray matter and white matter. Normalized images were finally transformed to the standard SPM template, re-sliced to 1.5 mm resolution in Montreal Neurological Institute (MNI) space.

Cortical thickness measurements across the whole cortex were obtained using FreeSurfer tools (<http://surfer.nmr.mgh.harvard.edu/>). Processing steps included removal of non-brain tissue, segmentation of the subcortical white matter and deep gray matter volumetric structures, tessellation of the gray and white matter boundary, registration to a spherical atlas which is based on individual cortical folding patterns to match cortical geometry across subjects and creation of a variety of surface based data. Cortical thickness is calculated as the closest distance from the gray/white boundary to the gray/CSF boundary at each vertex on the tessellated surface (Fischl et al., 1999).

## Diffusion Tensor Imaging (DTI)

DTI was processed using Functional MRI of the Brain (FMRIB) Software Library 5.0 (FSL), developed by the Analysis Group at the Oxford Centre for FMRIB (Smith et al., 2004). Diffusion-weighted images were corrected for motion and eddy current distortions ("Eddy Current Correction" option in the FMRIB Diffusion Toolbox [FDT] version 2.0 in FSL), and a whole-brain mask was applied using the FSL Brain Extracting Tool. A further rigorous image quality control was carried out to identify potential residual effects of head motion, which involved the visual inspection of each DTI slice for all 25DTI volumes in all participants. Volumes with slices with signal loss (greater than ~10%) or residual artifacts were identified by an expert researcher. DTI full examinations showing one or

more degraded images in more than 5 volumes were discarded. A total of 76 children were removed from the DTI analysis on the basis of this criterion (in addition to 10 cases showing gross image degradation). The final DTI sample involved 177 children showing a mean  $\pm$  SD of 23.5 (94%)  $\pm$  1.9 optimal-quality volumes. Subsequently, we estimated fractional anisotropy (FA) maps using FDT in FSL after local fitting of the diffusion tensor model at each voxel (“dtifit”). Next, diffusion data were processed using Tract-Based Spatial Statistics (Smith et al., 2006). Each FA data set was re-sliced to a 1 mm  $\times$  1 mm  $\times$  1 mm anatomical resolution and normalized to standard MNI space via the FMRIB58\_FA template using the FMRIB's Nonlinear Registration Tool.

## Magnetic Resonance Spectroscopy

Metabolite relative measurements were performed on the Advantage Windows, v. 4.2, workstation using the PROBE-SV software package, which includes automatic processing of the raw data that permits immediate display and evaluation of spectra. Measurements of choline-containing compounds (choline-to-total creatine ratio) were used to test the association of air pollution with membrane precursors in white matter (Blüml et al., 2013). N-acetylaspartate (NAA) spectra width and the ratio creatine-to-noise (root-mean-square ‘RMS’ noise) were used to assess spectra quality. The quality criteria to be retained for statistical analyses were NAA line width (full width at half maximum of peak) of 0.09 ppm or less and creatine RMS noise of 8 or greater. A total of 34 participants were excluded as a result of poor spectrum quality. The final sample for the spectroscopy analysis included 229 children.

## Functional MRI

Resting-state and task functional MRI preprocessing was carried out using SPM8 and involved motion correction, spatial normalization and smoothing using a Gaussian filter (full-width half-maximum, 8 mm). Data were normalized to the standard SPM-EPI template and re-sliced to 2 mm isotropic resolution in MNI space.

The following procedures were adopted to control for potential head motion effects: (i) Conventional SPM time-series alignment to the first image volume in each subject. (ii) Exclusion of 24 children in the resting-state analysis and 39 children in the task-activation analysis with large head motion. That is, outliers (and extremes) with regard to mean inter-frame motion were excluded using conventional boxplot criteria (cases beyond the quartile Q3 by one-and-a-half Q3 Q1 interquartile range [SPSS 15.0; SPSS Inc., Chicago IL]). The finally analyzed sample therefore included 239 children with valid resting-state and 224 children with valid task assessment. (iii) Both motion-related regressors (a total of 6 realignment parameters, including 3 translation and 3 rotation first-order

derivatives) and estimates of global brain signal fluctuations were included as confounding variables in first-level (single-subject) analyses. (iv) Within-subject, censoring-based MRI signal artifact removal (scrubbing) (Power et al., 2014) was used to discard motion-affected volumes. For each subject, inter-frame motion measurements (Pujol et al., 2014b) served as an index of data quality to flag volumes of suspect quality across the run. At points with interframe motion  $>0.2$  mm, that corresponding volume, the immediately preceding and the succeeding two volumes were discarded. Using this procedure, a mean  $\pm$  SD of  $11.2$  (6.2%)  $\pm$   $13.8$  volumes out of 180 fMRI resting-state sequence volumes and  $14.9$  (12.4%)  $\pm$   $15.8$  volumes out of the 120 fMRI task volumes were removed. (v) Potential motion effects were further removed using a summary measurement for each participant (mean inter-frame motion across the fMRI run) as a regressor in the second-level (group) analyses in SPM (Pujol et al., 2014b).

*Resting-state fMRI.* Four functional connectivity MRI maps were generated using coordinates taken from a classical study (Fox et al., 2005), converted to MNI in mm and located at the medial frontal cortex [ $x = 1, y = 54, z = 26$ ], posterior cingulate cortex [ $x = -2, y = -38, z = 38$ ], dorsal frontal cortex [ $x=28, y=-10, z=58$ ] and supplementary motor area [ $x= -2, y = -2, z = 55$ ]. The maps obtained using the medial frontal cortex and the posterior cingulate cortex regions typically include all the elements of the Default Mode Network (DMN), which is highly active in inner mental processes and is negatively correlated (anticorrelated) with networks participating in attention-demanding tasks (Kelly et al., 2008). On the other hand, maps from the frontal cortex and supplementary motor area regions both capture networks commonly participating in attention demanding tasks. As classically described, the dynamic relationship between the DMN and the anticorrelated task-related networks may reflect the largest-scale functional organization in the brain (Fox et al., 2005; Kelly et al., 2008). Interestingly, this network interaction matures significantly in the age period targeted in the present study (Sherman et al., 2014). Functional connectivity maps were generated using procedures detailed in previous reports (Harrison et al., 2013; Pujol et al., 2014a). For each location, the seed region was defined as a 3.5mm radial sphere (sampling  $\sim 25$  voxels in 2 mm isotropic space). This was performed using MarsBaR region of interest (ROI) toolbox in MNI stereotaxic space (Brett et al., 2003). Signals of interest were then extracted for each seed region respectively by calculating the mean ROI value at each time point across the time-series. To generate the seed maps, the signal time course of a selected seed region was used as a regressor to be correlated with the signal time course of every voxel in the brain in order to generate first-level (single-subject) voxel-wise statistical parametric maps (contrast images). The maps were estimated for each seed separately. A high-pass filter set at 128 s was used to remove low frequency drifts below  $\sim .008$  Hz. In addition, we derived estimates of white

matter, CSF and global brain signal fluctuations (using standard masks in MNI space from SPM) to include in the regression analyses as nuisance variables.

**Table 6.** Functional MRI results.

	<i>Non-adjusted</i>			<i>Adjusted by age and sex</i>		
	<i>ml</i>	<i>x y z</i>	<i>t</i>	<i>x y z</i>	<i>t</i>	
<b>Correlation with Air Pollution</b>						
<b><i>Medial frontal seed map</i></b>						
L Lateral frontal cortex – positive correlation	5.1	-48 46 16	3.6	-52 46 18	4.1	
L Parietal cortex – negative correlation	2.6	-50 -58 44	3.5	-48 -56 44	3.2	
R Parietal cortex – negative correlation	1.7	58 -56 46	3.5	58 -56 46	3.2	
<b><i>Dorsal frontal seed map</i></b>						
L Parietal cortex – positive correlation	3.2	-32 -64 32	3.6	-32 -64 32	3.5	
R Lateral frontal cortex – negative correlation	3.4	50 24 2	3.7	50 24 2	3.5	
R Insula – negative correlation	1.4	38 2 -2	4.3	38 2 -2	4.3	
<b><i>Posterior cingulated cortex seed map</i></b>						
R Lateral frontal cortex – positive correlation	1.5	56 36 -2	3.3	56 36 -2	3.2	
<b><i>Supplementary motor area seed map</i></b>						
L Prefrontal cortex – positive correlation	6.1	-28 38 28	4.4	-28 38 28	4.6	
R Prefrontal cortex – positive correlation	2.2	22 48 34	3.5	22 48 34	3.6	
L Parietal cortex – positive correlation	3.5	-58 -46 36	3.3	-56 -46 36	3.4	
R Parietal cortex – positive correlation	5.2	58 -46 40	4.1	58 -46 40	3.9	
Anterior cingulate cortex – negative correlation	6.2	-14 34 -12	3.6	-14 36 -12	3.7	
<b><i>Sensory task</i></b>						
R Somatosensory cortex – positive correlation	6.3	34 -44 64	3.7	34 -44 64	3.8	
L Premotor cortex – positive correlation	1.4	-10 0 60	3.7	-10 0 60	3.6	
<b>Correlation with Age</b>						
<b><i>Medial frontal seed map</i></b>						
	<i>ml</i>	<i>x y z</i>		<i>t</i>		
L Parietal cortex – positive correlation	10.7	-46 -70 52		4.9		
Medial frontal cortex – positive correlation	1.5	-6 52 48		3.3		
Cerebellum – positive correlation	5.8	-22 -48 -32		4.6		
L Lateral frontal/insula – negative correlation	9.7	-36 22 0		4.8		
R Lateral frontal/insula – negative correlation	10.4	40 16 2		3.5		
<b>Correlation with Performance (motor speed)</b>						
<b><i>Medial frontal seed map</i></b>						
	<i>ml</i>	<i>x y z</i>		<i>t</i>		
Medial frontal cortex – positive correlation	7.6	-10 46 26		3.6		
L Frontal lateral cortex – negative correlation	1.6	-32 44 -4		3.9		

x y z, coordinates given in Montreal Neurological Institute (MNI) space. Statistics at corrected  $P_{FWE} < 0.05$  estimated using Monte Carlo simulation. Cluster size in ml.

**Task-activation fMRI.** Functional interaction between brain systems may also be inferred using fMRI task paradigms by assessing the segregation between activated and deactivated areas during stimulation (Harrison et al., 2008; Pujol et al., 2012). Deactivated areas during our sensory task include part of the DMN, which are generally anticorrelated with networks participating in attention-demanding tasks (Chai et al., 2014; Kelly et al., 2008), although the deactivation pattern is not limited to the DMN. In the task analysis, single-subject (first-level)

SPM contrast images were estimated for activations (stimulation condition N rest) and deactivations (rest N stimulation condition). For these analyses, the fMRI signal response at each voxel was modeled using the SPM canonical hemodynamic response function.

Before the statistical analysis, all the processed images (anatomical 3D, DTI, and functional MRI) were visually inspected to detect processing-induced artifacts and verify the accuracy of anatomical segmentation and FreeSurfer surface reconstructions.

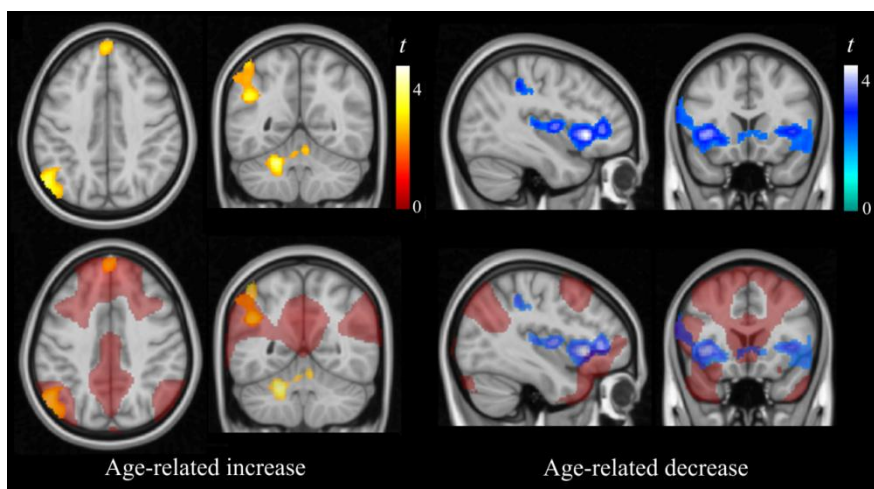


**Figure 10.** Correlations of age with functional connectivity in the medial frontal seed map. Age was associated with higher functional connectivity between the medial frontal (seed) region and the left angular gyrus, medial frontal cortex and cerebellum (left panels), and with lower functional connectivity between the seed and the lateral frontal cortex/insula region bilaterally (right panels). The right hemisphere corresponds to the right side of axial and coronal views.

### *Statistical Analysis*

Data was treated as quantitative variables and the analyses involved cross-correlations using SPM. After individual preprocessing of each imaging exam, separate second-level analyses were carried out to map voxel-wise the correlation across-subjects between individual brain images and individual age and pollutant measurements (obtained in the school of each participant). The correlations with pollutant measurements were performed both with and without adjusting by age and sex. The set of individual brain images included whole-brain estimates of regional white matter and gray matter volume and



concentration, cortical thickness, DTI fractional anisotropy, resting-state functional connectivity and task-activation/deactivation. The association with choline-to-creatine metabolite ratio was obtained using simple bivariate Pearson correlation. Total creatine was examined first for an association with traffic pollution. We found no association. As mentioned, the number of participants finally included in each analysis after exclusions on the basis of image quality criteria was: anatomic T1-weighted images, 253; DTI, 177; MR spectroscopy, 229; resting-state fMRI, 239; and sensory task fMRI 224. Finally, three additional children with outlier pollutant measurements were excluded from the correlation between brain measurements and air pollution. Results were considered significant with clusters of 1.032 ml (e.g., 129 voxels with a resolution of  $2 \times 2 \times 2$ mm) at a height threshold of  $p < 0.005$ , which satisfied the family-wise error (FWE) rate correction of  $P_{FWE} < 0.05$  according to Monte Carlo simulations (Pujol et al., 2014c). Resting-state fMRI data were additionally adjusted for multiple testing (four functional connectivity maps) using Bonferroni (significant cluster size  $\geq 1.4$  ml). Maps in figures are displayed at  $t > 2.3$ .

### 4.2.3 Results

Traffic-related pollution at the children's schools was assessed using the weighted average of two reliable vehicle exhaust indicators, namely particulate elemental carbon and  $\text{NO}_2$  (Methods). Table 5 reports ambient air concentrations of the measured pollutants. According to these data, air pollution levels at school in the city of Barcelona may be considered moderate-to-high when compared with other areas (Cyrys et al., 2012; Eeftens et al., 2012).

This summary pollution index was then whole-brain correlated with several MRI maps characterizing brain maturation. No significant association was identified between air pollution and any anatomical, structural or metabolic brain measurement. By contrast, the functional imaging analysis showed consistent results.

Our functional approach involved the generation of connectivity maps representative of key neural networks using coordinates taken from previous works (see Methods). The map obtained using the medial frontal cortex (seed) region of interest produced the most illustrative results. We found that traffic-related air pollution was significantly associated with weaker functional connectivity between regions belonging to the DMN (i.e., between the medial frontal cortex and the angular gyrus bilaterally), indicating lower intra-network integration (Fair et al., 2009). In addition, pollution also was associated with stronger functional connectivity between the (medial frontal cortex) seed region

and the frontal operculum at the lateral boundary of the DMN, indicating lower network segregation (Fair et al., 2009) (Fig. 9 and Table 6).

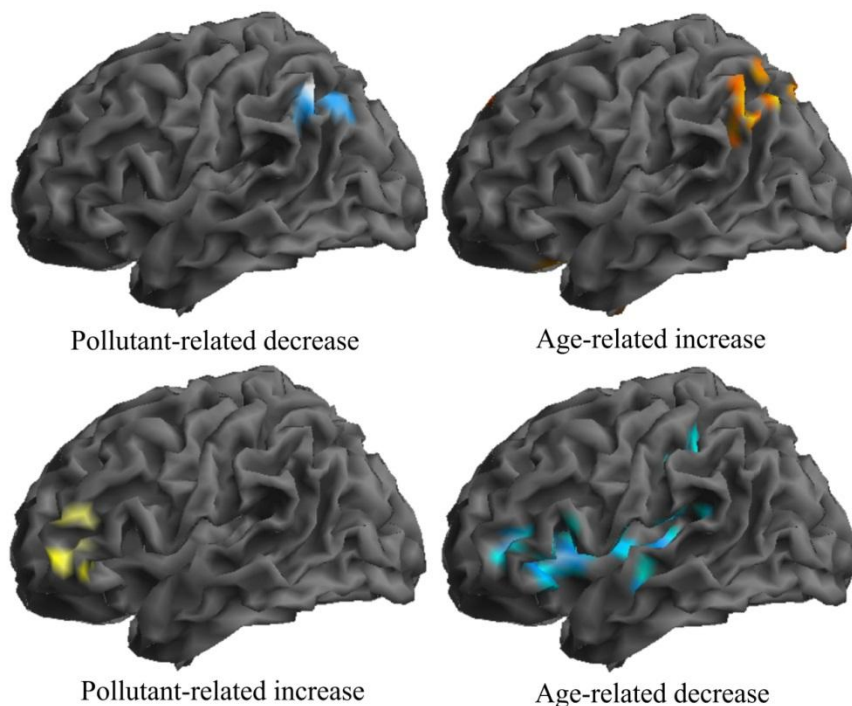


**Figure 11.** 3D rendering display of urban pollution and age effects in the medial frontal seed map. Age and air pollution were associated with opposite effects on functional connectivity in notably similar areas, thus indicating that higher exposure may interfere with the normal development of functional connections.

The analysis of the correlation between children's age and functional connectivity in the DMN was useful in establishing the detrimental nature of the results (Fig. 10). Indeed, the age effect on functional connectivity in this network was the opposite of the pollutant effect. Age was significantly associated with stronger functional connectivity within the elements of the DMN (integration) and significantly associated with weaker functional connectivity with the bordering network (segregation), as shown in a previous longitudinal study (Sherman et al., 2014). Fig. 11 illustrates the opposite effects of age and pollutants using a 3D rendering display.

The analyses based on additional functional connectivity maps mirrored such findings with results in the same direction. The maps included the DMN identified from a seed region located in the posterior cingulate cortex (Table 6) and

anticorrelated networks generated from dorsal frontal cortex (Supplementary Fig. 1) and supplementary motor area seeds (Supplementary Fig. 2). The potential effects of air pollution on brain function were further tested by mapping the correlation between pollutant measurements and fMRI task activations and deactivations. Air pollutants were significantly associated with lower deactivations (rest N task map) during passive viewing and listening in the supplementary motor area and somatosensory cortex (Fig. 12). No significant findings were observed in the task N rest map.

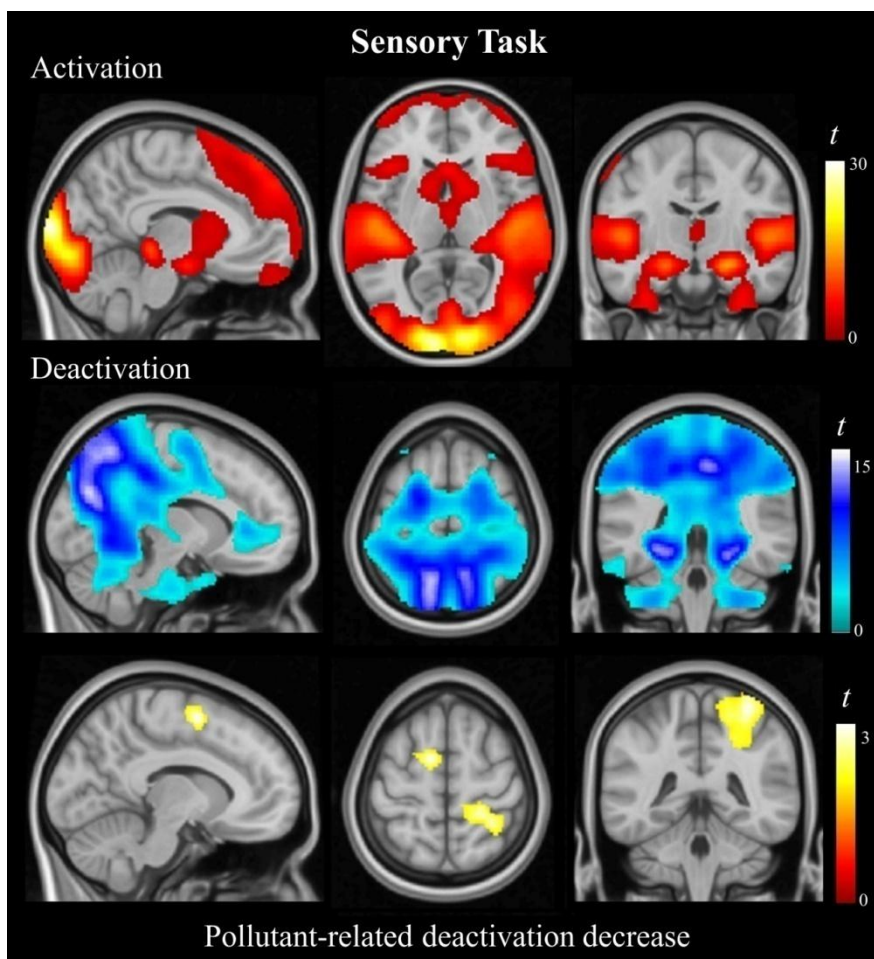


**Figure 12.** Sensory task results. One-sample group activation (top panel) and deactivation (middle panel) maps showing brain response to passive viewing and listening. Air pollution was associated with reduced deactivation in the supplementary motor area and somatosensory cortex included in the deactivation map (bottom panel). The right hemisphere corresponds to the right side of axial and coronal views.

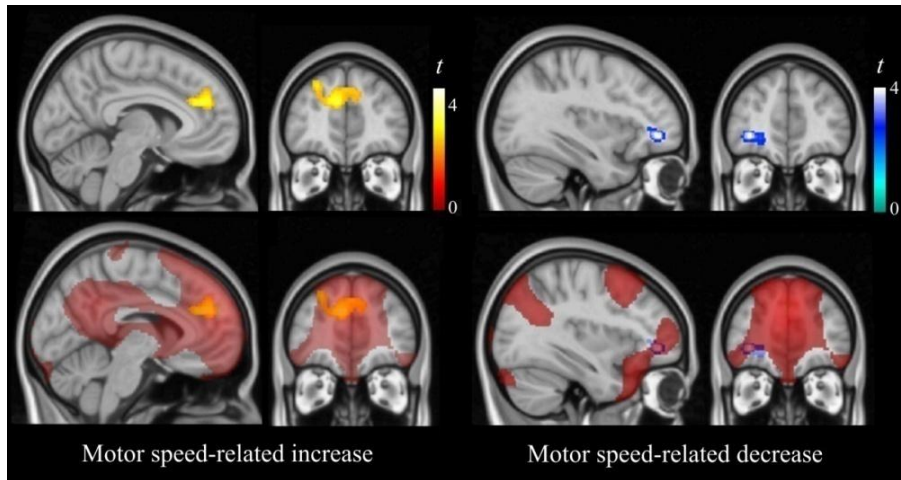


**Figure 13.** Correlations of performance (motor speed) with functional connectivity in the medial frontal seed map. Faster responses were associated with higher functional connectivity within a core region of the network (medial frontal cortex), and with lower functional connectivity in the lateral boundary of the network. The right hemisphere corresponds to the right side of coronal views.

To test whether measured pollution was associated with cognitive performance, we used children's performance in working memory, motor response speed and attention (Methods). The only significant result involved motor speed. Higher pollution predicted slower reaction time in 248 participants with complete MRI and behavioral testing (standardized  $\beta = 0.154$ ;  $p = 0.015$ ). A further imaging analysis was performed to correlate children's reaction time with functional connectivity in the DMN map (Fig. 13). Interestingly, a faster reaction time was associated with stronger connectivity within the DMN (network integration) and weaker connectivity in the frontal operculum (network segregation).

The effect of potential confounders was tested for each significant finding including age, sex, academic achievement, difficulties scores, obesity, parental education, home and school vulnerability index, distance from home to school and public/non-public school category as covariates. Each potential confounder was both individually entered into the model and combined with other confounders. No single confounder or combination showed a relevant effect. That is, decreases in  $\beta$  estimates after the inclusion of confounders in a regression model were very small (mean  $\pm$  SD, 1.2%  $\pm$  1.0%) with no variables affecting the primary results with  $\beta$  reductions greater than 7%.

#### 4.2.4 Discussion

Vehicle exhaust-related air pollution exposure was associated with brain changes of a functional nature, with no evident effect on brain anatomy, structure or membrane metabolism. Children from schools with higher traffic-related pollution showed lower functional integration and segregation in key brain networks. Age and performance (i.e., motor response speed) both showed the opposite effect to that of pollution on brain function, thus indicating that higher exposure is associated with slower brain maturation.

The functional findings were highly consistent, as similar effects were observed in different functional networks and the age-sensitive areas notably coincided with the areas showing significant correlation with air pollution. Similarly, the regions identified with the mapping of correlations with motor speed also showed a notable correspondence with the anatomy of findings from both pollutant and age analyses. Nonetheless, despite the evident effect on functional connectivity, the overall brain repercussion may, to some extent, be considered subtle, as changes did not involve any measurement of brain structure. In such a context, one may speculate on the reversibility of the brain damage and the potential effectiveness of actions addressed to reduce pollution. Epidemiological data also support the notion of a subtle repercussion, as large samples are required to demonstrate robust associations (Sunyer et al., 2015).

The effect of air pollution may, however, be more dramatic when the exposure involves early developmental periods. Indeed, Peterson et al. (2015) have provided evidence of brain structural alterations in later childhood associated with prenatal pollutant exposure affecting large areas of the left-hemisphere white matter, and a less severe effect associated with postnatal exposures at age 5 years. Also, recent studies have revealed that long-term ambient air pollution exposure may ultimately affect brain tissue volume in older people (Chen et al., 2015; Wilker et al., 2015).

We have used a general marker of vehicle exhaust traffic-related air pollution based on elemental carbon and NO<sub>2</sub>. Although this indicator reflects the amount of pollution from the traffic source, carbon and NO<sub>2</sub> are not necessarily the agents causing the toxic effect on the brain. Traffic pollution contains a variety of elements with greater potential neurotoxicity, such as manganese, aluminum, lead and copper (Amato et al., 2014). We have recently identified the effects of airborne copper pollution, which is road traffic-related, although a significant proportion also comes from industry, and a third source is the result of railway traffic (submitted). Brain alterations associated with copper were neural system specific and affected the basal ganglia with damage to both structure and function. In contrast, our current study based on a general indicator does not inform on which specific neurotoxicant or a combination thereof may be responsible for the identified effect restricted to functional measurements.

A concern in traffic pollution studies is potential residual confounding by socio-demographic characteristics (e.g., when a relationship exists between proximity to traffic and economically disadvantaged areas). In the city of Barcelona, however, there was a small and inverse relation between air pollution and socioeconomic vulnerability, with higher pollution levels in schools with lower vulnerability (Sunyer et al., 2015). Also, we found no significant associations between school pollution levels and parental education, employment or educational quality. Besides, the associations between air pollution and fMRI remained after adjusting for all the potential confounders (see Results), which is opposed to a potential role of these variables.

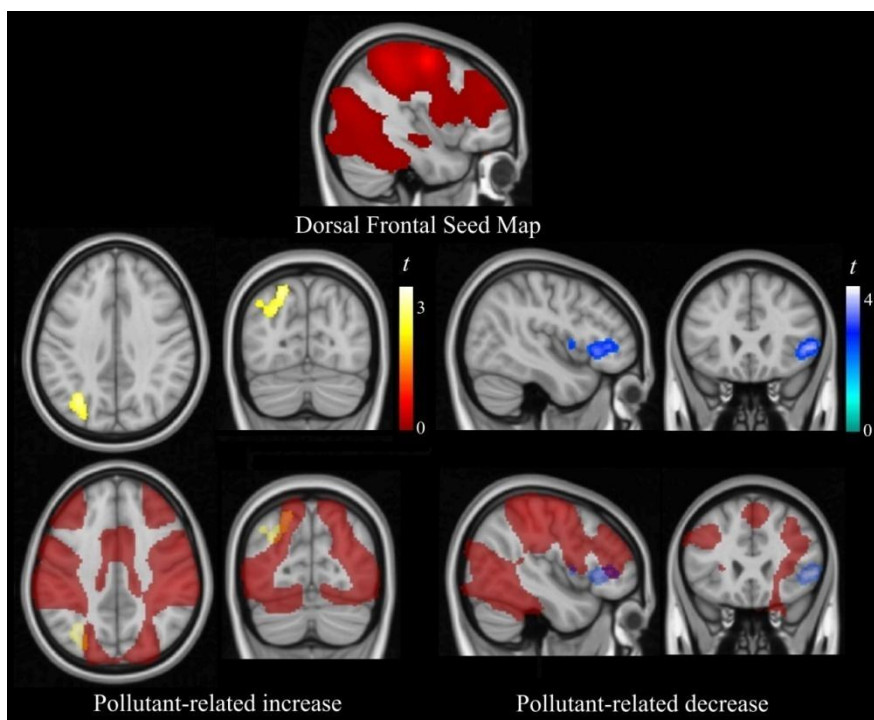
A general limitation when assessing children with MRI is the potential effect of head movements on image quality, particularly on functional MRI and DTI acquisitions. We considered this issue carefully and adopted several means to rigorously control the effects of motion (Methods). However, it is relevant to emphasize that a rigorous control of potential head motion may introduce spurious changes (e.g., regressing out global brain signal may introduce negative correlations) or even remove changes related to genuine neural activity (Pujol et al., 2014b). Also, a higher MRI signal may be obtained using a higher magnetic field (i.e., 3-Tesla magnets). Although we did have the 3-Tesla option, the present study was developed using a 1.5-Tesla magnet following the recommendations of the FP7-ERC Ethics Review Committee to limit magnetic field strength in children.

#### **4.2.5 Conclusion**

Although children's brains may be vulnerable at each developmental stage, preadolescence is notably transcendent in establishing solid bases for large-scale functional network organization. Urban traffic pollution appears to be capable of affecting the normal development of the proto-adult brain and significantly interfering with functional network maturation.

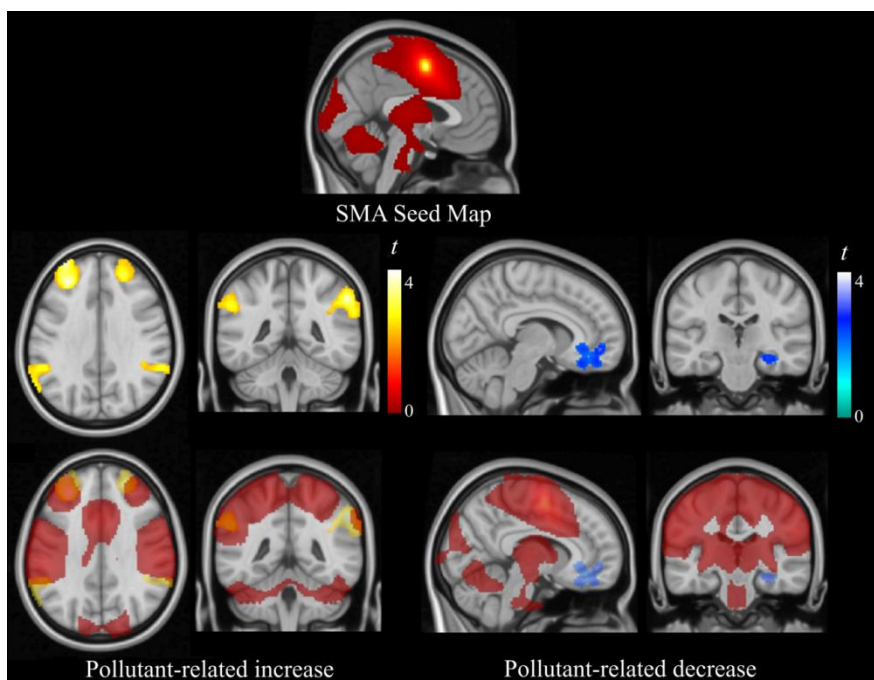
#### **Acknowledgements**

This work was supported by the European Research Council under the ERC [grant number 268479]—the BREATHE project. The Agency of University and Research Funding Management of the Catalonia Government participated in the context of Research Group SGR2014-1673. We acknowledge Cecilia Persavento, Judit González, Laura Bouso, Mónica López and Pere Figueras for their contribution to the field work. We also acknowledge all the families and schools participating in the study.



**Supplementary Figure 1.** Correlations of urban pollution with functional connectivity in the dorsal frontal seed map. Higher pollution levels were associated with higher functional connectivity between the dorsal frontal (seed) region and the parietal cortex (left panels), and lower functional connectivity between the seed and the lateral frontal cortex. Note that these results show the opposite direction to that of the medial frontal analysis (main text Figure 1). The right hemisphere corresponds to the right side of axial and coronal views.





**Supplementary Figure 2.** Correlations of urban pollution with functional connectivity in the supplementary motor area (SMA) seed map. Higher pollution levels were associated with higher functional connectivity between SMA and both the parietal and anterior prefrontal cortex bilaterally (left panels), and lower functional connectivity between SMA and both the anterior cingulate cortex and hippocampus (left panels). The right hemisphere corresponds to the right side of axial and coronal views.





### 4.3 Study III:

#### ***Video Gaming in School Children: How Much Is Enough?***

Jesús Pujol<sup>1,2</sup>, Raquel Fenoll<sup>1</sup>, Joan Forns<sup>3,4,5</sup>, Ben J. Harrison<sup>6</sup>, Gerard Martínez-Vilavella<sup>1</sup>, Dídad Macià<sup>1</sup>, Mar Álvarez-Pedrerol<sup>3,4,5</sup>, Laura Blanco-Hinojo<sup>1</sup>, Sofía González-Ortiz<sup>7</sup>, Joan Deus<sup>1,8,9</sup>, Jordi Sunyer<sup>3,4,5,10</sup>

<sup>1</sup> Magnetic Resonance Imaging Research Unit, Department of Radiology, Hospital del Mar, Barcelona, Spain

<sup>2</sup> Biomedical Research Center Network for Mental Health (CibersamG21), Barcelona, Spain

<sup>3</sup> Center for Research in Environmental Epidemiology, Barcelona, Spain

<sup>4</sup> Pompeu Fabra University, Barcelona, Spain

<sup>5</sup> Biomedical Research Center Network for Epidemiology and Public Health (Ciberesp), Madrid, Spain

<sup>6</sup> Melbourne Neuropsychiatry Centre, Department of Psychiatry, University of Melbourne, Melbourne, Australia;

<sup>7</sup> Department of Radiology, Hospital del Mar, Barcelona, Spain;

<sup>8</sup> Guttmann Neurorehabilitation Institute, Autonomous University of Barcelona, Barcelona, Spain

<sup>9</sup> Department of Clinical and Health Psychology, Autonomous University of Barcelona, Barcelona, Spain

<sup>10</sup> Hospital del Mar Medical Research Institute, Barcelona, Spain

#### ***Abstract***

***Objective:*** Despite extensive debate, the proposed benefits and risks of video gaming in young people remain to be empirically clarified, particularly as regards an optimal level of use. ***Methods:*** In 2,442 children aged 7 to 11 years, we investigated relationships between weekly video game use, selected cognitive abilities, and conduct-related problems. A large subgroup of these children (n 5 260) was further examined with magnetic resonance imaging approximately 1 year later to assess the impact of video gaming on brain structure and function. ***Results:*** Playing video games for 1 hour per week was associated with faster and more consistent psychomotor responses to visual stimulation. Remarkably, no further change in motor speed was identified in children playing >2 hours per week. By comparison, the weekly time spent gaming was steadily associated with conduct problems, peer conflicts, and reduced prosocial abilities. These negative implications were clearly visible only in children at the extreme of our game-playing distribution, with 9 hours or more of video gaming per week. At a neural level, changes associated with gaming were most evident in basal ganglia white matter and functional connectivity. ***Interpretation:*** Significantly better visuomotor skills can be seen in school children playing video games, even with relatively small amounts of use. Frequent weekly use, by contrast, was associated with conduct problems. Further studies are needed to determine whether moderate video gaming causes

*improved visuomotor skills and whether excessive video gaming causes conduct problems, or whether children who already have these characteristics simply play more video games.*

### **4.3.1 Introduction**

The pros and cons of video gaming in children remain openly debated (Bavelier et al., 2011; Ferguson et al., 2015). Although there is some evidence to suggest that video gaming can improve particular cognitive abilities in youth (Powers et al., 2013; Bavelier et al., 2012), other evidence links it with conduct related problems and increased risk toward disorders of addiction (Anderson et al., 2010; Gentile et al., 2011). One possibility is that video gaming per se is neither good nor bad, but its level of use makes it so, which begs the question, how much is enough?

We performed the current study in 2,442 school-age children to investigate relationships between average weekly video game use and both cognitive performance and conduct-related problems. Considering video gaming as a training exercise based on repetitive use and on the basis of previous research (Powers et al., 2013), we predicted that video gaming in school children would have a principal beneficial effect on speed of mental processing (eg, reaction time and chronometric measurements of attention) and a marginal influence on more innate cognitive capabilities (eg, working memory) (Melby-Lervag et al., 2013; Shipstead et al., 2012).

A subgroup of this population ( $n = 260$ ) was further examined with magnetic resonance imaging (MRI) approximately 1 year later to assess the impact of video gaming on brain structure and function. In the brain, video gaming could more notably reinforce neural connections, with a major effect presumably on frontal-basal ganglia circuits, which are central for the acquisition of new skills through practice (Doyon et al., 2003; Graybiel et al., 2008; Yin et al., 2006).

### **4.3.2 Methods**

#### *Participants*

This study was developed in the context of a large-scale project designed to assess the effects of environmental factors on brain (FP7-ERC-2010-AdG, ID 268479). Study design and participant selection have been described in full detail elsewhere (Sunyer et al., 2015; Pujol et al., 2016).

In short, the BREATHE project recruited 2,897 children from 39 schools to form a representative sample of children in Barcelona aged between 7 and 11 years (Sunyer et al., 2015). A representative subsample of 278 children was recruited from the larger cohort to participate in neuroimaging. For the present video

game study, we included children with complete cognitive and behavioral evaluation, and excluded statistically defined extreme video gamers ( $n = 23$  children playing  $\geq 18$  hours per week). The final sample comprised 2,442 children (mean  $\pm$  standard deviation [SD] age at the baseline =  $8.6 \pm 0.9$  years, range = 7.0–11.1 years, including 1,223 boys and 1,219 girls). The neuroimaging subsample comprised 260 children (mean  $\pm$  SD age at baseline =  $8.4 \pm 0.8$  years, range = 7.1–10.3 years, including 134 boys and 126 girls) with complete imaging assessment, after the exclusion of statistically defined extreme video gamers ( $n = 3$ ).

All parents or tutors signed the informed consent form approved by the Research Ethical Committee (No. 2010/41221/ I) of the Hospital del Mar Medical Research Institute, Barcelona, Spain and the FP7-ERC-2010-AdG Ethics Review Committee (268479-22022011).

### *Behavioral Measurements*

#### Video Game Use

At baseline, parents were asked to estimate how much time (in hours) their child was currently playing video games on an average weekday and weekend. A single score was computed from these estimates to indicate average hours of play per week. To document the video games most frequently used, 100 families from the MRI group completed a follow-up questionnaire indicating which games were most frequently played in the previous year. As shown in Table 7, 96% of children played visuomotor skill-based games (eg, Super Mario Bros), full-body active games (exergames; eg, Wii Sports), or both.

#### Cognitive Testing

The selected cognitive assessment included motor response speed, attention, and working memory. Speed of motor responses and attention were assessed using the computerized child version of the Attentional Network Test (ANT) (Rueda et al., 2004). Overall reaction time was used to index speed of motor responses to visual stimulation and its SD was used to index motor response consistency as a measurement of sustained attention (Lagner et al., 2013). Specific visual attention features additionally measured by the ANT task are “alerting,” “orienting,” and “interference.” Commission and omission errors were also registered. Cases with  $>30\%$  commission or omission errors were excluded from further analyses (total 9 cases in the whole sample and 2 cases in the MRI sample). In the final whole sample, commission errors were 3.1% and omission errors were 1.1%.

A computerized version of the N-Back task (Anderson et al., 2002) was used to assess working memory. “Detectability” (normalized hit rate minus normalized

false alarm rate) on 2-back and 3-back loads was used to overall index test performance accuracy. See Forns et al., 2014 for more detail.

## Behavioral Assessment

Parents completed the Strengths and Difficulties Questionnaire (SDQ) of child behavioral problems (Goodman et al., 2001). The questionnaire includes 25 questions on psychological attributes, some positive and some negative, which are rated from 0 to 2 points each. Responses are divided in 5 separate scales: “emotional symptoms,” “conduct problems,” “inattention/ hyperactivity,” “peer relationship problems,” and “prosocial behavior.” A “difficulties” score ranging from 0 to 40 was generated by summing the scores for the scales 1 to 4. Parents were also asked to report the average daily sleeping time (in hours) of their children. Overall school achievement was rated by teachers using a 5-point scale (from the worse = 1 to the best = 5).

## Additional Contextual Assessments

A neighborhood socioeconomic status vulnerability index (Urban Vulnerability Atlas of Spain, 2012; [http://www.fomento.gob.es/MFOM/LANG\\_CASTELLANO/DIRECCIONES\\_GENERALES/ARQ\\_VIVIENDA/SUELO\\_Y\\_POLITICAS/OBSERVATORIO/Atlas\\_Vulnerabilidad\\_Urbana/](http://www.fomento.gob.es/MFOM/LANG_CASTELLANO/DIRECCIONES_GENERALES/ARQ_VIVIENDA/SUELO_Y_POLITICAS/OBSERVATORIO/Atlas_Vulnerabilidad_Urbana/)), at both school and home addresses, was used as a composite measure of sociodemographic factors including level of education, unemployment, and occupation at the census tract. Parental education was registered using a 5-point scale (1 = illiterate; 2 = less than primary; 3 = primary; 4 = secondary; 5 = university).

## *MRI Acquisition*

MRI was administered a mean 6 SD of 1.2 6 0.4 years after study baseline. A 1.5T Sigma Excite system (General Electric, Milwaukee, WI) equipped with an 8-channel phased-array head coil and single-shot echo planar imaging (EPI) software were used. The imaging protocol included high-resolution T1-weighted 3-dimensional (3D) anatomical images, diffusion tensor imaging (DTI), and a 6-minute functional MRI sequence acquired in the resting state with eyes closed. Acquisition parameters for the 3 sequences are fully described in a previous report (Pujol et al., 2016).

**Table 7.** Frequency of Video Games used as a Percentage.

<i>Game</i>	<i>Use, %</i>
<i>Visuomotor skill-based Games<sup>1</sup></i>	78
Plataforms	
Mario Bros/ Super Mario Bros/ Luigi/ Super Mario Galaxy	46
Donkey Kong	12
Sports Simulation	
FIFA	33
Pro Evolution Soccer	8
Inazuma Eleven	8
NBA	4
Driving Simulation	
Mario Karts	7
Formula 1	3
Gran Turismo	2
Shooting	
Call of Duty	2
Fighting	
Dragon Ball	2
Adventure with Action	
Lego City	5
Grand Theft Auto	2
<i>Full-Body active games/exergames<sup>1</sup></i>	58
Wii Sports	48
Just Dance	20
Mario Party	17
Wii Party	4
<i>Adventure/Strategy Games<sup>1</sup></i>	49
Animal Crossing	12
Pokemon	11
Minecraft	6
Dogz/Horsez	4
Others	12
<i>Visuomotor skill-based Games and/or full-body Active Games</i>	96
<i>Adventure/Strategy Games alone</i>	4

Based on reports from 100 families indicating up to 3 games played the most in the year before magnetic resonance imaging.

<sup>1</sup> Alone or combined.

## *Image Preprocessing*

### Anatomical 3D

After visual inspection by a trained operator, images from 9 children were discarded as a result of poor image quality, and thus the final sample for the anatomical analysis included 251 children. Statistical parametric mapping (SPM) voxel-based morphometry algorithms with DARTEL registration were used to measure gray and white matter tissue concentration and volume at a voxel level. The preprocessing steps are detailed elsewhere (Pujol et al., 2016). Such a preprocessing approach implied the generation of a study-specific template.

Normalized images were transformed to the standard SPM template, re-sliced to 1.5mm resolution in Montreal Neurological Institute (MNI) space.

## DTI

The Functional MRI of the Brain (FMRIB) Software Library 5.0 (FSL), developed by the Analysis Group at the Oxford Centre for FMRIB (Smith et al., 2004) was used to process DTI images. Image quality control was rigorous in this study. A total of 86 children were removed from the DTI analysis on the basis of suboptimal image quality (see Pujol et al. 2013). The final DTI sample involved 174 children with a mean  $\pm$  SD of 23.5 ( $\pm$  1.9) optimal-quality volumes. Fractional anisotropy (FA) maps were estimated using FMRIB's Diffusion Toolbox in FSL after local fitting of the diffusion tensor model at each voxel ("dtifit"). Tract-Based Spatial Statistics (Smith et al., 2006) was used to process diffusion data. FA data sets were re-sliced to a 1mm  $\times$  1mm  $\times$  1mm anatomical resolution and normalized to standard MNI space via the FMRIB58\_FA template and the Nonlinear Registration Tool.

## Functional MRI

Preprocessing was carried out using SPM8 and involved motion correction, spatial normalization, and smoothing using a Gaussian filter (full-width half maximum = 8mm). Data were normalized to the standard SPM-EPI template and resliced to 2mm isotropic resolution in MNI space.

The comprehensive procedures adopted to control for potential head motion effects are fully described in our previous report (Pujol et al., 2016). In short, the procedures included: (1) conventional SPM time-series alignment; (2) exclusion of 24 children with outlier head motion (mean interframe motion > 0.12mm; the finally analyzed sample therefore included 236 children); (3) use of both motion-related regressors and estimates of global brain signal fluctuations as confounding variables in first-level analyses; (4) within-subject, censoring-based MRI signal artifact removal (scrubbing) (Power et al., 2014; Pujol et al., 2014a); and (5) use of the mean interframe motion across the functional MRI run for each participant as a regressor in the second-level analyses (Pujol et al., 2014b).

Based on the results obtained from the anatomical and DTI assessments, our functional connectivity analysis was focused on the left basal ganglia. To systematically explore basal ganglia, we targeted 4 key sub-regions: the dorsal and ventral aspects of both caudate nucleus and putamen. Based on a widely applied method for mapping basal ganglia functional connectivity, the regions of interest (or "seeds") were centered at MNI coordinates (in millimeters): (1) dorsal caudate nucleus ( $x = -13, y = 15, z = 9$ ); (2) dorsal putamen ( $x = -28, y = 1, z = 3$ ); (3) ventral caudate nucleus, corresponding approximately to the nucleus accumbens ( $x = -9, y = 9, z = -8$ ); and (4) ventral putamen ( $x = -20, y = 12, z = 23$ )

(Pujol et al., 2014b; Di Martino et al., 2017a; Harrison et al., 2009; Harrison et al., 2013). The procedures adopted to generate functional connectivity maps from the selected regions are detailed in our previous report (Pujol et al., 2016).

## *Statistical Analysis*

### Behavioral Data

Student t test was used to compare sex and age group means as to hours of play per week. Analysis of variance (ANOVA) adjusted by age and sex (ANCOVA) was used to compare gamers and non-gamers as to the behavioral variables. Assumptions under the ANCOVA were met in these analyses including homogeneity of variance, homogeneity of regression slopes of covariates, and non-collinearity. Linear regression adjusted by age and sex was used to assess the relationship between video game playing time and behavioral variables within the user group. Bonferroni correction was applied to account for multiple testing within each analysis. Only probability values  $< 0.006$  ( $0.05/8$ ) were considered significant. Finally, to easily illustrate the identified associations of gaming with behavior variables, the data were plotted as discrete groups on the basis of playing time in hours (Fig. 14 and 18).

### Imaging Analyses

ANOVA with age and sex as covariates (ANCOVA) and cross-correlations were estimated using SPM. Separate second-level (group) analyses were carried out for whole-brain estimates of regional white matter and gray matter volume, DTI fractional anisotropy, and resting-state functional connectivity. The behavioral results obtained in the large sample helped to guide the subsequent imaging analysis. Specifically, 3 groups of children were defined on the basis of video game use: 45 non gamers, 113 low-use gamers (playing 1–2 hours per week), and 102 high-use gamers (playing 3 or more hours per week). The cutoff between low and high use corresponds to the median of time of play per week in all gamers. In each case, ANCOVA allowed us to first identify brain areas showing overall differences among these groups. From each analysis, a plot was then generated using brain measurements extracted at representative peak differences to characterize the direction of findings with no bias. That is, the 3-group model allowed us to fairly capture any change combination among the 3 groups (non-playing, low use, and high use) in a single model sensitive to both the effect of playing versus non-playing and the effect of low versus high use. Finally, post hoc whole-brain t tests were used to compare non gamers with high-use gamers. In addition, we mapped voxelwise the correlation across subjects between individual brain images and the child's age at the time of MRI acquisition.



Results were considered significant with clusters of 1.032ml (e.g, 129 voxels with a resolution of 2 x 2 x 2mm) at a height threshold of  $p < 0.005$ , which satisfied the family wise error (FWE) rate correction of  $P_{FWE} < 0.05$  according to Monte Carlo simulations (Pujol et al., 2014c).

### 4.3.3 Results

#### *Behavioral Results*

The overall study sample comprised 428 non gamers and 2,014 gamers (i.e, playing 1 hour or more per week). As a group, gamers played a mean of  $4.0 \pm 2.9$  hours per week (see Fig. 14 for participant distribution according to playing time). Boys overall played video games 1.7 hours per week more than girls (95% confidence interval [CI] = 1.4–1.9 hours). There was also a significant effect of age, with older children (above sample median age) playing 0.4 hours per week more than younger children (95% CI = 0.2–0.7 hours). Although the correlation between age and gaming hours was significant in the whole group ( $p = 0.0004$ ), collinearity between both variables was very low ( $r = 0.07$ , tolerance = 0.995).

No significant differences were found between gamers and non gamers as to parents' education. For example, 59.1% of mothers of gamers had university-level education versus 61.0% in non gamers (chi-square = 0.5,  $p = 0.511$ ). All further statistical analyses were adjusted for sex and age (i.e, age and sex were included as covariates in both group comparisons and correlations).

Video gamers showed faster motor response to visual stimulation (i.e, shorter reaction time) than non gamers, with a mean group difference of 65 milliseconds (Table 8). Such a difference was statistically robust ( $t = 8.1$ ,  $p = 6e^{-16}$ ) and was also significant in the smaller subsample of children who underwent MRI ( $t = 4.5$ ,  $p = 0.0001$ ). Video game use was also associated with higher consistency of motor responses, measured as reaction time SD (see Table 8). However, there were no effects on specific attentional features or working memory. Remarkably, most of the advantage in motor responsiveness was observed in children playing 1 hour per week (mean difference of 52 milliseconds with respect to nongamers), with minimal further change observed after 2 hours per week (illustrated in Fig.18).

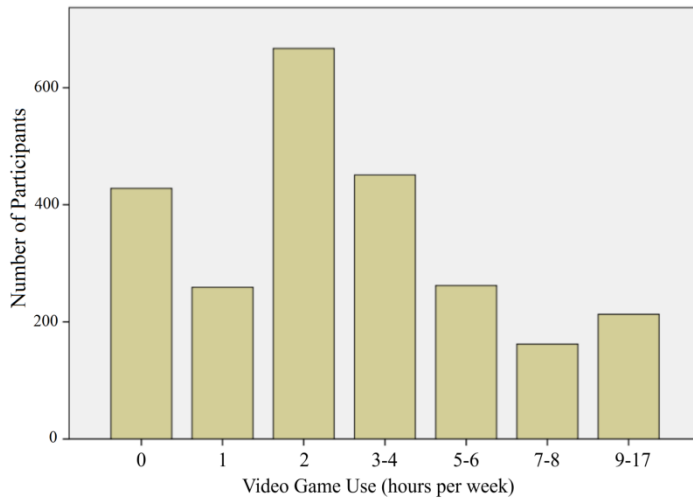


**Figure 14.** Participant distribution according to playing time.

By contrast, in the gaming group, the weekly time spent gaming was steadily associated with higher scores in parental ratings of strengths and difficulties (SDQ), particularly in regard to conduct problems (see Fig. 15), peer conflicts, and reduced prosocial abilities (see Table 8). In our post hoc analyses, children gaming in the range of 9 to 17 hours per week showed significantly more behavioral problems than nongamers (e.g. conduct problems;  $t = 3.3, p = 0.001$ ). In addition, the amount of time that was spent gaming was negatively associated with sleeping time. However, as a group, gamers and non gamers did not differ as to strengths and difficulties ratings. Interestingly, gamers showed significantly higher school achievement scores (see Table 8).

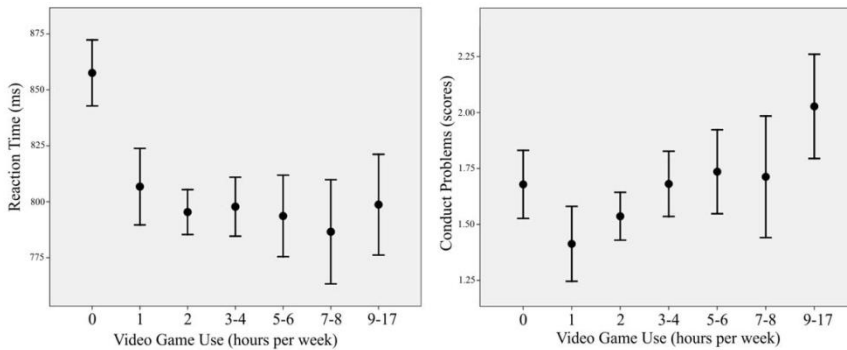


**Figure 15.** Mean reaction time (left) and conduct scores (right) plotted for discrete playing time groups. Both plots are adjusted by age and sex display 95% confidence interval estimates.

A further analysis stratified by sex and age showed that the identified associations were notably consistent across the subgroups. In both boys and girls, most of the attained group difference in motor responsiveness was observed playing 1 hour per week, as in the older children subgroup. It is relevant, however, that further improvement was observed up to 3 to 4 hours of play in the younger children. In each stratified group, differences between gamers and non-gamers were highly significant (boys,  $p = 2e^{-10}$ ; girls,  $p = 5e^{-8}$ ; younger,  $p = 3e^{-1}$ ; older,  $p = 9e^{-9}$ ). However, such differences between gamers and non-gamers were significantly stronger in girls compared to boys (interaction  $t = 2.6$ ,  $p = 0.008$ ). No significant interaction was identified for age. Similarly, gamers showed a significant linear correlation between playing hours and conduct problems in each subgroup analysis (boys,  $p = 0.001$ ; girls,  $p = 1e^{-5}$ ; younger,  $p = 8e^{-6}$ ; older,  $p = 0.002$ ). No significant interaction was found in the correlation analysis. Also, we found no significant differences between gamers and non-gamers in any subgroup (boys, girls, younger, and older children) as to conduct problems. All associations remained highly significant when analyses were further adjusted for other potential confounding variables, including parental education and neighborhood vulnerability index as the most representative indicators of children's close environment.

### *Imaging Results*

Age and sex were included as covariates in all imaging analyses.

#### T1-Weighted 3D Anatomical Images

When examining differences among non-gamers and low- and high-use gamers in white matter volume measurements (ANCOVA), significant results were observed in a region adjacent to the ventral and lateral aspect of the striatum and extending to the temporal lobe (Fig. 16 and Supplementary Table 1). A plot of white matter volume measurements from the left ventral striatal region revealed a similar increase of white matter volume in both low- and high-user groups compared with nonusers. Fig. 16 illustrates this effect in post hoc comparison between nonusers and high users. In addition, the primary ANCOVA identified significant effects in the brainstem (see Supplementary Table 1), which were not observed in the post hoc analysis. No significant results were obtained for gray matter volume.

#### DTI Fractional Anisotropy

ANCOVA consistently showed significant differences among groups in a region adjacent to the lateral aspect of the striatum (see Fig. 16, Supplementary Table 1). The plot of FA measurements from this left striatal region revealed a relevant

FA increase, but only in the high-use group (see Fig. 16). Direct comparison of non-gamers with high-use gamers confirmed the increase of FA in this region and detected additional significant changes in the ventral striatal region bilaterally, as well as the right thalamus and left occipital white matter.

## Basal Ganglia Functional Connectivity

Video gaming was associated with higher functional connectivity in the putamen and caudate nucleus maps (Fig. 17 and Supplementary Table 1). Specifically in the putamen maps, a significant connectivity increase was identified with the left motor cortex and prefrontal cortex in both low- and high-use groups. In the ventral caudate map, the most relevant finding involved the dorsal anterior cingulate cortex (ACC), which demonstrated a strong effect in the high-use group and an intermediate effect in the low-use group compared with non-gamers. The post hoc analysis confirmed a robust connectivity increase with the ACC and additionally with the left and right anterior insula region (Fig. 17 and Supplementary Table 1).

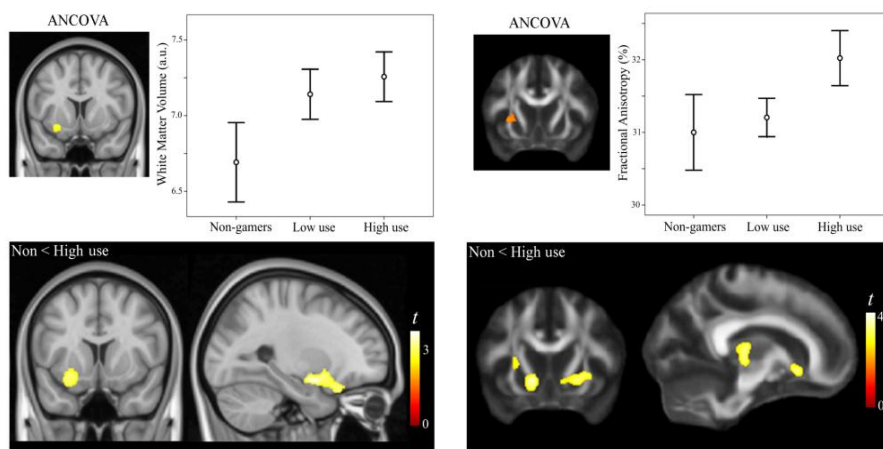


**Figure 16.** Gaming group differences in white matter volume measurements (top left) and diffusion tensor imaging fractional anisotropy (top right). Analysis of variance adjusted by age and sex (ANCOVA) indicated significant changes adjacent to the striatum in both analyses. Mean and 95% confidence intervals are plotted for each modality, reflecting regional peak differences among gaming groups. The bottom left and right images illustrate corresponding differences identified between non-gamers versus high-use gamers. The left hemisphere corresponds to the left side of coronal views.

## Correlation Analysis with Age

White matter volume increased with age in the visual system and sensorimotor projection tracts at the level of basal ganglia and thalamus, with no areas showing negative correlations with age (Fig. 18). FA increased significantly with age mostly in the internal capsule and basal ganglia. Therefore, the identified associations of video gaming with white matter measurements were generally consistent with the effects of age in terms of their positive direction and (partial) anatomical overlap. Similarly, age was associated with higher functional connectivity between the putamen and motor cortex in the area associated with video game use, albeit significant only for right hemispheric effects. For the ventral caudate, age was instead negatively associated with its functional connectivity with a medial frontal area adjacent to the ACC region that was positively associated with gaming use (and additionally with the upper brainstem and amygdala).

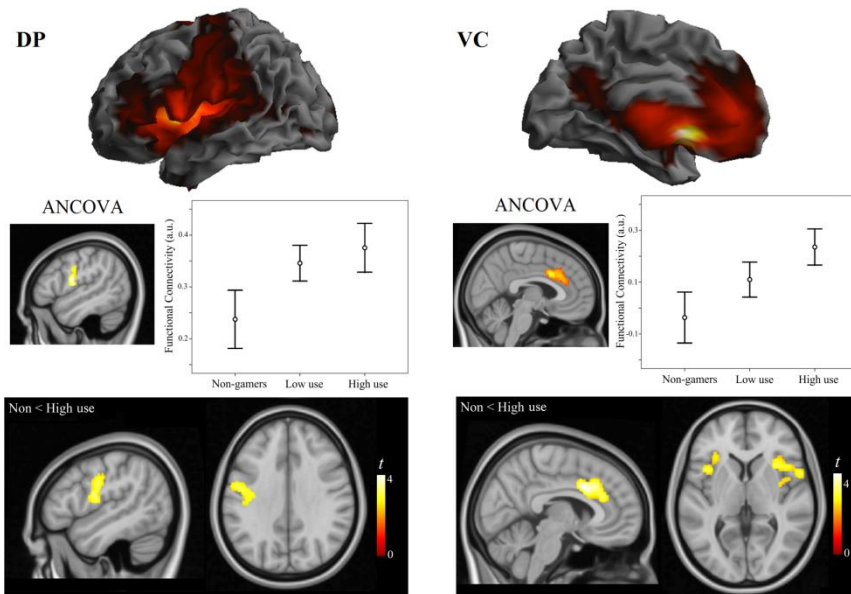


**Figure 17.** Group differences in basal ganglia functional connectivity. Analyses of covariance (ANCOVA) indicated significant changes in functional connectivity between the dorsal putamen (DP) and motor cortex at the level of the frontal operculum. In the ventral caudate (VC) analysis, the most relevant finding involved the anterior cingulate cortex. Mean and 95% confidence intervals are plotted, reflecting regional peak differences among gaming groups. Bottom left and right images illustrate corresponding differences identified between non-gamers and high use gamers. The left hemisphere corresponds to the left side of axial views.

### 4.3.4 Discussion

In the cognitive domain, video game use was associated with faster motor response to visual stimulation. Importantly, no further change in motor speed was identified in children playing >2 hours per week, suggesting an early ceiling effect for this measurement. Video games, overall, did not demonstrate more problematic behavior than non-gamers, although, within the gaming group, we observed a positive association between time weekly spent gaming and conduct problems, peer conflicts, and reduced prosocial abilities, as well as a negative association with sleeping time. At a neural level, structural and functional brain changes associated with gaming use were most evident with respect to basal ganglia circuitry.

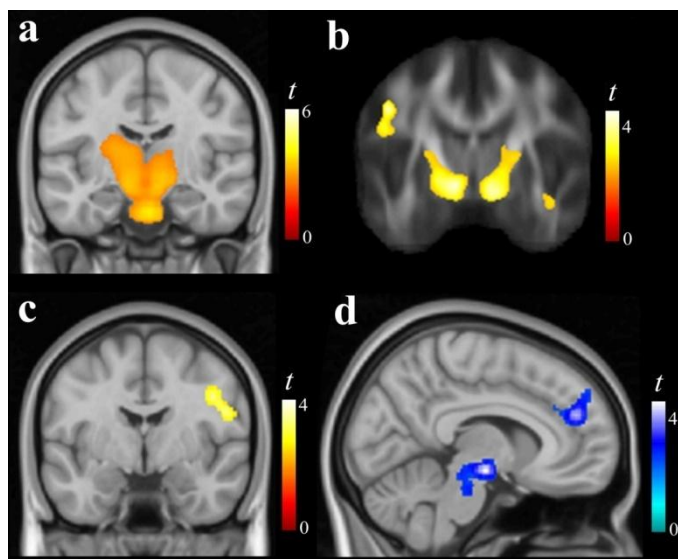


**Figure 18.** Correlation of age with brain measurements. White matter volume (A) increased significantly with age in projection tracts (and the visual system). Fractional anisotropy (B) increased with age mostly in the internal capsule and basal ganglia. Age was associated with higher functional connectivity between the putamen and motor cortex (C) and weaker functional connectivity between the caudate nucleus and the medial frontal cortex (D) and additionally with the upper brainstem (and amygdala).

Our cognitive assessment selectively measured processing speed, attention, and working memory as primary cognitive domains of interest. In the literature, there is some consensus that gaming may improve speed of information processing and motor response (Powers et al., 2013; Latham et al., 2013; Dye et al., 2009); however, the reported effects on executive function and working memory, as well

as general intelligence, have been less consistent (Powers et al., 2013). For example, working memory has been shown to improve in some studies, whereas others reported only partial associations or negative results (Oei et al., 2013; Black et al., 2014; Boot et al., 2008).

In our study, larger differences in reaction time than in working memory support the contention that several abilities are more trainable than others with commercial video games (Powers et al., 2013; Melby-Levag et al., 2013; Doyon et al., 2003).

We observed an association between gaming use and changes in basal ganglia circuits in the form of structural (white matter) and functional connectivity increases. These findings are intuitive in many respects, as it is well known that basal ganglia circuits are critical for procedural learning based on the acquisition of new skills through practice (Melby-Levag et al., 2013; Shipstead et al., 2012; Doyon et al., 2003). Our results are also generally consistent with other imaging studies reporting significant effects of gaming use on the frontobasal ganglia system structure and function (Kim et al., 2015; Lorenz et al., 2015; Kühn et al., 2014a; Hyun et al., 2013; Erickson et al., 2010). Specifically, Erickson et al., 2010 showed that the acquisition of skills on demanding video games may be predicted by variations in the volume of the striatum. Children traditionally acquire procedural skills through action, for instance in relation to sports and outdoor games. Neuroimaging research now suggests that training with desktop virtual environments is also capable of modulating brain systems that support procedural learning. However, the type of video game is likely to be particularly relevant with regard to the modulation of specific neural systems. For example, the use of logic and “platform jumping” games has been associated with anatomical changes implicating the hippocampal system in adults (Kühn et al., 2014b; Kühn et al., 2014c).

Reviews of the literature generally conclude that excessive video game use has negative effects on some aspects of behavior in children (Bavelier et al., 2011; Powers et al., 2013; Anderson et al., 2010; Straker et al., 2014). Most of the identified problems relate to the extent to which gaming can become a behavioral addiction, or to the violent content of some of the games themselves. We did not include children with probable gaming addiction, and the amount of time spent on playing in our population (mean = 4 hours per week, = range 0–17 hours) was far less than the gaming level that has been associated with severe psychosocial health disturbances. Despite this, gaming use in our study was positively related to the presence of conduct problems, peer conflicts, and reduced prosocial abilities. This finding is in agreement with the results of a national survey of 10- to 15-year old children in the United Kingdom, in which gaming use of >3 hours per day was associated with similar behavioral problems (Przybylski et al., 2014). Thus, frequent video game use does appear to be associated with behavioral problems in children even in the absence of a recognized gaming disorder, although the direction of the relationship is less clear (Gentile et al.,

2011). That is, children with peer conflicts and reduced prosocial abilities may show a tendency to isolate and spend more time playing video games. Conversely, highly frequent use likely consumes a proportion of the child's leisure time and invades other activities that may ultimately affect the normal development of prosocial abilities.

Our study was limited in that we applied a selective cognitive and behavioral assessment that did not comprehensively cover all domains. Also, we estimated the time spent gaming from parental reports but with no formal assessment of the fidelity of these reports in terms of their reliability and accuracy. It is also relevant to mention that the estimation of video game use was based on a single cross-sectional measurement. Finally, the type of video games played varied, and we were unable to perform specific analyses stratified by game content or type.

### **4.3.5 Conclusion**

In conclusion, we have investigated relationships between weekly video game use, selected cognitive abilities, conduct-related problems, and brain correlates in a large group of children. Relatively small amounts of video gaming were associated with better performance in certain visuomotor skills and, by contrast, a frequent use was associated with the presence of conduct problems. Whereas motor response differences between gamers and nongamers were already established with 2 hours per week of video gaming, conduct problems appear to be more common in school children playing 9 hours weekly or more. It is important to emphasize that this is a correlational study and, as such, does not permit direct inferences regarding causal relationships. Further studies will be needed to explore the extent to which better visuomotor skills and conduct problems are a cause or consequence of gaming.

### **Acknowledgements**

This work was supported by the European Research Council (grant number 268479; the BREATHE project). The Agency of University and Research Funding Management of the Catalonia Government participated in the context of Research Group SGR2014-1673. We thank C. Persavento, J. González, L. Bouso, M. López, and P. Figueras for their contribution to the field work; and the families and schools participating in the study.



Table 8. Behavioral Results.

Measure	Group Comparison				Correlation with Weekly Play Time, Users, N=2,014			
	Nonusers N=428, Adj. Mean (95% CI)	Users, N=2,014, Adj. Mean (95%)	Difference (95%)	t	p	$\beta$	t	p
<b>Cognitive Tests</b>								
Reaction time, ms	861 (847 to 875)	796 (790 to 802)	65 (49 to 81)	8.1 <sup>a</sup>	6e-16a	-0.559	-0.5	0.619
Reaction time SD, ms	286 (278 to 294)	267 (264 to 271)	19 (10 to 28)	4.0 <sup>a</sup>	0.00005 <sup>a</sup>	-0.201	-0.3	0.761
Alerting, ms	43 (35 to 50)	49 (46 to 53)	-6 (-15 to 2)	-1.5	0.128	1.161	2.0	0.045
Orienting, ms	32 (25 to 40)	35 (31 to 38)	-3 (-11 to 6)	-0.6	0.575	-1.102	-2.0	0.057
Interference, ms	66 (60 to 72)	63 (60 to 66)	3 (-3 to 10)	1.0	0.340	1.082	2.3	0.021
2B working memory, d'	2.2 (2.1 to 2.3)	2.3 (2.2 to 2.3)	-0.08 (-0.2 to 0.05)	-1.2	0.229	-0.015	-1.6	0.118
3B working memory, d'	1.1 (1.0 to 1.2) <sup>b</sup>	1.2 (1.2 to 1.3) <sup>c</sup>	-0.07 (-0.2 to 0.04)	-1.3	0.210	-0.012	-1.5	0.124
<b>Behavior</b>								
School achievement	3.41 (3.31 to 3.51)	3.60 (3.55 to 3.64)	-0.19 (-0.26 to -0.03)	-3.2 <sup>a</sup>	0.001 <sup>a</sup>	-0.002	-0.3	0.780
Sleeping time, h	9.63 (9.56 to 9.7)	9.56 (9.53 to 9.59)	0.07 (-0.007 to 0.1)	1.8	0.076	-0.029	-5.3 <sup>a</sup>	1e-7a
Total SDQ score	8.6 (8.1 to 9.1)	8.3 (8.1 to 8.6)	0.27 (-0.30 to 0.21)	0.9	0.353	0.188	4.6 <sup>a</sup>	5e-6a
Conduct problems	1.7 (1.5 to 1.8)	1.6 (1.6 to 1.7)	0.04 (-0.13 to 0.21)	0.4	0.661	0.065	5.4 <sup>a</sup>	8e-8
Problems with pee	1.2 (1.0 to 1.3)	1.1 (1.1 to 1.2)	0.07 (-0.09 to 0.23)	0.8	0.420	0.061	5.2 <sup>a</sup>	2e-7a
Emotional symptoms	1.9 (1.7 to 2.1)	1.9 (1.9 to 2.0)	-0.03 (-0.22 to 0.17)	-0.3	0.787	0.030	2.1	0.33
Inattention/ hyperactivity	3.8 (3.6 to 4.1)	3.7 (3.6 to 3.8)	0.19 (-0.08 to 0.46)	1.4	0.169	0.033	1.7	0.094
Prosocial behavior	8.5 (8.3 to 8.7)	8.5 (8.4 to 8.6)	<-0.006 (-0.18 to 0.16)	-0.1	0.941	-0.039	-3.2 <sup>a</sup>	0.002 <sup>a</sup>

All the analysis were adjusted by sex and age. 2B and 3B indicate 2-back and 3-back, respectively.

<sup>a</sup> Significant after Bonferroni correction.

<sup>b</sup> n=408

<sup>c</sup> n=1967

Adj.:=Adjusted; CI=Confidence interval; d'=Detectability; SD=Standard deviation; SDQ=Strengths and Difficulties Questionnaire.

**Supplementary Table 1.** MRI results.

	<i>Cluster size, ml</i>	<i>x y z</i>	
<b>White Matter Volume ANCOVA</b>			
L Ventral striatum region-anterior temporal	1.2	-29 3 -15	F=7.2
Posterior mesencephalon	1.4	-3 -39 -18	F=6.3
Anterior pons	1.1	3 -12 -30	F=6.9
<b>Post-Hoc High Users &gt; Non-Users</b>			
L Ventral striatum region-anterior temporal	6.1	-30 5 -14	t=3.7
<b>DTI Fractional Anisotropy ANCOVA</b>			
L Lateral Striatum Region	1.4	-28 2 16	F=9.6
<b>Post-Hoc High-Users &gt; Non-Users</b>			
L Lateral striatum region	1.5	-28 4 14	t=3.8
L Ventral striatum region	1.5	-13 17 -6	t=4.0
R Ventral striatum region	1.4	11 19 -7	t=3.7
R Thalamus	1.7	16 -22 11	t=3.9
L Occipital lobe	1.9	-24 -68 4	t=3.7
<i>Functional Connectivity</i>			
<b>Dorsal Putamen Map ANCOVA</b>			
L Motor Cortex	1.2	-50 -4 18	F=7.7
<b>Post-Hoc High-Users &gt; Non-Users</b>			
L Motor Cortex	6.7	-50 -4 18	t=3.9
<b>Ventral Putamen Map ANCOVA</b>			
L Lateral prefrontal cortex	1.9	-42 32 18	F=9.8
Medial frontal cortex	1.3	-2 16 50	F=7.1
<b>Post-Hoc High Users &gt; Non-Users</b>			
L Lateral prefrontal cortex	4.0	-42 34 18	t=4.1
L Motor cortex	1.2	-58 -4 14	t=3.3
<b>Ventral Caudate Map ANCOVA</b>			
Anterior cingulate cortex	4.0	4 12 34	F=10.6
L Parietal operculum	2.2	-58 -4 14	F=13.9
<b>Post-Hoc High-Users &gt; Non-Users</b>			
Anterior cingulate cortex	9.9	6 10 34	t=4.5
R Anterior insula region	6.1	35 16 0	t=4.0
R Anterior insula region	2.0	-40 12 6	t=3.7

x y z, coordinates given in Montreal Neurological Institute (MNI) space. Statistics at corrected threshold PFWE < 0.05 estimated using Monte Carlo simulations.



## 4.4 Study IV:

### *Anomalous White Matter Structure and the Effect of Age in Down Syndrome Patients*

Raquel Fenoll<sup>1</sup>, Jesús Pujol<sup>1,2</sup>, Susana Esteba-Castillo<sup>3</sup>, Susana de Sola<sup>4,5</sup>, Núria Ribas-Vidal<sup>3</sup>, Javier García-Alba<sup>6</sup>, Gonzalo Sánchez-Benavides<sup>4</sup>, Gerard Martínez-Vilavella<sup>1</sup>, Joan Deus<sup>1,7,8</sup>, Mara Dierssen<sup>5,9</sup>, Ramón Novell-Alsina<sup>3</sup>, Rafael de la Torre<sup>4,10,11</sup>

<sup>1</sup> MRI Research Unit, Department of Radiology, Hospital del Mar, Barcelona, Spain

<sup>2</sup> Centro Investigación Biomédica en Red de Salud Mental, CIBERSAM G21, Barcelona, Spain

<sup>3</sup> Specialized Department in Mental Health and Intellectual Disability, Institut d'Assistència Sanitària (IAS), Girona, Catalonia, Spain.

<sup>4</sup> Integrative Pharmacology and Neuroscience Systems Research Group, Hospital del Mar Medical Research Institute, Barcelona, Spain.

<sup>5</sup> Cellular & Systems Neurobiology, Centre for Genomic Regulation (CRG)

<sup>6</sup> Adults with Down Syndrome Department, Hospital Universitario de La Princesa, Madrid, Spain.

<sup>7</sup> Guttmann Neurorehabilitation Institute, Autonomous University of Barcelona, Spain

<sup>8</sup> Department of Clinical and Health Psychology, Autonomous University of Barcelona, Spain

<sup>9</sup> Centro de Investigación Biomédica en Red de Enfermedades Raras (CIBERER), Madrid, Spain.

<sup>10</sup> Centro de Investigación Biomédica en Red de Fisiopatología de la Obesidad y Nutrición (CIBEROBN), Madrid, Spain.

<sup>11</sup> Departament de Ciències Experimentals i de la Salut Universitat Pompeu Fabra (CEXS-UPF), Barcelona, Spain

### **Abstract**

**Background:** Neural tissue alterations in Down syndrome are fully expressed at relatively late developmental stages. In addition, there is an early presence of neurodegenerative changes in the late life stages. The aims of this study were both to characterize white matter abnormalities in the brain of adult Down syndrome patients using diffusion tensor imaging (DTI) and to investigate whether degenerative alterations in white matter structure are detectable before dementia is clinically evident. **Methods:** Forty-five adult non-demented Down syndrome patients showing a wide age range (18-52 years) and a matched 45-subject control group were assessed. DTI fractional anisotropy (FA) brain maps were generated and selected cognitive tests were administered. **Results:** Compared with healthy controls, non-demented Down syndrome patients showed lower DTI fractional anisotropy (FA) in white matter involving the major pathways, but with more severe alterations in the frontal-subcortical circuits. White matter FA decreased with age at a similar rate in both DS and

control groups. **Conclusions:** *Our results contribute to characterizing the expression of white matter structural alterations in adult Down syndrome. However, an accelerated aging effect was not demonstrated, which may suggest that the FA measurements used are not sufficiently sensitive or, alternatively, age-related white matter neurodegeneration is not obvious prior to overt clinical dementia.*

**Keywords:** *neurodegeneration, MRI, diffusion tensor imaging, accelerated aging.*

#### **4.4.1 Introduction**

Although research in Down syndrome has substantially progressed in the understanding of basic mechanisms via which gene overexpression interferes with brain development, there is less information as to the general organization of the adult brain and the effect of age (Wiseman et al., 2015; Ballard et al., 2016). The brain contains billion of neurons that communicate with each other via axons to create complex neural networks. The structural mapping of these networks is essential for understanding brain function (Mori et al., 2006). However, although new imaging techniques have emerged in recent years, our knowledge of structural connectivity in Down syndrome is still limited.

Diffusion tensor imaging (DTI) is a non-invasive method that provides information about the microstructural properties of brain tissue by measuring the magnitude and direction of water molecule diffusion (Jones et al., 2013). In white matter, the diffusion of water molecules is less restricted along the long axis of a group of aligned tissue fibers than perpendicular to it. This condition of directionally-dependent diffusion is referred to as “anisotropic”. The most commonly used measure for diffusion anisotropy is fractional anisotropy (FA), which serves to characterize white matter tracts by mapping directional diffusion restrictions related mainly to fiber density, axonal diameter and myelination degree (Mori et al., 2006; Jones et al., 2013).

DTI has been used to characterize both age-related changes and disease (Madden et al., 2009; Gens et al., 2016; Langley et al., 2016; Adluru et al., 2014). Results from leading studies have shown that age-related changes are associated with FA decreases (Madden et al., 2009). DTI findings have been validated by post-mortem histological studies showing that advanced age is linked to alterations of almost all white matter components. Segments of axons degenerate and swell, myelin becomes less compact and glial cells accumulate cellular debris, form glial scars and increase in number (Marner et al., 2003; Peters et al., 2002; Tang et al., 1997).

In Down syndrome, a number of magnetic resonance imaging (MRI) studies have identified a variety of anatomical (Shapiro et al., 1989; Weis et al., 1991; Kesslak et al., 1994; Paz et al., 1995; White et al., 2003; Teipel et al., 2004) and functional (Pujol et al., 2014a; De la Torre et al., 2016) alterations. The frontal lobes (White et al., 2003; Teipel et al., 2004; Pujol et al., 2014a; De la Torre et al., 2016;

Carducci et al., 2013) and related circuits (Pujol et al., 2014a; De la Torre et al., 2016), as representative of late maturing structures, generally show the most relevant alteration. By contrast, some studies have reported a relative preservation of tissue volume in temporal and parietal regions (White et al., 2003; Carducci et al., 2013; Pinter et al., 2001). Nevertheless, white matter alterations and their functional significance have not been fully characterized using FA measurements. There is one previous study indicating that white matter in adult Down syndrome is abnormal in terms of FA, particularly when dementia is clinically evident (Powell et al., 2014). Nevertheless, the number of Down syndrome patients without dementia was small in this study (n=10) and the study design did not allow a distinction between the effect of aging and pre-existing changes. It is not currently evident whether the neurodegenerative effect on white matter structure is detectable before dementia is expressed. If this were indeed the case, age-related FA changes could serve as early markers of neurodegeneration, which could be of high practical interest given the difficulty in identifying the cognitive deficits related to dementia in a population with significant baseline alteration in cognition (Wiseman et al., 2015; Ballard et al., 2016).

The aims of this study were both to characterize white matter abnormalities in the brain of adult non-demented Down syndrome patients using DTI and to investigate whether degenerative changes in white matter structure are detectable before dementia becomes clinically evident. We predicted that Down syndrome patients would exhibit both widespread FA reduction in white matter and an accelerated aging effect, and that the alteration would be associated with poorer cognitive performance.

#### **4.4.2 Methods**

##### *Participants*

Sixty-eight Down syndrome patients were initially recruited in the study. Candidates were recruited from the community via parent organizations and underwent comprehensive medical, psychiatric, neuropsychological and laboratory evaluation. Individuals with seizure or neurological disease (other than Down syndrome) and non-stable medical conditions were not considered eligible. Participants were selected on the basis of age (18 y.o. upwards), Down syndrome confirmed by karyotype, capability to understand MRI instructions, follow commands and keep still, and also optimal attitude and willingness (patients and parents) to participate. Five patients did not complete the image acquisition protocol and a further 18 subjects were ultimately excluded due to head motion during MRI (see below). The final sample, therefore, included 45 relatively high-functioning Down syndrome patients (29 females, 16 males) with

genotype-confirmed trisomy 21 and a mean  $\pm$  SD age of  $35.3 \pm 10.8$  years, range 18-52 (Table 9). The included and excluded patient subgroups did not significantly differ as to age, performance IQ, semantic fluency and working memory. Excluded patients, however, were predominantly males (6 females, 17 males).

A control group of 45 healthy volunteers were selected matched for age with the patient sample ( $34.6 \pm 10.0$  years, range 19-51) and showing similar sex distribution (Table 9). Participants were either friends or family of subjects participating in the current and other studies, or were recruited from local advertisements. A complete medical interview was carried out to exclude individuals with relevant medical or neurological disorders, cerebrovascular risk factors, substance abuse, psychiatric disease or undergoing medical treatment. In all included control subjects the brain showed a normal appearance on high resolution anatomical MRI scans.

This study was conducted according to the principles expressed in the Declaration of Helsinki. Anxiolytics were not administered in this study. The study protocol was approved by the Clinical Research Ethical Committee of the Parc de Salut Mar of Barcelona. Written informed consent was obtained from parents and control subjects. Verbal or written assent was additionally obtained from Down syndrome patients.

### *Cognitive Testing*

Selected cognitive assessment in all Down syndrome patients included Performance IQ estimated with the Kaufman Brief Intelligent Test, Second Edition (K-BIT) (Kaufman et al., 2004) matrices subtest as a general cognitive assessment, the Wechsler Adult Intelligence Scale (WAIS) backward digit span task as one of conventional measurements of working memory (Lanfranchi et al., 2009), and semantic fluency as a sensitive measurement of verbal output (Del Hoyo et al., 2015).

Additionally, each patient underwent comprehensive neurological and psychiatric history and subsequent tailored neuropsychological testing to clinically rule out the presence of dementia (and mild cognitive impairment- MCI) in terms of cognitive deterioration overlapping with developmental cognitive deficits associated with Down syndrome. Clinical diagnosis (or exclusion) of dementia in Down syndrome by experienced clinicians is recommended as being more accurate and reliable than operative diagnostic tools at a relatively early stage of the disease (Sheehan et al., 2015). Nevertheless, apart from expert clinical diagnosis (by SE and SdS), no patient met International Classification of Diseases (ICD)-10 (World Health Organisation, 1992) or Diagnostic and Statistical Manual of Mental Disorder-IV-Text Revision (DSM-IV-TR) (American Psychiatric Association, 2000) criteria for dementia. A total of 3 patients, however, did meet criteria for mild MCI (Petersen et al., 2011), adapted to adults

with intellectual disability (Krinsky-McHale et al., 2013). The clinical diagnosis of MCI in these 3 cases was established by an experienced neuropsychologist (SEC) on the basis of (i) a report of cognitive impairment by the patient (confirmed by a reliable informant) or by a reliable informant that implies a change from previous capacities, (ii) abnormal performance in the corresponding neuropsychological testing and (iii) no clinically relevant decline in overall adaptive skills and insufficient ICD-10 and DSM-IV-TR criteria for dementia.

**Table 9.** Characteristics of study participants.

	Down Syndrome	Healthy Controls
Age (mean, SD years) <sup>a</sup>	35.3 (10.8)	34.6 (10.0)
Gender (men / women)	16/29	19/26
Medical Background (%)		
Cardiovascular	28%	-
Respiratory	24.4%	-
Metabolic /Endocrine	46.7%	-
Ophthalmological	66.7%	-
Otorhinolaryngological	6.7%	-
Disability Levels (%) <sup>DSM-IV-TR</sup>		
Mild	57.8%	-
Moderate	42.2%	-
Severe	0%	-
Profound	0%	-
Knowledge (%)		
Illiterate	51.1%	-
Read / Write	48.9%	-
Years of Schooling (mean, SD years)	9.3 (3.9)	-
Neuropsychological Assessment:		
Performance IQ, K-IT (mean, SD) <sup>b</sup>	60.5 (8.0)	-
Semantic Fluency (mean, SD) <sup>c</sup>	9.8 (3.4)	-
Digit Span Test (mean, SD) <sup>d</sup>		
Forward Span	2.7 (1.2)	-
Backward Span	1.2 (1.1)	-
Forward Score	3.3 (1.5)	-
Backward Score	1.2 (1.2)	-
Total Score	4.5 (2.3)	-

Key: SD, standard deviation.

<sup>a</sup> Between-group differences for age were not significant ( $p=0.76$ ).

<sup>b</sup> K-BIT, Kaufman Brief Intelligent Test (2nd edition); matrices test.

<sup>c</sup> Semantic fluency, animals in 1 minute.

<sup>d</sup> Digit span, verbal short-term memory test.

### *MRI Acquisition*

A 1.5 Tesla Signa Excite System (General Electric, Milwaukee, WI, USA) equipped with an eight-channel phased-array head coil and single-shot echoplanar imaging (EPI) software was used. Diffusion-weighted scans were obtained using spin-



echo single-shot echo-planar sequences of 25 directions with a B-factor of 1000 s/mm<sup>2</sup>. Acquisition parameters were repetition time 8300 ms; echo time 94 ms; thickness 5 mm, no gap; pulse angle 90°; field of view 26 cm; 128 x 128 acquisition matrix reconstructed into a 256 x 256 matrix, and scan duration was 3 m 52 s. Twenty-six slices were prescribed parallel to the anterior-posterior commissure line covering the whole brain. Participants were instructed to relax, stay awake and lie still.

### *Image Preprocessing*

DTI was processed using Functional MRI of the Brain (FMRIB) Software Library 5.0 (FSL), developed by the Analysis Group at the Oxford Centre for FMRIB (Smith et al., 2004). Diffusion-weighted images were aligned to the B0 image using affine registration and corrected for motion and eddy current distortions (“Eddy Current Correction” option in the FMRIB Diffusion Toolbox [FDT] version 2.0 in FSL). A whole-brain mask, generated with the FSL Brain Extracting Tool, was applied to the DTI images. Subsequently, we estimated fractional anisotropy (FA) maps using FDT in FSL by local fitting of the diffusion tensor model at each voxel (“dtifit”). FA maps were then aligned to a common target (FMRIB58\_FA template) using Tract-Based Spatial Statistics (Smith et al., 2006), re-sliced to a 1mm × 1mm × 1 mm anatomical resolution and normalized to standard MNI space via the FMRIB58\_FA template using the FMRIB’s Non-linear Registration Tool. All the images were visually inspected by a trained researcher before and after the preprocessing steps to avoid the inclusion of poor-quality images. An additional rigorous image quality control was carried out to identify potential effects of head motion on raw images, which involved the visual inspection of each DTI slice for all 25 DTI volumes in all participants. The effect of motion can generally be observed as signal loss in the whole or a part of one slice compared with the other slices. Volumes with slices showing signal loss (greater than ~ 10% compared with slices normal in signal and measured using the conventional MRICron display tool) or residual artifacts were identified by an expert researcher. DTI full examinations showing more than 5 degraded volumes were discarded. A total of 18 participants were removed from the DTI analysis on the basis of this criterion (in addition to 5 cases showing gross image degradation). The final DTI sample involved 45 patients with a mean ± SD of 23.0 (92%) ± 1.6 optimal-quality volumes.

After the full pre-processing, FA maps were transferred to the SPM8 platform and smoothed with an 8 mm Gaussian Kernel to carry out group statistical analyses.

### *Statistical Analyses*

Individual FA maps were included in second-level (group) SPM analyses using 2-sample *t*-test between the 45 Down syndrome patients and 45 healthy controls.

Voxel-wise analyses in SPM were also performed to map the correlation between age and whole-brain FA measurements in both groups. Finally, voxel-wise analyses were performed to map the correlation between individual ratings in the selected cognitive tests and FA measurements in the Down syndrome group. Results were considered significant with clusters of 1.032 ml (1,032 voxels) at a height threshold of  $p < 0.005$ , which satisfied the family-wise error (FWE) rate correction of  $PFWE < 0.05$  according to Monte Carlo simulations (Pujol et al., 2014c).

### 4.4.3 Results

#### *Fractional Anisotropy Differences between Down Syndrome and Control Subjects*

Down syndrome patients showed a widespread white matter FA reduction compared with healthy controls involving parts of the frontal lobes, semioval centers, corpus callosum, external capsule, internal capsule, putamen, thalamus, pyramidal tracts and brainstem (Table 10). Therefore, the major brain pathways were affected, although the alterations were more severe in the frontal-subcortical circuits (Fig. 19). For example, 21 out of 25 sub-clusters showing the largest between-group differences ( $t > 5$ ) involved the frontal-subcortical circuits and only 4 did not ( $\chi^2 = 11.5$ ,  $p < 0.001$ ). In the opposite contrast, a region of significantly larger FA was found in Down syndrome at the temporo-parietal junction (Fig. 19).

#### *Correlations with Cognitive Performance in Down Syndrome*

No significant correlations were found between FA measurements and both performance IQ (K-BIT matrices) and working memory scores (WAIS digit span). By contrast, FA showed significant positive correlation with semantic fluency (i.e., lower FA values, poorer performance) in a variety of regions involving the frontal lobes, corpus callosum, semioval centers, arcuate fasciculus, caudate nucleus, external capsule, thalamus and hippocampus (Fig. 20 and Table 10).

#### *Age-Related Effect on Fractional Anisotropy*

In both groups, FA decreased as a function of age. Healthy controls showed FA age-related changes in the frontal lobes, corpus callosum, basal ganglia (caudate), thalamus, semioval centers, and pyramidal tracts (Fig. 21 and Table 10). In Down syndrome, significant correlations with age were found in the frontal lobes, left arcuate fasciculus, right external capsule and hypothalamus (Fig. 21 and Table 10). We found no significant between-group differences relating to the strength

of the correlations (i.e., no significant correlation interaction), which is illustrated in Fig. 22.

#### 4.4.4 Discussion

Our results indicate that white matter in Down syndrome patients showed generally lower FA compared with healthy participants. The most affected structures were the frontal lobes, subcortical white matter and some parts of the brainstem. Lower FA in Down syndrome was associated with poorer semantic fluency, which illustrates a degree of correspondence between white matter integrity and performance in patients. White matter FA did indeed decrease with age in both study groups, but we did not find the expected accelerated age effect in the Down syndrome group.

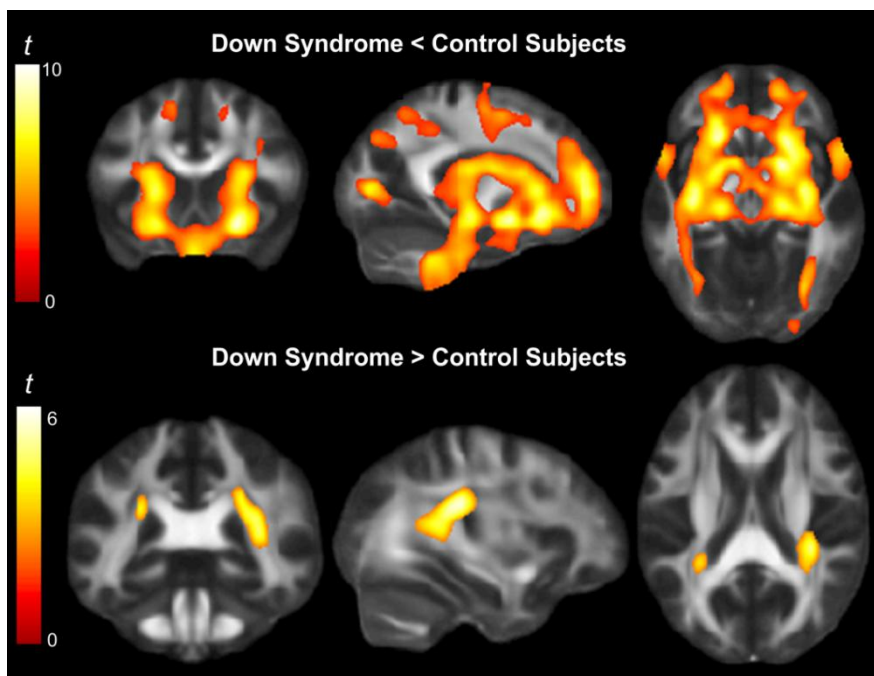


**Figure 19.** Fractional anisotropy (FA) differences between Down syndrome and control subjects. Down syndrome patients showed a general pattern of lower FA in white matter, although the changes were more severe in the frontal-subcortical circuits (TOP). By contrast, regions with significantly higher FA in Down syndrome patients than controls were limited to the temporo-parietal junction (BOTTOM). The right hemisphere corresponds to the right side of axial and coronal images.

FA is a tissue measurement primarily independent of tissue volume that may generally express the extent to which an anatomical structure is composed of white matter tracts showing one dominant direction. In brain regions containing tracts with a single direction, FA increases as a result of brain maturation (Jones et al., 2013; Douaud et al., 2011). In this context, our results indicate that Down syndrome subjects have a less developed white matter structure than controls in many white matter tracts. This is a remarkable finding due to the few studies based on DTI in non-demented Down syndrome patients. Our results are consistent with studies of brain anatomy showing generally reduced white matter volumes in Down syndrome compared with healthy controls (Weis et al., 1991; White et al., 2003). However, our data may further contribute to characterizing white matter alterations in Down syndrome in that they would indicate that the changes are not limited to general volume reductions, but may also implicate a less developed structural connectivity pattern.

Although FA abnormalities involved the major brain pathways, the frontal-subcortical circuits showed more severe alterations. As a general trend, the results are consistent with the profile of cognitive deficits in Down syndrome typically progressing with deep impairment in language production and executive functions, which are cognitive domains notably dependent on the frontal lobes (Chapman et al., 2000; Lott et al., 2010; Grieco et al., 2015).

We also observed that Down syndrome individuals showed higher FA at the temporo-parietal junction. This observation is partly consistent with studies reporting relatively larger white matter volume in temporal and parietal regions (White et al., 2003; Carducci et al., 2013; Pinter et al., 2001), which may reflect a particular abnormality in white matter maturation. Indeed, in complex structures with tracts crossing in different directions (as in the temporo-parietal junction), higher FA may paradoxically denote less mature or less structured tissue (Jones et al., 2013; Douaud et al., 2011). The multimodal temporo-parietal junction is certainly a complex area in terms of white matter connectivity. In Down syndrome, the pattern of connectivity would seem to be incomplete at this level. This event appears in parallel with a more general FA reduction in several other brain structures. In this general effect, the alteration may denote poor development of white matter pathways showing a predominant direction or a simpler structure.

A relevant problem in evaluating cognitive abilities in Down syndrome is the notable lack of consistency and reproducibility of ratings in some neuropsychological tests (Silverman et al., 2010). We used the K-BIT matrices subtest to estimate general intelligence, the digit span to evaluate working memory and semantic verbal fluency to test verbal output. Only verbal fluency was associated with FA alterations in Down syndrome in a rather general manner, thus indicating a certain parallelism between the identified pattern of white matter alterations and cognitive performance. Nevertheless, we failed to find similar associations with performance IQ and working memory. We now, a

posteriori, consider that these tests are not perhaps the most suitable to reliably predict brain alterations in Down syndrome. The development of more specific and sensitive tools to evaluate cognition in Down syndrome, as recently proposed (De Sola et al., 2015), could be helpful in future studies.

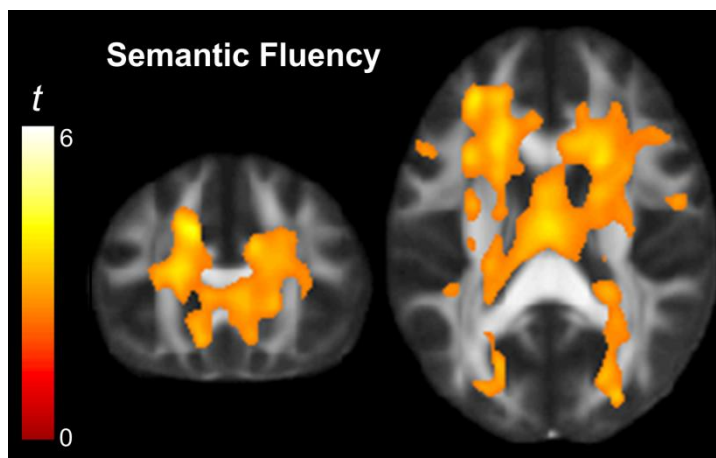


**Figure 20.** Significant positive correlation between semantic fluency and fractional anisotropy (FA) measurements in the direction of lower FA values, the poorer performance. The right hemisphere corresponds to the right side of the images.

Our study did not find significant between-group differences in age-related white matter changes. That is to say, although both groups suffered a variation of white matter structure with age, there were no between-group differences. In our Down syndrome group, none of the participants were diagnosed with Alzheimer's disease and only 3 patients had MCI according to clinical criteria. Therefore, we were unable to demonstrate the anticipated premature aging effects on white matter using FA measurements, which contrast with positive findings in studies on familial Alzheimer's disease (summarized in a recent report (Sánchez-Valle et al., 2016)). This brings us to the conclusion that DTI FA measurements are perhaps not sufficiently sensitive to capture brain pathology related to the acceleration of aging in subclinical populations. Alternatively, age-related white matter neurodegeneration may be a later event, which is not obvious prior to overt clinical dementia. In the study by Powell et al. (Powell et al., 2014), FA alterations were indeed more evident when dementia was clinically evident in Down syndrome patients.

It is important to mention, however, that the identified FA decrease with age in the control group is not the expression of the white matter structure involution or degeneration occurring in the senile brain (also expressed in the form of additional FA decrease (Madden et al., 2012), as age in the control group showed

a mean of 34.6 years and range 19-51 years. Age-related FA changes may better reflect the normal active evolution of white matter tracts in the adult brain. Our findings are consistent with previous studies in normal populations showing FA peaks from early 20s to late 30s and subsequent subtle FA decreases starting around mid-adulthood with notably different timings across different tracts (Yap et al., 2013). FA studies in normal populations further emphasize early proposals that white matter remodeling is a biological process active over the entire lifespan (Yakovlev et al., 1961; Pujol et al., 1993).

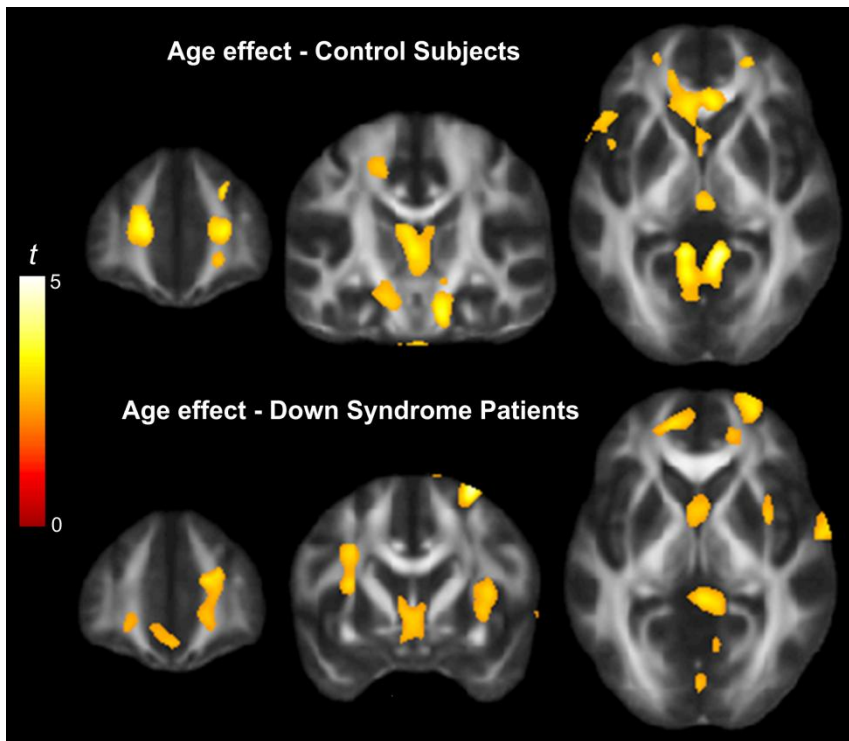


**Figure 21.** Age-related effect on fractional anisotropy (FA). FA decreased as a function of age in both control subjects and Down syndrome patients. No significant between-group differences were identified.

One challenge in the assessment of DTI is the control of head-motion effects on the measurement, which may be relevant in low-performance populations. We have considered this issue carefully and adopted several means to rigorously control such effects. We decided to exclude cases with detectable image degradation, as no correction procedure is wholly efficient once the images have been acquired. The regular use of MRI practice sessions with mock scanners may minimize the problem in future studies. A post-hoc analysis on DTI using less

rigorous exclusion criteria (n=54) showed similar but weakened DTI results, indicating that the data obtained in the more selective sample (n=45) was most probably not due to motion effects. Although accurate control of head motion effects may be strength of the study, it is important to mention that strict participant selection is also a limitation. In this context, our findings cannot generalize to all Down syndrome population, but conclusions should be limited to relatively highly performing individuals. A final limitation relates to using a 1.5-T system, as opposed to a 3-T system with higher MRI signal.

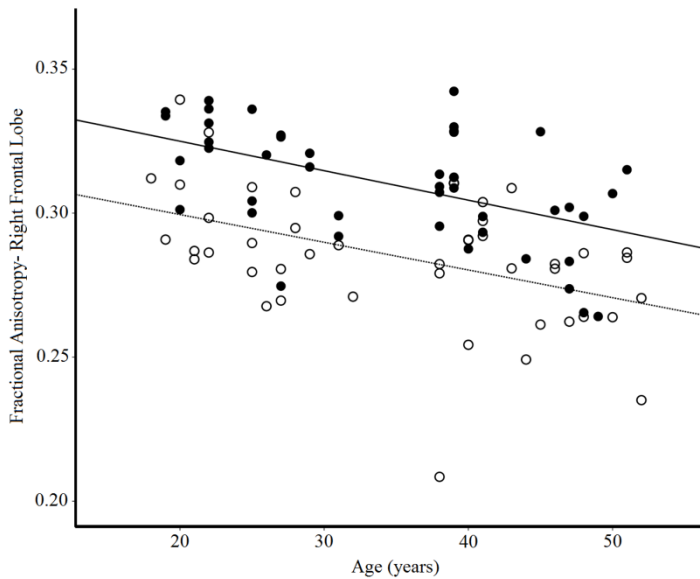


**Figure 22.** Correlation between age and FA at the right frontal lobe. Down syndrome patient data are represented by the dashed line and open circles, and control subject data by solid line and solid circles.

#### 4.4.5 Conclusions

Results from our imaging approach indicate that the brain in relatively high-functioning Down syndrome patients shows generally lower FA, suggesting underdevelopment of white matter tracts. The altered white matter structure was associated with poorer performance at neuropsychological assessment. Finally, age-related reduction of FA did not significantly differ between the control group and our non-demented Down syndrome patients. Probably, the adopted DTI approach was not sufficiently sensitive to detect alterations related to the dementia process in subclinical stages of Alzheimer-like pathology. Further studies should focus on the temporal evolution of white matter structure

involution and the development of dementia in Down syndrome adults and provide biomarkers for detecting early signs of premature aging.

## **Funding**

This study was supported in part by the Spanish Government (Grants SAF2010-19434, PI11/00744 and PI/120219) and the Jérôme Lejeune Foundation, Paris.

## **Acknowledgements**

We thank the Fundació Catalana de Síndrome de Down (FCSD, Spain) for their assistance with the recruitment of participants and the TESDAT Study Group members for their contribution (Lancet Neurology, May 12, 2016 [http://dx.doi.org/10.1016/S1474-4422\(16\)30034-5](http://dx.doi.org/10.1016/S1474-4422(16)30034-5)). We thank the Agency of University and Research Funding Management of the Catalonia Government for their participation in the context of Research Groups SGR 2009/1450 and SGR 2009/718.



**Table 10.** Diffusion Tensor Imaging (DTI) fractional anisotropy (FA) results.

	<i>Cluster size, ml</i>	<i>x y z</i>	<i>t (r)</i>	<i>t* (r)</i>
<b>Down &lt; Controls</b>				
R semioval center	354.0*	18 -7 53	6.3	5.9
L semioval center	*	-13 2 51	6.1	5.7
R frontal lobe	*	20 45 15	7.9	7.5
L frontal lobe	*	-19 47 13	8.2	7.8
Corpus callosum	*	4 30 -3	4.3	4.0
R putamen	*	24 13 16	7.4	7.0
L putamen	*	-21 11 17	8.0	7.7
R thalamus	*	10 -9 17	7.2	7.0
L thalamus	*	-11 -11 18	8.4	8.3
R pyramidal tract	*	19 -18 -7	7.9	7.4
L pyramidal tract	*	-19 22 -6	9.2	8.7
Brainstem	*	1 -32 -23	8.3	7.8
<b>Down &gt; Controls</b>				
Temporo-parietal junction	6.7	37 -42 12	5.9	5.9
<b>FA correlation – Semantic fluency in DS</b>				
R frontal lobe	148.7*	27 48 4	4.4 (0.6)	4.2 (0.6)
L frontal lobe	*	-14 24 33	4.9 (0.6)	4.6 (0.5)
Corpus callosum	*	13 27 3	3.3 (0.5)	3.3 (0.5)
R semioval center	*	12 2 36	3.5 (0.5)	3.3 (0.5)
L semioval center	*	-11 -2 43	4.5 (0.6)	4.3 (0.6)
L arcuate fasciculus	*	-30 13 14	5.4 (0.6)	5.2 (0.6)
R caudate nucleus	*	13 27 3	3.3 (0.5)	3.3 (0.5)
L caudate nucleus	*	-19 20 18	4.4 (0.6)	4.5 (0.6)
R external capsule	*	35 1 -2	4.4 (0.6)	4.2 (0.6)
L external capsule	*	-30 13 14	5.3 (0.6)	5.2 (0.6)
R thalamus	*	8 -23 8	3.4 (0.5)	3.8 (0.5)
L thalamus	*	-3 -21 10	4.0 (0.5)	4.0 (0.5)
<b>FA correlation – Age in healthy controls</b>				
R frontal lobe	704.1*	24 48 7	4.2 (-0.4)	4.2 (-0.4)
L frontal lobe	*	-15 46 12	4.4 (-0.4)	4.4 (-0.4)
Corpus callosum	*	5 30 4	4.0 (-0.4)	4.0 (-0.4)
Thalamus	*	-1 -20 7	3.8 (-0.4)	3.7 (-0.4)
R pyramidal tract	*	13 -20 -25	4.0 (-0.4)	4.0 (-0.4)
L pyramidal tract	*	-15 -26 -13	3.5 (-0.4)	3.5 (-0.4)
<b>FA correlation – Age in DS patients</b>				
R frontal lobe	4.0	19 42 17	3.8 (-0.4)	3.3 (-0.3)
L arcuate fasciculus	2.4	-31 6 30	3.5 (-0.4)	3.2 (-0.3)
R external capsule	5.5	35 11 -2	3.0 (-0.3)	3.0 (-0.3)
Hypothalamus region	1.9	0 6 -2	3.4 (-0.3)	3.4 (-0.4)

Key; DS, Down Syndrome; \* Same cluster; *t\**, without 3 patients with mild cognitive impairment-MCI. *x y z* coordinates given in Montreal Neurological Institute (MNI) space. Statistics at corrected threshold  $P_{FWE} < 0.05$  according to Monte Carlo simulations.

## 4.5 Study V:

### ***A Longitudinal Study of Brain Anatomy Changes preceding Dementia in Down Syndrome***

Jesus Pujol, MD<sup>1,2</sup>; Raquel Fenoll, MSc<sup>1</sup>, Núria Ribas-Vidal, MSc<sup>3</sup>; Gerard Martínez-Vilavella, MSc<sup>1</sup>; Laura Blanco-Hinojo, PhD<sup>1,2</sup>; Javier García-Alba, PhD<sup>4</sup>; Joan Deus, PhD<sup>1,5</sup>; Ramón Novell, MD<sup>3</sup>; Susanna Esteba-Castillo, PhD<sup>3</sup>

<sup>1</sup> MRI Research Unit, Department of Radiology, Hospital del Mar, 08003 Barcelona, Spain

<sup>2</sup> Centro Investigación Biomédica en Red de Salud Mental, CIBERSAM G21, 08003 Barcelona, Spain

<sup>3</sup> Specialized Service in Mental Health and Intellectual Disability, Institut Assistència Sanitària (IAS), Parc Hospitalari Martí i Julià, 17190 Girona, Spain.

<sup>4</sup> Adults with Down Syndrome Department, Hospital Universitario de La Princesa, 28006 Madrid, Spain.

<sup>5</sup> Department of Clinical and Health Psychology, Autonomous University of Barcelona, 08193 Barcelona, Spain

#### ***Abstract***

**Objective:** We longitudinally assessed Down syndrome individuals at the age of risk to develop dementia to measure changes in brain anatomy and their relationship to cognitive impairment progression. **Methods:** Forty-two Down syndrome individuals were initially included, of whom 27 (mean age 46.8 years) were evaluable on the basis of finishing the 2-year follow-up and success in obtaining good quality MRI exams. Voxel-based morphometry was used to estimate regional brain volumes at baseline and follow-up 3D anatomical images. Longitudinal volume changes for the group and their relationship with change in general cognitive status and change in specific cognitive domains were mapped. **Results:** As a group, significant volume reduction was identified in the substantia innominata region of the basal forebrain, hippocampus, lateral temporal cortex and left arcuate fasciculus. Volume reduction in the substantia innominata and hippocampus was more prominent in individuals that changed the clinical status from cognitively stable to mild cognitive impairment or dementia during the follow-up. Of relevance, longitudinal memory score change was specifically associated with volume change in the hippocampus, prospective memory with prefrontal lobe and verbal comprehension with language-related brain areas. **Conclusions:** Results are notably concordant with the well-established anatomical changes signaling the progression to dementia in Alzheimer's disease, despite dense baseline pathology that developmentally accumulates in Down syndrome. This communality supports the potential value of Down syndrome as genetic model of Alzheimer's neurodegeneration and may serve to further claim that Down syndrome patients are full candidates to benefit from treatment research in Alzheimer's disease.

### 4.5.1 Introduction

Down syndrome (DS) or chromosome 21 trisomy is the most common genetic cause of intellectual disability (Ballard et al., 2016). In addition to interference with brain development, aging is also disturbed in DS with an early presence of neurodegenerative changes (in virtually all DS individuals from 40 years of age) and clinical dementia in up to 70% of cases by the age of 60 (Dekker et al., 2015; Wiseman et al., 2015). The brain in older DS individuals displays many of the neuropathological features found in Alzheimer's disease (Head et al., 2016). This communality is of capital importance as it indicates a direct link between a genetic anomaly and neurodegeneration that may potentially contribute to elucidate the pathogenesis of Alzheimer's disease (Wiseman et al., 2015).

Previous neuroimaging research is prominent in indicating that demented DS patients indeed show brain alterations in systems with typical degeneration in Alzheimer's disease (Emerson et al., 1995; Teipel and Hampel, 2006; Haier et al., 2008; Beacher et al., 2009; Powell et al., 2014; Sabbagh et al., 2015; Rafii et al., 2015; Lin et al., 2016). Nevertheless, existing cross-sectional studies are still not conclusive in distinguishing baseline DS dense brain pathology established during brain development from ongoing degenerative changes at time of progression to dementia. We present a longitudinal study on DS patients at the age of risk to develop dementia aimed at measuring changes in brain anatomy and their relationship to cognitive deterioration.

### 4.5.2 Methods

#### *Participants*

Forty-two DS individuals were initially included in the study. Candidates were recruited from the community via parent organizations and were selected on the basis of age (40 years old upwards), DS confirmed by karyotype, capability to understand and follow MRI instructions, and also optimal attitude and willingness (participants and parents) to participate. Individuals with non-stable medical conditions were not considered eligible. Eight participants were excluded due to head motion during baseline MRI, 3 participants were lost in the follow-up and 4 more were excluded due to head motion during follow-up MRI. The final evaluable sample for MRI analysis included 27 relatively high-functioning DS individuals (15 females, 12 males) with genotype-confirmed trisomy 21 and a mean  $\pm$  SD age of  $46.8 \pm 5.6$  years, range 40-63 years (Table 11). The included and excluded participant subgroups did not significantly differ as to age, sex distribution, performance IQ and specific neuropsychological testing.

This study was conducted according to the principles expressed in the Declaration of Helsinki. The study protocol was approved by the Clinical Research Ethical Committee of the Parc de Salut Mar of Barcelona. Written informed consent was obtained from parents. Verbal or written assent was additionally obtained from Down syndrome individuals.

**Table 11.** Characteristics of study participants and cognitive testing.

	Primary Sample (n=42)		Final Sample (n=27)	
Age (mean, SD years) <sup>a</sup>	46.0 (5.3)		46.8 (5.6)	
Gender (men / women)	21/21		12/15	
Medical Background (%)				
Cardiovascular	28.6%		37.0%	
Respiratory	11.9%		11.1%	
Metabolic /Endocrine	57.1%		48.1%	
Ophthalmological	71.4%		70.4%	
Otorhinolaryngological	4.8%		7.4%	
Disability Levels (%) <sup>DSM-IV-TR</sup>				
Mild	33.3%		29.6%	
Moderate	66.7%		70.4%	
Severe	0%		0%	
Profound	0%		0%	
Performance IQ, K-IT (mean, SD) <sup>a</sup>	59.3 (9.2)		60.7 (9.0)	
Knowledge (%)				
Illiterate	33.3%		29.6%	
Read/Write	66.7%		70.4%	

	Primary Sample (n=42)		Final Sample (n=27)	
<b>Cognitive Testing (mean, SD)</b>	Baseline	Follow-up	Baseline	Follow-up
Memory-Word List Learning	24.3 (7.7)	25.8 (8.8)	25.7 (7.2)	25.8 (8.5)
Verbal Comprehension	8.9 (2.4)	9.2 (2.4)	9.0 (2.6)	9.2 (2.0)
Block Construction	6.2 (2.3)	5.2 (1.9)*	6.1 (2.3)	5.2 (1.9)*
Object Recognition	3.3 (1.5)	3.8 (1.3)	3.2 (1.3)	3.8 (1.2)
Prospective Memory	3.0 (1.4)	2.6 (1.9)	3.2 (1.4)	2.7 (1.7)

SD, standard deviation. <sup>a</sup>K-BIT, Kaufman Brief Intelligent Test (2nd edition); matrices test.

\*significant score reduction at  $p < 0.01$ .

### *Clinical Assessment*

Each participant underwent comprehensive medical, neurological and psychiatric history and subsequent tailored neuropsychological testing to clinically establish (or rule out) the diagnoses of mild cognitive impairment (MCI) and dementia in terms of cognitive deterioration overlapping with developmental cognitive deficits associated with DS. The diagnosis of MCI and dementia was based on expert clinical judgment as it is recommended in DS (Sheehan et al. 2015; Krinsky-McHale and Silverman, 2013). Operatively, a diagnosis of MCI was established on the basis of (i) a report of cognitive

impairment by the patient (confirmed by a reliable informant) or by a reliable informant that implies a change from previous capacities, (ii) abnormal performance in the corresponding neuropsychological testing and (iii) no clinically relevant deterioration in adaptive skills and general cognition (Fenoll et al., 2017). The diagnosis of dementia was established when the patient met MCI criteria (i) and (ii), and (ii) showed perceptible worsening in adaptive skills in association with memory impairment and at least one of the following: aphasia, apraxia, agnosia or disturbance in executive functioning. At baseline, 2 DS individuals met MCI criteria and no one for dementia.

### *Specific Neuropsychological Testing*

To establish the correlation between regional brain volume changes over time and cognitive decline, one neuropsychological test was selected for each major Alzheimer's disease domain: memory impairment, aphasia, apraxia, agnosia and disturbance in executive functioning:

**Memory.** A version of the Rey Auditory-Verbal Learning Test (Geffen et al., 1990) adapted for people with intellectual disability (Esteba-Castillo et al., 2017) was used. The test measures learning, delayed recall and recognition. Only performance on learning was used. Participants were read a list of 12 words and were asked to evoke as many words as they could remember. The same list was repeated over five trials. Word list learning over trials was measured as sum of recalled words on trials 1 to 5.

**Verbal Comprehension - Verbal Abstract Reasoning.** This test combines an adapted version of the conventional "similarities" subtest (4 items) used in many intelligence batteries (participants are given two words or concepts and have to describe how they are similar) with comprehension of verbal sentences (5 items) reflecting different social situations (Esteba-Castillo et al., 2017). Each response was rated as 0 (incorrect), 1 (partial) or 2 (correct) with total maximum scoring of 18.

**3D Block Construction.** As a measurement of constructional apraxia, we used a variation of the cubes subtest of the Developmental Neuropsychological Assessment-NEPSY battery (Korkman et al., 1998) adapted for people with intellectual disability (Esteba-Castillo et al., 2017). The participant used hand movements to construct 3D block patterns with methacrylate cubes to match a model. A total of 10 models were consecutively presented and scores of 1 were given for each correct construction (maximum score, 10).

**Object Recognition.** The recognition of objects (unusual views) subtest of the Cambridge Examination for Mental Disorders of Older People with Down's

syndrome and Others with Intellectual Disabilities-CAMDEX-DS (Ball et al., 2006) validated for Spanish population was used (Esteba-Castillo et al., 2013). The test involves the recognition of objects (6 items) on pictures taken from unusual angles. The number of correct answers was registered.

**Prospective Memory.** This task requires the interaction of executive and mnemonic components to remember intentions (Fish et al., 2010). We used two prospective memory items of the Rivermead Behavioral Memory Test (RBMT) (Wilson et al., 1985) adapted for people with intellectual disability (Esteba-Castillo et al., 2017). In the first situation, the participant had to remember, after a delay of 20 m with interference, to ask for setting the next hospital appointment at the moment the explorer gives a cue. In the second situation, the participant had to claim a previously hidden object also after a given cue. Scores are lower when the number of cues given in each situation is higher (i.e., higher scores indicates better performance). The sum of scores from both situations was used.

### *MRI acquisition*

A 1.5-Tesla Signa Excite system (General Electric, Milwaukee, WI) equipped with an eight-channel phased array head coil and single-shot echoplanar imaging (EPI) software was used. High-resolution 3D anatomical images were obtained using an axial T1-weighted three-dimensional fast spoiled gradient inversion recovery prepared sequence. A total of 134 contiguous slices were acquired with inversion time 400 ms, repetition time 11.9 msec, echo time 4.2 msec, flip angle 15°, field of view 30 cm, 256 x 256 pixel matrix, and slice thickness 1.2 mm. Each participant received an MRI practice session with a specifically designed mock scanner to allow habituation and minimize the probability of head motion during actual MRI sessions.

### *Image Pre-Processing*

All the anatomical images were visually inspected before analysis by a trained operator to detect artefacts and any motion effect. Eight participants were discarded at baseline and 4 at follow-up as a result of poor image quality. Gray and white matter tissue volumes were estimated at a voxel level using Statistical Parametric Mapping (SPM). SPM voxel-based morphometry (VBM) DARTEL algorithms were used with the following processing steps: segmentation of anatomical images into gray and white matter tissue probability maps in their native space; estimation of the deformations that best align the images together by iteratively registering the segmented images with their average; finally, generating spatially normalized and smoothed segmentations (10x10x10 mm FWHM) using the deformations estimated in the previous step. The analyses were performed with scaling by Jacobian determinants (estimates of volume

change during the normalization) to consider tissue volume. Normalized images were finally transformed to the standard SPM template, re-sliced to 1.5 mm resolution in Montreal Neurological Institute (MNI) space.

### *Image Analysis*

As in a previous longitudinal assessment of brain volume changes over time (Soriano-Mas et al., 2011), we generated difference images (baseline voxel values minus follow-up voxel values) for both gray matter and white matter segments that served to map regional volume change in the whole sample (using one-sample t-test) and to compare the degree of anatomical change between individuals with and without cognitive deterioration during follow-up (using two-sample t-test). In addition, we estimated voxel-wise the correlations between volumetric longitudinal changes (i.e., the generated difference images) and cognitive longitudinal changes (baseline cognitive scores minus follow-up cognitive scores) using linear regression in SPM.

Results were considered significant with clusters of 1,701 ml (504 voxels) at a height threshold of  $P < 0.005$ , which satisfied the FWE (family wise error) rate correction of  $P_{FWE} < 0.05$  according to Monte Carlo simulations. Results below this threshold are also reported (FWE small volume corrected) for the hippocampus, which is a primary interest anatomical structure with a narrow section diameter.

## **4.5.3 Results**

### *Behavioral Results*

Study follow-up had mean duration of 23 months (SD, 2 months). Five participants changed their clinical status from cognitively stable to MCI and 2 more from cognitively stable to dementia. Therefore, 26% of cases ( $n=7$ ) in our sample showed clinical evidence of cognitive impairment progression in a period of approximately 2 years. In the whole group, score change for the selected cognitive tests was not significant, except for constructional apraxia assessment with Block Construction (Table 11).

### *Imaging Results*

Significant gray matter volume reduction over time in the whole DS sample was identified in a region located at the basal forebrain and ventral aspect of the basal ganglia involving the substantia innominata, in the right orbitofrontal cortex and in the lateral aspect of the right temporal lobe (Fig. 23 and Table 12). Changes in the homologous temporal lobe region in the left hemisphere were not significant,

although volume reduction was present at a lower cluster size threshold (Table 12). Significant white matter volume reduction was identified in a region implicating the right hippocampus and in the left arcuate fasciculus (Fig. 23 and Table 12).

DS individuals with cognitive impairment progression showed significant gray matter volume reduction compared with the remaining sample also in the region of the substantia innominata, and in the left hippocampus (Fig. 24 and Table 12). Although less extensive, volume reduction in the substantia innominate region notably overlapped with changes in the whole sample. Figure 1 shows a box-plot of volume reduction in individuals with and without cognitive impairment progression at the brain coordinate showing the largest (peak) volume reduction in the whole sample.

In the analysis of correlations between anatomical and cognitive longitudinal change, the following results were observed: a correlation between memory score reduction and gray matter volume reduction in a small portion of the left hippocampus and amygdala. A correlation between verbal comprehension score reduction and gray matter volume reduction within the Wernicke area (and related auditory cortex) and volume reduction in part of the left arcuate fasciculus. A correlation between prospective memory score reduction and both gray and white matter volume reduction in an extensive portion of the prefrontal lobe bilaterally, bilateral gray matter volume reduction in the paracentral lobule, and bilateral white matter volume reduction involving inferior temporal cortex and the hippocampus (Fig. 25 and Table 12).

All these associations were observed in the expected positive direction (i.e., tissue volume reduction in parallel with cognitive score reduction). In addition, the analysis generated two results in the opposite direction involving a negative correlation between memory score change and volume change in the right thalamus, and between object recognition score change and volume change in white matter adjacent to the left caudate nucleus (Table 12).

#### **4.5.4 Discussion**

Despite challenges inherent to longitudinal assessments particularly in individuals with a degree of intellectual disability, our study shows that identifying brain anatomical changes that precede dementia in DS is feasible. Significant volume reduction after two years was identified in the substantia innominata region of the basal forebrain, the hippocampus, lateral temporal cortex and left arcuate fasciculus. Volume reduction in the substantia innominata and hippocampus was more prominent in the individuals showing variation in



their general cognitive status during this period. Score change in different cognitive domains correlated with anatomical changes in specific brain systems. Of relevance were the associations of longitudinal change in the domain of memory with hippocampus, prospective memory with the prefrontal lobe and verbal comprehension with language-related brain areas.

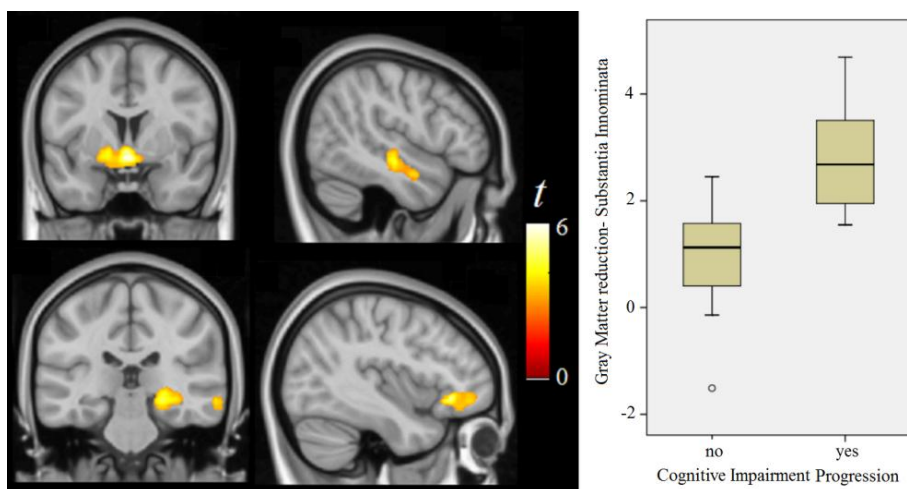


**Figure 23.** Significant gray matter (top images) and white matter (bottom images) volume reduction over time in the whole DS sample. The box-plot corresponds to volume reduction (arbitrary units) for individuals with and without changes in their cognitive status at the brain coordinates showing the greatest (peak) volume reduction in the whole sample. The right side of coronal views corresponds to the right hemisphere. The sagittal image at the figure top corresponds to the right hemisphere and the sagittal image at the figure bottom to the left hemisphere.

Neurons of the cholinergic basal forebrain show neurofibrillary tangles in the earliest and presymptomatic stages of Alzheimer’s disease (Theofilas et al., 2015; Mesulam et al., 2004; Mesulam 2013), and both neurofibrillary tangle accumulation and neuronal loss are parallel to the cognitive decline (Mesulam et al., 2004; Liu et al., 2015). The nucleus basalis of Meynert is the major element of the cholinergic complex located at the region of the substantia innominata below the anterior commissure and basal ganglia (Liu et al., 2015). In young persons with DS, the nucleus basalis contains fewer neurons than controls and the difference may accentuate in older individuals (Casanova et al., 1985, Mann et al., 1984) in whom developmental and degenerative changes are combined. In our study, we have established a direct link between basal forebrain volume reduction and cognitive decline in the early stages of dementia in DS. So, basal forebrain degeneration may appear to be a marker of progression to dementia also in DS.

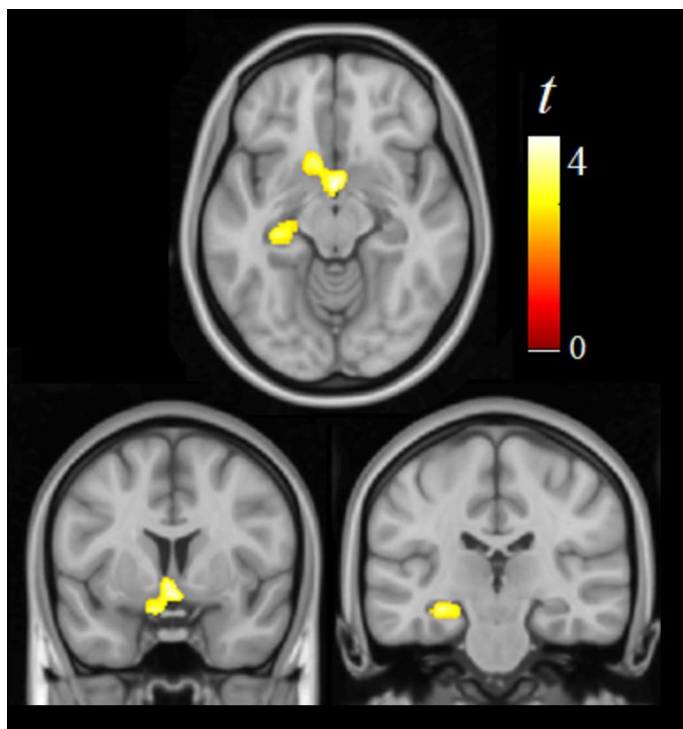


**Figure 24.** Regions showing significant gray matter volume reduction in DS individuals with clinical evidence of cognitive impairment progression compared with the remaining sample. The right side of coronal views corresponds to the right hemisphere.

Hippocampal volumetry is one of the most validated, accessible and widely used biomarkers in Alzheimer’s disease, capable to reliably predict time-to-progression from mild cognitive impairment to Alzheimer’s dementia (Mak et al., 2016; Jack et al., 2010). In cross-sectional studies, the hippocampus volume is consistently smaller in young DS individuals compared with control subjects. However, volume alteration again is more important in older and demented individuals superimposed to the developmental deficiency (Teipel and Hampel, 2006; Aylward et al. 1999; Beacher et al., 2009; Krasuski et al., 2002). Our results indicate that longitudinal assessment of hippocampal volume in DS may sufficiently distinguish the degenerative component from baseline alterations. We are aware of only one longitudinal assessment of brain volumetry published in DS, which precisely focused on the hippocampus. In the follow-up study by Aylward et al. (1999), changes in hippocampus volume over time were not statistically significant for either demented (n= 6) or non-demented (n= 13) DS subjects probably due to the small sample size.

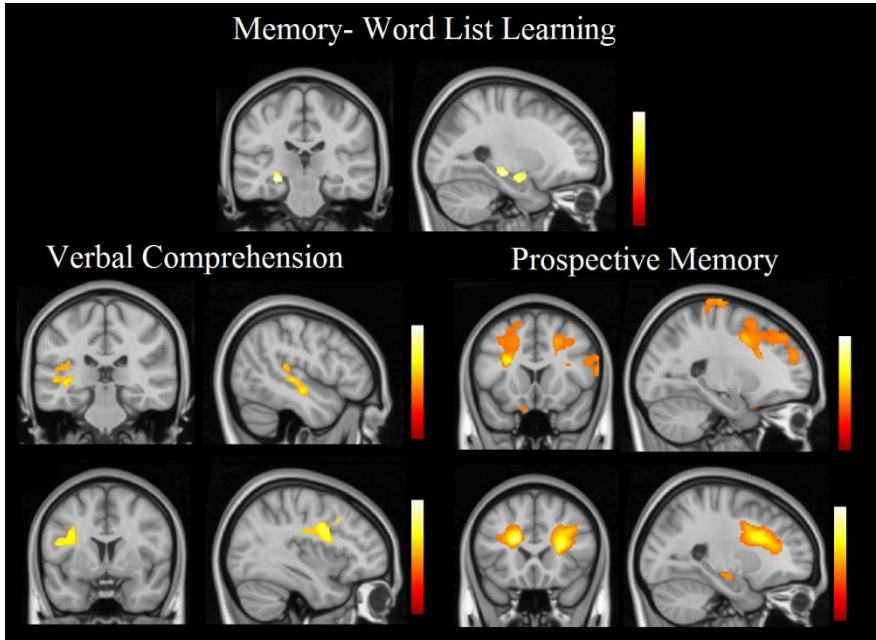


**Figure 25.** Correlations between anatomical and cognitive longitudinal changes. The right side of coronal views corresponds to the right hemisphere and all sagittal views correspond to the left hemisphere.

A set of neocortical areas with relevant vulnerability to Alzheimer’s disease neuropathology have collectively been called the cortical signature of Alzheimer’s disease based on that cortical thinning relates to symptom severity in the earliest stages (Dickerson et al., 2009) and clinical progression (Verfaillie et al., 2016), and may even be detectable in asymptomatic individuals nearly a decade before dementia (Dickerson et al., 2011). Overall, the major elements of the cortical Alzheimer’s disease signature were the superior prefrontal, inferior parietal and anterior temporal cortices. Previous research has shown that individuals with DS have a significantly greater age-related reduction in volume compared with normal control subjects in regions corresponding broadly to the vulnerable Alzheimer’s disease cortical signature with a particularly large effect in the prefrontal cortex (Beacher et al., 2010). Our study shows a significant association between longitudinal volume change in an extensive portion of the superior aspect of the prefrontal lobe and prospective memory score change.

Prospective memory is a relatively complex task requiring the interaction of mnemonic and executive components to remember intentions after delay and interference (Fish et al., 2010). Neuroimaging studies in normal subjects have shown a consistent activation of the prefrontal lobe during prospective memory paradigms (Burgess et al., 2011). Our results suggest that prospective memory

could reflect the functional status of the prefrontal lobe during the progression to dementia in DS, despite being one of the most developmentally affected brain structures (Pujol et al., 2014a; Fenoll et al., 2017). Longitudinal behavioral studies also support that frontal lobe symptoms, in the form of disturbance in executive functioning, are early signs of dementia in DS (reviewed in Dekker et al., 2015).

The only apparently non-consistent findings in our study were the negative correlation between volume change in the thalamus and verbal comprehension score change, and between white matter adjacent to the left caudate nucleus and visual recognition. We consider that they may correspond to spurious associations, but paradoxically larger (Fortea et al., 2010) or relatively preserved (Benzinger et al., 2013) caudate nucleus volumes were also identified in mutation carriers in familial AD before dementia.

One challenge in MRI studies in populations with intellectual disability is avoiding excessive head motion during the acquisition. In this sample we used MRI practice sessions with a specifically designed mock scanner to minimize the problem. In addition, we decided to exclude cases with detectable image degradation, as no correction procedure is wholly efficient once the images have been acquired. Although accurate control of head motion effects may be strength of the study, strict participant selection is also a limitation. In this context, our findings cannot generalize to all DS, but conclusions should be limited to relatively highly performing individuals. A final limitation relates to using a 1.5-T system, as opposed to a 3-T system with higher MRI signal.

#### **4.5.6 Conclusions**

Volume changes identified in our longitudinal assessment and their associations with cognitive impairment progression are overall notably consistent with the well-established anatomical changes signaling the progression to dementia in Alzheimer's disease. So, brain involution in the older DS individuals seems to approach Alzheimer's disease degenerative process despite taking place in a complex situation with dense baseline pathology and a high potential for interactions between developmental and age-associated changes. Brain systems early affected in Alzheimer's disease as the basal forebrain, hippocampus and the prefrontal lobe were selectively affected in DS preceding dementia in our study. Lastly, we would also emphasize the bidirectional implications of our findings, firstly giving support to the potential value of DS as genetic model of Alzheimer's disease-type neurodegeneration, and then serving to further claim that patients at risk for developing dementia in DS are full candidates to benefit from treatment research in AD

**Table 12.** Regional brain volume change and correlation with change in cognitive scores.

<b>Volume Reduction Whole Sample</b>	<b>Number of voxels (ml)</b>	<b>x y z</b>	<b>t</b>
Substantia Innominata Region (gray matter)	2,358 (8.0)	1.5 0 -10.5	5.9
R Lateral Temporal Cortex (gray matter)	573 (1.9)	49.5 -18 -10.5	4.3
L Lateral Temporal Cortex (gray matter)	316 (1.1)*	-63 -18 -6	4.0
R Orbitofrontal Cortex (gray matter)	550 (1.9)	19.5 37.5 -21	5.4
R Hippocampus Region (white matter)	1,375 (4.6)	27 -33 -6	5.0
L Arcuate Fasciculus (white matter)	1,314 (4.4)	-43.5 30 -7.5	5.8
<b>Volume Reduction Cognitive Impairment Progression Group &gt; Remaining Sample</b>			
Substantia Innominata Region (gray matter)	907 (3.1)	0 1.5 -10.5	4.8
L Hippocampus (gray matter)	365 (1.2)	-30 -25.5 -13.5	4.1
<b>Correlation Between Change in Volume and Change in Cognitive Score</b>			
<b>Memory- Word List Learning</b>			
L Hippocampus-Amygdala (gray matter)	444 (1.5)	-25.5 -25.5 -10.5	3.9
R Thalamus (gray matter)	665 (2.4)	10.5 -16.5 1.5	-4.2
<b>Verbal Comprehension</b>			
L Wernicke Area (gray matter)	759 (2.6)	-49.5 -15 -10.5	4.0
L Arcuate Fasciculus (white matter)	1,402 (4.7)	-36 0 30	4.0
<b>Object Recognition</b>			
L Caudate Nucleus (adjacent white matter)	1,591 (5.4)	-12 18 1.5	-4.7
<b>Executive Function-Prospective Memory</b>			
L Prefrontal (gray matter)	6,578 (22.2)	-25.5 6 37.5	5.3
R Prefrontal (gray matter)	2,773 (9.4)	39 49.5 22.5	4.3
Paracentral Lobule (gray matter)	4,850 (16.4)	12 -15 70.5	4.5
L Prefrontal (white matter)	5,154 (17.4)	19.5 16.5 24	6.5
R Prefrontal (white matter)	6,478 (21.9)	24 31.5 18	6.9
L Inferior Temp./Hippocampus (white matter)	1,019 (3.4)	-28.5 -18 -13.5	3.8
R Inferior Temp./Hippocampus (white matter)	2,079 (7.0)	39 -28.5 -21	3.9

x y z, coordinates (mm) given in Montreal Neurological Institute (MNI) space. Statistics at corrected threshold  $P_{FWE} < 0.05$  estimated using Monte Carlo simulations. \*subthreshold.

## **4.6 Study VI: Preliminary Results**

### ***Abnormal Hypothalamus and related Brain Regions in Prader-Willi syndrome evaluated by Diffusion Tensor Imaging***

#### **4.6.1 Introduction**

Prader-Willi syndrome (PWS) is a genetic disorder caused by the lack of expression of the paternally inherited genetic material located in 15q11-q13. It is characterized by neonatal hypotonia, intellectual disabilities, obesity and behavioral disturbance. Patients present with several neuroendocrinological abnormalities, such as growth hormone deficiency, hypogonadotropic hypogonadism, and hyperphagia, as the result of possible involvement of the hypothalamo-hypophyseal system. There's growing evidence from structural and functional studies that suggest abnormalities in white matter developmental trajectory. But, few studies have explored this issue. To our knowledge there's only one research in Prader-Willi patients using DTI and it was not focused in the hypothalamo-hypophyseal region (Yamada et al., 2006). So, specific white matter alterations in Prader-Willi syndrome remain unknown yet.

Thus, the objective of the present study was to evaluate the hypothalamus and related brain regions in adult patients with Prader-Willi syndrome using DTI.

#### **4.6.2 Methods**

Twenty patients (11M, 9F, aged  $28.3 \pm 7.4$ ) with PWS and twenty age- and gender-matched control subjects (11M, 9F, aged  $28.1 \pm 7.0$ ) were recruited for this study. MRI data was acquired from all participants using a 1.5 Tesla Sigma Excite system (General Electric, Milwaukee, WI, USA). Diffusion-weighted scans were obtained using spin-echo single-shot echo-planar sequences of 25 directions with a B-factor of  $1000 \text{ s/mm}^2$ . Twenty-six slices were acquired with repetition time [TR] 8300 ms; echo time 94 ms; thickness 5 mm, no gap; pulse angle  $90^\circ$ ; field of view 26 cm;  $128 \times 128$  acquisition matrix reconstructed into a  $256 \times 256$  matrix. The twenty-six slices were prescribed parallel to AC-PC line.

DTI images were preprocessed and Fractional Anisotropy (FA) maps were calculated using Functional MRI of the Brain (FMRIB) Software Library 5.0 (FSL).

Data was re-sliced to a  $1\text{mm} \times 1\text{mm} \times 1\text{mm}$  anatomical resolution and normalized to standard MNI space. After, a smoothing (8mm) was applied and voxel-wise two sample  $t$ -test was done between groups using SPM8.

Individual FA DTI maps were included in second-level (group) SPM analyses using 2-sample  $t$ -test. Results were considered significant with clusters of 1.032 ml (1.032 voxels) at a height threshold of  $p < 0.005$ , which satisfied the family-wise error (FWE) rate correction of  $P_{\text{FWE}} < 0.05$  according to Monte Carlo simulations.

### 4.6.3 Results

We found a significant reduction in FA values in a number of brain regions in Prader-Willi syndrome patients than in controls (Fig. 26 and Table 13) based on a voxel-wise approach. FA was significantly reduced in the lenticular nucleus (bilateral), hypothalamus, amygdala and sub-genu. The observed diffusivity characteristics indicate developmental abnormalities in these white matter areas, which are highly consistent with the clinical features of Prader-Willi syndrome.

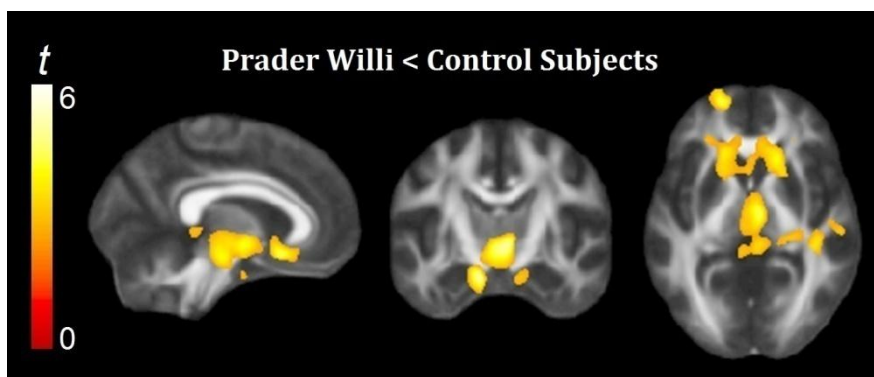


**Figure 26.** Fractional Anisotropy (FA) differences between Prader-Willi patients and control subjects. FA is significantly reduced in the hypothalamus and anatomo-functionally connected structures such as the amygdala, the striatum and the subgenual part of the anterior cingulate cortex.

### 4.6.4 Conclusions

DTI results confirm the presence of extensive structural anomalies in white matter connecting the hypothalamus with related brain structures may underlay endocrinological disorders and hyperphagia in these patients.

**Table 13.** Differences between groups.

	<i>Cluster size, ml</i> <i>(voxels)</i>	<i>x y z</i>	<i>t</i>
<b><i>Prader- Willi &lt; Control Subjects</i></b>			
R Lenticular nucleus	799270	20 4 -9	5.00
L Lenticular nucleus	799270	-23 3 -12	4.65
Hypothalamus	799270	4 -11 -3	5.25
Amygdala	799270	-12 -8 -21	5.61
Sub-Genu	799270	-5 17 -12	4.80

x y z, coordinates given in Montreal Neurological Institute (MNI) space. Statistics at  $p < 0.005$ .





# **5. GENERAL DISCUSSION**



## 5. General Discussion

The importance of white matter status for correct brain functioning and its influence on diverse cognitive domains is undeniable. Also, many studies have revealed its susceptibility of being modulated by many genetic and environmental factors. Specifically, neurodevelopmental genetic disorders alter the trajectory of white matter pathways and generate neuropsychiatric and irreversible cognitive consequences. But, although the main characteristics of white matter development are determined by nature, they are not exempt to be modified in response to certain environmental exposures. Main findings support that some experiences can influence myelin formation and its influence on improving skills.

Our DTI results about the pollutants influence on children confirms our initial hypothesis; airborne copper is significantly associated with poorer motor performance and detectable white matter damage in basal ganglia. Specifically, in the direction of copper exposure findings, children with slower reaction time and less consistent motor response exhibited changes in this region. These alterations are highly consistent with the well-known consequences of copper excess on the brain with basal ganglia as the main target. Although a normal oral diet contains a considerable amount (~1 mg) of copper (Morris et al., 2006), data suggest that relatively lower levels are neurotoxic in chronic airborne exposures. Long-term occupational copper exposure has been associated with increased risk for Parkinson's disease (Gorell et al. 2004; Caudle et al., 2015) and increased rate of mild cognitive impairment conversion to full Alzheimer's disease (Squitti et al., 2014c; Squitti et al., 2014b). In this context, evidence indicates that copper may play a causal role in late-onset neurodegenerative disorders (Bandmann et al., 2015).

Our associations have been demonstrated with copper common levels in urban environments, thus suggesting a risk to large populations with potentially significant implications for public health. Children may be particularly vulnerable to copper as an agent capable of interfering with brain development during critical developmental stages. Consistent with our results, a recent study has reported a significant association between high copper levels in blood and poorer cognitive performance in normal school children (Zhou et al. 2015). Our conclusion is that the effect of copper in basal ganglia is subtle, but biologically meaningful.

Despite the results obtained with copper, we've not been able to find out the impact of other pollutants on white matter pathways. We studied traffic-related pollution using the weighted average of two reliable vehicle exhaust indicators,

namely particulate elemental carbon and NO<sub>2</sub> and no significant association was identified between the pollution index and our white matter measure (FA). By contrast, the functional imaging analysis showed consistent results. The reason of negative findings in DTI may be that vehicle exhaust-related air pollution exposure was commonly associated with brain changes of functional nature, with no evident effect on brain anatomy, structure or membrane metabolism.

Children from schools with higher traffic-related pollution showed lower functional integration and segregation in key brain networks. Age and performance both showed the opposite effect to that of pollution on brain function, thus indicating that higher exposure is associated with slower brain maturation. The functional findings were highly consistent, similar effects were observed in different functional networks and the age-sensitive areas notably coincided with the areas showing significant correlation with air pollution. Fortunately, despite the evident effect on functional connectivity, the overall brain repercussion may, to some extent, be considered subtle, as changes did not involve any measurement of brain structure. So, we can speculate on the reversibility of the brain damage and the potential effectiveness of actions addressed to reduce pollution. The effect of air pollution may, however, be more dramatic when the exposure involves early developmental periods and long-term exposures. Also, recent studies have revealed that long-term ambient air pollution exposure may ultimately affect brain tissue volume in older people (Chen et al., 2015; Wilker et al., 2015).

On the other hand, our DTI video game findings showed that video game use was associated with faster motor response to visual stimulation. At the neural level, structural white matter changes associated with gaming use were most evident in basal ganglia circuitry. There were significant differences among groups in a region adjacent to the lateral aspect of the striatum. The plot of FA measurements from this left striatal region revealed a relevant FA increase, but only in the high-use group. Direct comparison of non-gamers with high-use gamers confirmed the increase of FA in this region and detected additional significant changes in the ventral striatal region bilaterally, as well as the right thalamus and left occipital white matter.

The observed associations between video games use and changes in basal ganglia circuits in the form of structural (white matter) and functional connectivity increases support that several abilities are more trainable than others with video games. It's well known that basal ganglia circuits are critical for procedural learning based on the acquisition of new skills through practice (Doyon et al., 2003). So, our results are generally consistent with other imaging studies reporting significant effects of gaming use on the fronto-basal ganglia system structure and function. Specifically, Erickson et al. (2010) showed that the

acquisition of skills on demanding video games may be predicted by variations in the volume of the striatum. Children traditionally acquire procedural skills through action, for instance in relation to sports and outdoor games. Neuroimaging research now suggests that training with desktop virtual environments is also capable of modulating certain white matter brain systems that support procedural learning.

In summary, by studying these two examples of environment modulators, we've confirmed that white matter development is an active process influenced by distinct active and passive environmental factors. Nevertheless, all white matter modulators effects are not predictable or even reversible. It's well known that neurodevelopment genetic diseases bring about a disturbed white matter organization since birth that becomes more evident in adulthood.

Our findings in Down syndrome sample indicate that white matter in Down syndrome patients shows generally lower FA compared with healthy participants, suggesting underdevelopment of white matter tracts. The most affected structures were the frontal lobes, subcortical white matter and some parts of the brainstem. Lower FA in Down syndrome was associated with poorer semantic fluency, which illustrates a degree of correspondence between white matter integrity and performance in patients. White matter FA did indeed decrease with age in both Down syndrome and healthy controls, but we didn't find the expected accelerated age effect in the Down syndrome group.

Our results are consistent with studies of brain anatomy showing generally reduced white matter volumes in Down syndrome compared with healthy controls (Weis et al., 1991; White et al., 2003). However, our data may further contribute to characterizing white matter alterations in Down syndrome in that they would indicate that the changes are not limited to general volume reductions, but may also implicate a less developed structural connectivity pattern. Although FA abnormalities involved the major brain pathways, the frontal-subcortical circuits showed more severe alterations.

As a general trend, the results are consistent with the profile of cognitive deficits in Down syndrome typically progressing with deep impairment in language production and executive functions, which are cognitive domains notably dependent on the frontal lobes (Lott et al., 2010). A relevant problem in evaluating cognitive abilities in Down syndrome is the notable lack of consistency and reproducibility of ratings in some neuropsychological tests. We used an extensive neuropsychological assessment but only verbal fluency was associated with FA alterations in Down syndrome in a rather general manner, thus indicating a certain parallelism between the identified pattern of white matter alterations and cognitive performance. Nevertheless, we failed to find similar

associations with performance IQ and working memory. We consider now that these tests are not the most suitable to predict brain alterations in Down syndrome. The development of more specific and sensitive tools to evaluate cognition in Down syndrome could be helpful in future studies.

Also, we didn't find significant results between-group differences in age-related white matter changes. It means, although both groups suffered a variation of white matter structure with age, there were no between-group differences. In our Down syndrome group, none of the participants were diagnosed with Alzheimer's disease and only 3 patients had mild cognitive impairment according to clinical criteria. Therefore, we were unable to demonstrate the anticipated premature aging effects on white matter using FA measurements, which contrast with positive findings in studies on familial Alzheimer's disease. Probably, the adopted DTI approach was not sufficiently sensitive to detect alterations related to the dementia process in subclinical stages of Alzheimer-like pathology.

Despite challenges are inherent to longitudinal assessments particularly in individuals with intellectual disability, our longitudinal study in Down syndrome shows that identifying brain anatomical changes that precede dementia in Down syndrome is feasible. Our results are focused on significant volumetric reductions after two years in the substantia innominata region of the basal forebrain, the hippocampus, lateral temporal cortex and left arcuate fasciculus. Nevertheless, we didn't find significant changes in FA in these specific regions. The volume changes identified in our longitudinal assessment and their associations with cognitive impairment progression are overall notably consistent with the well-established anatomical changes signaling the progression to dementia in Alzheimer's disease. So, brain involution in the older Down syndrome individuals seems to approach Alzheimer's disease degenerative process despite taking place in a complex situation with dense baseline pathology and a high potential for interactions between developmental and age-associated changes. Brain systems early affected in Alzheimer's disease as the basal forebrain, hippocampus and the prefrontal lobe were selectively affected in Down syndrome preceding dementia in our study. Lastly, we would also emphasize the bidirectional implications of our findings, firstly giving support to the potential value of Down syndrome as genetic model of Alzheimer's disease-type neurodegeneration, and then serving to further claim that patients at risk for developing dementia in Down syndrome are full candidates to benefit from treatment research in Alzheimer's disease.

One of main criticisms someone could make to this research is why we didn't describe changes in white matter tracts measured with DTI if we've shown volume reductions in white matter analyzed with VBM. Actually, we found

significant FA reductions after two years in right temporal gyrus and right frontal projection tracts (Fig.27) but are not coincident with our VBM results.

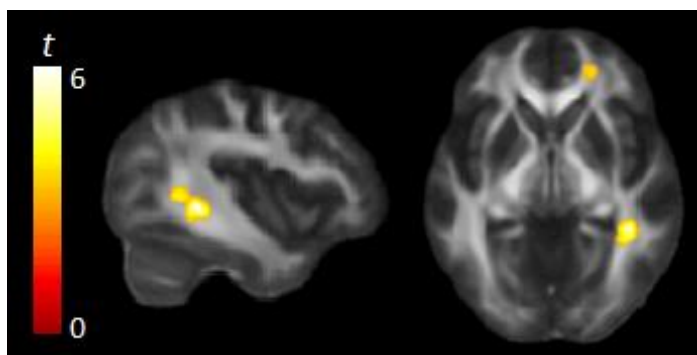


**Figure 27.** Significant FA reductions over time in the whole Down syndrome sample.

Despite this, our FA results match with a previous VBM study based on mild cognitive impairment and healthy participants (Wang et al., 2010) that showed significant clusters of reduced white matter volume in mild cognitive impairment patients relative to controls in bilateral temporal gyrus, the right anterior cingulate, the bilateral superior, medial frontal gyrus and right parietal angular gyrus.

At present, the pathogenesis of the white matter abnormality in Alzheimer's disease and specially Down syndrome population remains certainly unclear. Recent studies postulated that myelin breakdown is the primary process leading to Alzheimer disease (Bartzokis et al., 2003). As we all know, extracellular amyloid  $\beta$ -peptide ( $A\beta$ ) oligomer deposition is an important early event in the pathogenesis of Alzheimer disease. Scientific literature indicates that myelin can be directly damaged by oligomerized  $A\beta$  (Marnier et al., 2003). Furthermore, homeostatic responses to this myelin breakdown increase intracortical toxicity and might explain the progressive neuronal damage of Alzheimer disease. However, the distribution of myelin breakdown is not global. Rather, the most susceptible regions to neurodegeneration are the cortical association areas that myelinate late in life (Braak et al., 2000; Bartzokis et al., 2004).

In our DTI results, the distribution of the white matter abnormalities in the brain supports the myelin breakdown hypothesis. First, according to the theory, the late-myelinating regions such as the temporal lobes and the nearby neocortical association areas are the focus of the very first  $A\beta$  deposits and myelin breakdown. Second, the frontal lobes and parietal lobes that myelinate late in life are more susceptible to myelin breakdown than the occipital lobes. Our findings



of white matter abnormalities distribution provide evidence of myelin damage pattern that appears to be the reverse of myelination. The results of Wang et al. (2010) are consistent with some previous studies of Alzheimer disease or MCI using DTI method, which have reported white matter changes by the measurement of FA value (Medina et al., 2006; Huang et al., 2007; Stahl et al., 2007). Some studies used voxel-based methods to analyze DTI differences in patients with Alzheimer disease, mild cognitive impairment and controls (Xie et al., 2006). Many of them found impaired white matter integrity in the medial temporal white matter, splenium of the corpus callosum, parietal lobe and cingulum bundle with greater posterior than anterior involvement. Our findings of impaired white matter regions including temporal gyrus and frontal projections are consistent with previous mild cognitive impairment studies. Sadly, these findings have not been replicable in Down syndrome patients with mild cognitive impairment or Alzheimer-like dementia yet.

We've been talking about Down syndrome for a while, but, although Down syndrome has higher incidence rate than other genetic diseases, it's not the only neurodevelopmental disease that show behavioral and cognitive alterations, suggesting an abnormal brain development. Our preliminary Prader-Willi results confirm that the presence of extensive structural anomalies in white matter connecting the hypothalamus with related brain structures may underlay endocrinological disorders and hyperphagia in these patients. These and previous findings on Down syndrome sample confirm the undeniable effect of diverse neurodevelopmental diseases on white matter growth and maturation.

## **Limitations**

A general limitation when assessing special populations like children or people with intellectual disability is avoiding excessive head motion during the acquisition. Specifically in Down syndrome sample we used MRI practice sessions designed to minimize the problem.

In addition, we decided to exclude cases with detectable image degradation, as no correction procedure was wholly efficient once the images have been acquired. Although accurate control of head motion effects may be a strong point of the study, strict participant selection is also a limitation.

Also, our DTI findings in Down syndrome sample cannot be generalized to all Down syndrome patients because we used high performing individuals. So, our conclusions should be limited to relatively highly-performing Down syndrome individuals.

A final limitation relates to using a 1.5-T system, as opposed to a 3-T system with higher MRI signal, following the recommendations of the FP7-ERC Ethics Review Committee to limit magnetic field strength in children.



# 6. CONCLUSIONS



## 6. Conclusions

The main conclusions of this thesis, derived from our studies, can be summarized as follows:

- I. Airborne copper is associated with poorer motor performance and basal ganglia alterations in developing children.
- II. Vehicle exhaust-related air pollution exposure is associated with functional brain changes, with no evident effect on brain anatomy.
- III. Video game playing is associated with faster motor response to visual stimulation and changes in the basal ganglia circuitry. A excess of playing is associated with conduct problems.
- IV. Down syndrome patients show generally lower FA, suggesting underdevelopment of white matter tracts.
- V. Changes in regional brain volumes, but not in FA, in Down syndrome are concordant with the well-established anatomical changes signaling the progression to dementia in Alzheimer's disease.
- VI. Prader-Willi patients show extensive structural anomalies in white matter connecting the hypothalamus with related brain structures.



# **7. RESUMEN ABREVIADO EN CASTELLANO**





## **7. Resumen Abreviado en Castellano**

### ***INFLUENCIA DE FACTORES GENÉTICOS Y AMBIENTALES SOBRE LA ESTRUCTURA DE LAS VÍAS DE SUSTANCIA BLANCA MEDIDA CON TENSOR DE DIFUSIÓN***

#### **7.1 Introducción**

---

##### **7.1.1 Sustancia Blanca**

Imaginemos que fuéramos capaces de echar un vistazo al interior de cráneo y ver qué es lo que hace a un cerebro ser diferente de otro, o qué características cerebrales anatómicas y funcionales están debajo de un trastorno genético. Actualmente, disponemos de técnicas de imagen que nos permiten observar la estructura y función cerebral que están revelando grandes sorpresas como que una gran variedad de moduladores genéticos y ambientales pueden modificar las vías de desarrollo y maduración de la sustancia blanca, generando diversas consecuencias a lo largo de la vida.

Resumidamente, la sustancia gris se compone principalmente de cuerpos celulares y por debajo de ella, está la sustancia blanca que ocupa casi la mitad del volumen cerebral (Zhang et al., 2000; Liu et al., 2017). La sustancia blanca está compuesta por millones de “cables” que permiten la comunicación a través de los axones gracias la mielina.

Para entender cómo funciona la sustancia blanca, es esencial comprender su desarrollo. Los principios de maduración de la sustancia blanca cerebral siguen las leyes generales del desarrollo: crecimiento inicial y posterior maduración. De hecho, el proceso de envoltura del axón produce en diferentes etapas. En el nacimiento, encontramos muy poca cantidad de mielina y se va expandiendo progresivamente por todo el cerebro hasta los 25-30 años. Es un proceso que va desde la parte posterior del córtex hasta la anterior. Los lóbulos frontales son los últimos en mielinizarse, por eso se dice que hasta pasados 20 años no se adquieren por completo las habilidades de razonamiento, planificación y juicio. Durante décadas los neurocientíficos han mostrado relativamente poco interés en la sustancia blanca, considerando la mielina como una mera capa aislante y a los axones que están en su interior como simples transmisores de información pasivos. Sin embargo, en las últimas décadas está apareciendo un creciente interés en lo que se refiere a la transmisión de información entre regiones

cerebrales. Nuevos estudios revelan que la extensión de sustancia blanca varía en personas en función de los diferentes ambientes a los que han sido expuesto o ante la presencia de ciertas disfunciones y/o patologías (Pujol et al., 2011; Via et al., 2014).

### **7.1.2 Factores Moduladores de la Sustancia Blanca**

Con esta nueva perspectiva sobre la sustancia blanca no es difícil imaginar cómo una transmisión defectuosa podría conducir a ciertas anomalías cerebrales (Soriano-Mas et al., 2011). Después de décadas de intentar explicar las causas de algunas discapacidades mentales mediante alteraciones de la sustancia gris, nuevos estudios tienen pruebas de que la sustancia blanca juega un papel destacado en ellas (Pujol et al., 2004).

El desarrollo de las vías de sustancia blanca no es un proceso inmutable a través de la vida y puede ser influenciado por diversos factores. En el siguiente texto nos centraremos en factores ambientales y genéticos de acuerdo a los objetivos principales de esta tesis.

En primer lugar, vamos a describir los hallazgos relevantes hasta la fecha sobre los efectos de diferentes moduladores ambientales sobre el desarrollo de la materia blanca y sus posibles consecuencias. Hemos decidido centrarnos en dos ejemplos de factores ambientales: los contaminantes y los videojuegos. Por un lado la contaminación, ya que es un factor externo que penetra pasivamente en el cerebro y puede influir en las trayectorias de desarrollo. Y por otro lado, los videojuegos que son un buen ejemplo de comportamiento activo que puede modificar el desarrollo del cerebro.

En segundo lugar, explicaremos el efecto de dos patologías genéticas sobre las vías de la sustancia blanca a través de la vida. Hemos escogido el síndrome de Down y síndrome de Prader-Willi como síndromes genéticos representativos que pueden interferir en el crecimiento de la sustancia blanca porque, aunque el síndrome de Down tiene una tasa de incidencia superior al síndrome de Prader-Willi, ambos muestran alteraciones cognitivas y conductuales, sugiriendo un desarrollo y maduración cerebral anómalos.

#### **7.1.2.1 Ambiente**

Aunque el desarrollo de la sustancia blanca es un proceso determinado por la naturaleza, no está exento de ser modificado en respuesta a ciertas experiencias y exposiciones ambientales. Muchos hallazgos sugieren que algunas experiencias influyen en la formación de mielina que sustenta los procesos de aprendizaje y la

mejora de habilidades cognitivas (Bavelier et al., 2012). Pero, ¿todas las experiencias y factores ambientales nos traen proporcionan beneficios?

### **7.1.2.1.1 Contaminantes**

Uno de cada seis niños tiene una discapacidad relacionada con el desarrollo y en la mayoría de los casos éstas afectan al sistema nervioso. Los trastornos del neurodesarrollo más comunes incluyen alteraciones del aprendizaje, déficits sensoriales y retrasos en el desarrollo (Boyle et al., 1994), procesos estrechamente relacionados con la sustancia blanca.

El cerebro humano en desarrollo es mucho más susceptible a lesiones causadas por agentes tóxicos que el cerebro de un adulto (Dobbing et al., 1968). La sensibilidad de lactantes y niños a los productos químicos industriales se ve reforzada por el grado de exposición, las elevadas tasas de absorción y la disminución de la capacidad de eliminar del organismo determinados compuestos exógenos, en relación con los adultos (Ginsberg et al., 2004).

Durante varias décadas se han ido acumulado evidencias sobre que los productos químicos industriales pueden causar daño en el desarrollo neurológico. Un estudio pionero sobre diversos contaminantes mostró que el plomo era una sustancia tóxica para el cerebro en desarrollo (Landrigan et al., 1975). A partir de entonces, se planteó la existencia de un vínculo entre sustancias químicas y anomalías anatómicas/funcionales cerebrales y cambios neurocomportamentales generalizados. Estos resultados estaban de acuerdo con otros tantos que indicaban que existían otros contaminantes ambientales que también podían resultar tóxicos durante el desarrollo temprano del cerebro (Grandjean et al., 2002) y podrían ser capaces de modificar la trayectoria de maduración cerebral. Otros estudios han ido más allá, clasificando la contaminación atmosférica como un importante neurotóxico para el desarrollo (Grandjean et al., 2014). En los niños, la exposición a contaminantes atmosféricos relacionados con el tráfico durante el embarazo y la infancia, cuando el cerebro se está desarrollando rápidamente, se ha relacionado con diversos retrasos cognitivos (Suglia et al., 2008; Guxens et al., 2012).

Los niños pasan una gran parte de su día en la escuela, incluyendo el período en que la contaminación diaria del tráfico alcanza su punto máximo. Muchos colegios se encuentran en las proximidades de carreteras muy concurridas, lo que aumenta el nivel de contaminación del aire. Actualmente, existe muy poca evidencia sobre el papel de la contaminación relacionada con el tráfico sobre las funciones cognitivas de los niños en edad escolar (Wang et al., 2009). Sin embargo, algunos estudios han demostrado que el desarrollo cognitivo se ve

mermado en niños expuestos a niveles altos de contaminantes relacionados con el tráfico durante su estancia en el colegio (Sunyer et al., 2015, Van Kempen et al., 2012).

### **7.1.2.1.2 Videojuegos**

Dado el aumento dramático del uso diario de la tecnología, diversas investigaciones han considerado que tiene un impacto notable sobre la cognición y el desarrollo humano (Greenfield et al., 1984; Hunt et al., 2012). En las últimas décadas, estos efectos han sido intensamente estudiados y debatidos (Oei et al., 2014).

Una visión general de la literatura existente sobre los videojuegos indica que proporcionan beneficios en varios dominios cognitivos, contrariamente a lo que se pensaba sobre el tema. Concretamente, se ha documentado que los jugadores de videojuegos asiduos tienen un mejor rendimiento que los no jugadores en varios aspectos de la cognición como la memoria visual a corto plazo (Anderson y otros, Boot et al., 2008), la cognición espacial (Greenfield et al., 2009), capacidad multitarea (Green et al, 2006a), y algunos aspectos de la función ejecutiva (Anderson et al., 2011). Sin embargo, los beneficios más notables se observan en el tiempo de reacción y el equilibrio entre la velocidad y la exactitud de respuesta, que corresponden a regiones cerebrales estrechamente ligadas con vías de sustanciablanca que son esenciales para la adquisición de nuevas habilidades a través de la práctica.

Por otro lado, hay una creciente prevalencia de los problemas que presentan los jugadores habituales. Varios investigadores han comenzado a probar científicamente el concepto de uso de videojuegos de forma patológica, ligado a una adicción (Fisher et al., 1994). Se ha asumido que sería similar al juego patológico. El paralelismo parece justificable porque se supone que ambos son adicciones conductuales que comienzan como entretenimiento que pueden estimular respuestas emocionales y liberación de dopamina (Koepp et al., 1998). A pesar de esto, los videojuegos no son una actividad patológica inicialmente; se convierten en patológicos para algunos individuos cuando la actividad se torna disfuncional, dañando el funcionamiento social, ocupacional, familiar, escolar y psicológico del individuo.

En resumen, aunque hay algunas pruebas que sugieren que los videojuegos pueden mejorar las habilidades cognitivas particulares durante la juventud (Bavelier et al., 2012), otras estudios lo vinculan a la presencia de problemas conductuales y un mayor riesgo de padecer trastornos relacionados con la adicción (Anderson et al., 2010, Gentile et al., 2010).

### **7.1.2.2 Genética**

Los trastornos genéticos del neurodesarrollo son un grupo de patologías en las que se altera el desarrollo del sistema nervioso central. Esto produce un desarrollo atípico cerebral que puede manifestarse a través de problemas neuropsiquiátricos, deterioro de la función motora, problemas de aprendizaje, alteración del lenguaje o problemas de comunicación no verbal. Algunos trastornos del neurodesarrollo modifican la trayectoria de las vías de la sustancia blanca y generan consecuencias neuropsiquiátricas y cognitivas que pueden ser más evidentes en la edad adulta. Al estudiar las anomalías de estos trastornos, pueden surgir datos claves acerca de los mecanismos biológicos subyacentes estas patologías.

#### **7.1.2.2.1 Síndrome de Down**

El síndrome de Down, o trisomía 21, es un trastorno cromosómico relativamente frecuente y la causa más común de discapacidad intelectual (Nadel et al., 1999). La investigación en el síndrome de Down ha progresado sustancialmente en lo que se refiere a la comprensión de los mecanismos biológicos básicos a través de los cuales la sobreexpresión genética interfiere en el desarrollo cerebral (Capone et al., 2001), pero existe una falta de información acerca de la organización general del cerebro y sus consecuencias a largo plazo (Pujol et al., 2014a). Sorprendentemente, hay muy pocos estudios de neuroimagen hechos en población infantil con síndrome de Down, tal vez porque las principales diferencias con sujetos sanos son más evidentes en la edad adulta cuando el cerebro está completamente desarrollado. De hecho, existe una gran variedad de estudios centrados en síndrome de Down adultos y en el riesgo de desarrollar demencia de tipo Alzheimer (Stanton et al., 2004).

En los pacientes adultos con síndrome de Down, un gran número de estudios de resonancia magnética han definido un patrón neuroanatómico completamente diferente al de controles sanos, hallazgos que coinciden con informes post-mortem realizados sobre la neuropatología del síndrome de Down (Schapiro et al., 1989, Kesslak et al., 1994, Raz et al., 1995, White et al., 2003, Teipel et al., 2004). Muchos de estos estudios también han reportado gran variedad resultados relacionados con la enfermedad de Alzheimer en estos pacientes; un hallazgo importante debido a la alta tasa de aparición de demencia en individuos con síndrome de Down mayores de 40 años (Wisniewski et al., 1985). Por otra parte, los principales estudios muestran que los adultos con síndrome de Down tienen, en general, una sustancia blanca más desestructurada que los controles sanos de la misma edad, particularmente en los lóbulos frontales (Powell et al., 2014, Head et al., 2016) que concuerda con un declive de las funciones ejecutivas

evidenciable mediante pruebas neuropsicológicas (Hartley et al., 2014, Madden et al., 2009). Estos estudios de imagen han proporcionado una mayor comprensión de las posibles repercusiones cognitivas de algunas de las alteraciones estructurales que tienen este tipo de pacientes (Raz et al., 1995; Aylward et al., 1999; Ikeda et al., 2002, Krasuski et al., 2002).

A pesar de estos hallazgos, es un reto detectar los primeros síntomas sub-clínicos de demencia en pacientes con síndrome de Down y sería interesante investigar si los cambios involutivos en las vías de sustancia blanca son detectables antes de que la demencia de que se manifieste clínicamente para obtener un diagnóstico eficaz y diseñar mejores intervenciones.

### **7.1.2.2.2 Síndrome de Prader-Willi**

El síndrome de Prader-Willi es un trastorno genético complejo asociado a múltiples manifestaciones clínicas resultantes del fracaso de la expresión de alelos paternos en la región 15q11.2-q13 del cromosoma 15 (Grugni et al., 2016) en la mayoría de los casos.

El síndrome muestra un fenotipo característico que abarca hipotonía neonatal, fracaso en el crecimiento normal, hiperfagia progresiva con obesidad precoz (si no se controla), deterioro del desarrollo con problemas de aprendizaje, alteraciones conductuales y psiquiátricas, características dismórficas y anomalías endocrinas (Cassidy et al., 2012). La mayoría de los pacientes tienen la capacidad de secreción de la hormona del crecimiento reducida e hipogonadismo hipogonadotrópico, lo que sugiere una disfunción hipotálamo-pituitaria (Burman et al., 2001).

Los estudios de neuroimagen que se han realizado en estos pacientes revelan que el síndrome de Prader-Willi se acompaña de determinadas anomalías en áreas específicas del cerebro (Yamada et al., 2006, Mantura et al., 2011, Ogura et al., 2011, Ogura Et al., 2013). A continuación se presentan algunos de los hallazgos más importantes relacionados con la sustancia blanca.

Algunos estudios han demostrado que hay regiones cerebrales atípicas en el síndrome de Prader-Willi. Curiosamente, las alteraciones observadas en la difusividad que indican anomalías del desarrollo son coherentes con las características clínicas de síndrome. Hay una reducción significativa de los valores de FA en una serie de regiones cerebrales en el síndrome de Prader-Willi que no está presente en controles sanos. Un análisis basado en regiones de interés usando como medida la FA mostró cambios generalizados en las siguientes regiones: hipotálamo, cápsula interna derecha e izquierda, cerebelo

derecho e izquierdo y todas las subregiones del cuerpo calloso (I, II, III, VI y V). Específicamente, el cuerpo calloso, hipotálamo y cápsula interna derecha presentaban una reducción significativa de FA en los pacientes con Prader-Willi (Tant et al., 2009; Yamada et al., 2006). Por lo tanto, se ha demostrado que la utilización de imágenes de tensor de difusión permite detectar anomalías focales en sustancia blanca entre pacientes con Prader-Willi y sujetos sanos. Pero a pesar de todo el conocimiento sobre el síndrome de Prader-Willi que tenemos actualmente, hay algunos aspectos que siguen siendo una incógnita, como la repercusión de las alteraciones de sustancia blanca sobre la función cognitiva y los síntomas psiquiátricos y comportamentales.

### **7.1.3 Medidas de Sustancia Blanca**

A pesar de que existen muchas técnicas para explorar las características de la sustancia blanca como buscar diferencias específicas en determinadas regiones de interés o la segmentación de sustancia blanca realizada con morfometría basada en voxel, la técnica más utilizada para explorar la sustancia blanca es la el tensor de difusión. Esta técnica nos permite visualizar, a *grosso modo*, la velocidad de difusión del agua a lo largo de los axones. Por lo tanto, puede utilizarse para explorar las diferentes vías de sustancia blanca.

En el tensor de difusión, la señal de resonancia decae cuando el agua está difundiendo (Stejskal et al., 1965) y es posible diseñar un protocolo de resonancia que detecte las direcciones primarias de la difusión del agua en cada vóxel del cerebro.

#### **7.1.3.1 Tensor de Difusión**

La imagen de tensor de difusión es un método no invasivo que proporciona información sobre las propiedades microestructurales de la sustancia blanca (Le Bihan et al., 1985, Le Bihan et al., 2001) midiendo la magnitud, dirección y anisotropía de las moléculas de agua (Schmithorst et al. 2010). Este método nos da muchas mediciones de la sustancia blanca, pero nos centraremos en la anisotropía fraccional (FA) porque es la medida más informativa sobre los niveles de maduración de las vías de la sustancia blanca.

##### **7.1.3.1.1 Anisotropía Fraccional**

El movimiento aleatorio de las moléculas de agua, también conocido como movimiento *browniano*, puede ser cuantificado y refleja las características



intrínsecas de la microestructura del tejido *in vivo* (Pierpaoli et al., 1996). En el agua o líquido cefalorraquídeo, la difusión de las moléculas de agua no tiene restricciones. Esta situación es denominada como "isotrópica" y a menudo representada como una esfera (Lerner et al., 2014) (Figura 2). Pero en el tejido cerebral, la difusión de agua se reduce sustancialmente por estructuras como vainas de mielina, membranas celulares y tractos de materia blanca. En general, en la sustancia blanca la difusión de las moléculas de agua está menos restringida a lo largo del eje longitudinal de un grupo de fibras alineadas que en el eje perpendicular a él (Dong et al., 2004). Esta condición de difusión dependiente de una dirección se denomina "anisotrópica" y puede estar representada por una elipsoide alargada (Lerner et al., 2014). La medida más utilizada para medir la anisotropía de difusión es anisotropía fraccional que mide los cambios en rangos de 0 (difusión que es igual en todas las direcciones) a 1 (difusión predominantemente en una dirección) (Pfefferbaum et al., 2003, Assaf et al., 2008). Como resultado, el tensor de difusión proporciona un gran marco para la adquisición, análisis y cuantificación de las propiedades de difusión de la sustancia blanca durante el desarrollo y los efectos y/o consecuencias de diferentes moduladores a lo largo de la vida.

## 7.2 Objetivos e Hipótesis

---

### ***7.2.1 Estudio I: La Exposición al Cobre Ambiental en la Escuela está asociado con un peor Rendimiento Motor Y Alteraciones en los Ganglios de la Base***

#### **7.2.1.1 Objetivos**

El desarrollo de las vías de sustancia blanca no es un proceso inmutable a lo largo de la vida, existen etapas, como la niñez, que son más susceptibles de generar cambios en consecuencia a la exposición a distintos factores ambientales. Existe una gran variedad de contaminantes ambientales que han sido identificados como neurotóxicos a elevadas concentraciones. Sin embargo, actualmente no está determinado si pueden generar alteraciones permanentes en el cerebro en desarrollo. Uno de los contaminantes que sí interfiere en el neurodesarrollo es el cobre. A pesar de que este elemento sea necesario para el metabolismo celular, niveles anormales pueden producir daño cerebral.

Así pues, el objetivo principal de este estudio fue investigar los efectos neurotóxicos de la exposición al cobre en las vías de sustancia blanca.

Entre los objetivos secundarios encontramos:

- I. Identificar los efectos perjudiciales de la exposición al cobre ambiental en niños entre 8-12 años.
- II. Explorar los potenciales efectos del cobre sobre las vías de sustancia blanca.
- III. Examinar el impacto del cobre sobre varias habilidades motoras, como el tiempo de la reacción y la consistencia de la respuesta motora.
- IV. Relacionar los hallazgos encontrados en DTI con las alteraciones en las habilidades motoras.

### **7.2.1.2 Hipótesis**

Hipotetizamos que los niños expuestos al cobre ambiental presentarían un peor rendimiento motor y cambios en la estructura de los ganglios basales.

## ***7.2.2 Estudio II: La Exposición a la Contaminación producida por el Tráfico está asociada con Alteraciones de la Conectividad Funcional de los Niños en Edad Escolar***

### **7.2.2.1 Objetivos**

Los niños son más vulnerables a los efectos moduladores de factores ambientales debido a su etapa de desarrollo. La exposición a ambientes urbanos contaminados se ha asociado en numerosas ocasiones con alteraciones en la cognición infantil a causa de la respuesta inflamatoria que provocan determinados contaminantes.

Así pues, este estudio pretendía detallar el efecto que tiene en el desarrollo de las vías de sustancia blanca la exposición prolongada a contaminantes urbanos y sus consecuencias sobre el rendimiento cognitivo.

En resumen, los objetivos de este estudio eran:

- I. Determinar el impacto de la exposición a contaminantes urbanos en una gran muestra de niños entre 8-12 años.
- II. Empleando la técnica del tensor de difusión, explorar los efectos que tiene la exposición continuada a contaminantes en sobre las vías de sustancia blanca.

- III. Utilizando una evaluación cognitiva adecuada, determinar cuáles son las principales repercusiones cognitivas de la exposición prolongada a contaminantes.
- IV. Relacionar los hallazgos encontrados en neuroimagen con las alteraciones en la cognición.

### **7.2.2.2 Hipótesis**

Nuestra principal hipótesis era que los potenciales efectos de la contaminación ambiental serían más evidentes durante el proceso de desarrollo cerebral y que esto se tendría que reflejar como cambios de difusión del agua dentro de tractos de sustancia blanca.

### **7.2.3 Estudio III: Videojuegos en Edad Escolar: ¿cuánto es suficiente?**

#### **7.2.3.1 Objetivos**

Los beneficios y riesgos de jugar a videojuegos en la población infantil es un tema que suscita gran debate, sobre todo a lo que se refiere en el tiempo óptimo de uso. A pesar de que existen evidencias que sugieren que pueden mejorar determinadas habilidades cognitivas que se adquieren con la prácticas, existen otras que afirman que es una fuente de problemas conductuales y que incrementa el riesgo de desarrollar una adicción.

De este modo, el principal objetivo de este estudio se basó en determinar qué consecuencias tiene jugar a videojuegos sobre la sustancia blanca cerebral y su relación con el rendimiento cognitivo.

Los objetivos secundarios incluyeron:

- I. Empleando una aproximación adecuada para detectar cambios y/o anomalías en la sustancia blanca (DTI), explorar las posibles repercusiones de jugar a videojuegos sobre las vías de sustancia blanca.
- II. Usando una evaluación motora adecuada, examinar el impacto de los videojuegos sobre las habilidades motoras.
- III. Relacionar los hallazgos encontrados en sustancia blanca con los resultados de la evaluación motora.

### **7.2.3.2 Hipótesis**

Nosotros predcimos que jugar a videojuegos en edad escolar, entendiendo los videojuegos como un entrenamiento basado en actividades repetitivas, tendrían efecto sobre la velocidad de procesamiento de la información y tiempos de reacción.

A nivel cerebral, los videojuegos podrían reforzar vías de sustancia blanca, con un impacto mayor sobre ganglios de la base, que son esenciales para la adquisición de nuevas habilidades mediante la práctica.

### ***7.2.4 Estudio IV: Anormalidades en la Sustancia Blanca Cerebral y el Efecto de la Edad en pacientes con Síndrome de Down***

#### **7.2.4.1 Objetivos**

Las anormalidades en tejido neural de los sujetos con síndrome de Down se hacen más notables en las etapas tardías del desarrollo. Además, la aceleración del envejecimiento en estos pacientes concurre con la aparición temprana de enfermedades neurodegenerativas. Un amplio abanico de estudios de resonancia magnética ha identificado una gran variedad de alteraciones anatómicas y funcionales. Pero los cambios en sustancia blanca y su repercusión funcional todavía permanecen sin caracterizar.

Así pues, con este estudio se pretendía caracterizar las anormalidades de sustancia blanca en adultos con síndrome de Down e investigar si estos cambios podrían ser usados como marcadores de demencia en este tipo de pacientes.

Los objetivos de este estudio incluían:

- I. Caracterizar las anormalidades en sustancia blanca cerebral en sujetos adultos no demenciados con síndrome de Down empleando la técnica de tensor de difusión.
- II. Investigar si los cambios involucionales de la sustancia blanca estructural son detectables antes del desarrollo de una demencia.

#### **7.2.4.2 Hipótesis**

Se predijo que los pacientes con síndrome de Down mostrarían una reducción de anisotropía fraccional de la sustancia blanca de forma generalizada y una

aceleración del envejecimiento, y que estas alteraciones podrían estar asociadas con un mal rendimiento cognitivo.

### ***7.2.5 Estudio V: Estudio Longitudinal sobre los Cambios Anatómicos que preceden a la Demencia en el Síndrome de Down***

#### **7.2.5.1 Objetivos**

La investigación en neuroimagen indica que los pacientes con síndrome de Down muestran alteraciones cerebrales típicas de la degeneración de la enfermedad de Alzheimer (Emerson et al., 1995; Haier et al., 2008; Beacher et al. 2009; Powell et al., 2014). A pesar de esto, los estudios no son concluyentes a la hora de distinguir la patología basal del Down de los cambios degenerativos que se producen en la demencia.

Así pues, el objetivo principal de esta investigación fue caracterizar a pacientes con síndrome de Down con riesgo de desarrollar demencia mediante la medición de cambios en la estructura de la sustancia blanca y su relación con el deterioro cognitivo.

En resumen, los objetivos eran:

- I. Caracterizar los cambios de la sustancia blanca en pacientes con síndrome de Down con riesgo de desarrollar una demencia.
- II. Relacionar la progresión del deterioro cognitivo de los pacientes con síndrome de Down con el declive cognitivo característico de la enfermedad de Alzheimer.
- III. Relacionar los cambios identificados en sustancia blanca con la progresión del deterioro cognitivo.

#### **7.2.5.2 Hipótesis**

Nosotros hipotetizamos que el cerebro de un paciente con síndrome de Down mayor posee características propias de la enfermedad de Alzheimer y esto podría ser un punto de unión entre una anomalía genética y la neurodegeneración que podría contribuir a caracterizar la patogénesis de la enfermedad de Alzheimer.

## ***7.2.6 Estudio VI: Anomalías Hipotalámicas y en regiones relacionadas en el Síndrome de Prader-Willi evaluadas mediante Tensor de Difusión***

### **7.2.6.1 Objetivos**

Los pacientes con síndrome de Prader-Willi presentan graves alteraciones neuroendocrinológicas, como déficit de hormona de crecimiento, hipogonadismo hipogonadotrópico e hiperfagia, consecuencia de una posible alteración del sistema hipotálamo-hipofisario. Existe una creciente evidencia que apunta hacia un desarrollo atípico de la sustancia blanca. Sin embargo, sólo existe un artículo centrado en este tema con este tipo de pacientes y no está centrado en la región hipotálamo-hipofisaria de interés (Yamada et al., 2006). Así que las posibles alteraciones en sustancia blanca en pacientes con Prader-Willi siguen siendo una incógnita.

Así pues, el objetivo de este estudio fue evaluar el hipotálamo y regiones adyacentes en paciente adultos con síndrome de Prader-Willi empleando el tensor de difusión.

Los objetivos de este estudio se resumen en:

- I. Usando un método capaz de detectar anomalías en las vías de sustancia blanca, caracterizar las anomalías en sustancia blanca en regiones relacionadas con estructuras con función neuroendocrinológica.
- II. Relacionar las anomalías en sustancia blanca con hormonas relacionadas con la conducta alimentaria en pacientes con síndrome de Prader-Willi.

### **7.2.6.2 Hipótesis**

Nosotros predecimos la presencia de anomalías estructurales en la sustancia blanca que conectan el hipotálamo con áreas adyacentes que podrían ser la causa directa de las características clínicas del síndrome de Prader-Willi.

## **7.3 Metodología**

---

La presente tesis consta de cinco estudios y unos resultados preliminares que examinan las funciones cognitivas y las características de imagen estructural y funcional durante desarrollo normal y patológico. Para llevar a cabo esta tesis, se

han estudiado tres muestras diferentes y se han empleado tres aproximaciones cognitivas y de imagen distintas. Todos los estudios fueron aprobados por el comité de ética del Hospital del Mar (Barcelona) y todos los sujetos y sus respectivas familias firmaron un consentimiento informado antes de ser incorporados a las investigaciones. Una descripción detallada de las características de las muestras, las aproximaciones metodológicas, las valoraciones cognitivas y/o conductuales y las técnicas de resonancia están detalladas en cada estudio.

### 7.3.1 Muestras

La muestra de niños en edad escolar se adquirió en el contexto de un proyecto a gran escala diseñado para explorar los efectos de factores ambientales sobre el desarrollo cerebral de los niños (BREATHE, Comisión Europea FP7-ERC-2010-AdG, ID 268479). Un total de 2.897 niños de 39 escuelas de la ciudad de Barcelona, fueron invitados a participar en el estudio de resonancia magnética por correo postal, correo electrónico o por teléfono. 810 de ellos dieron una respuesta positiva inicial. La muestra del estudio se reclutó posteriormente de este grupo con el objetivo de incluir a niños de todas las escuelas participantes. Se contactó directamente con los padres de 491 niños. El consentimiento para participar finalmente no fue obtenido en 165 casos, 27 niños se perdieron antes de la evaluación y 21 niños no eran elegibles ya que eran portadores *brackets* dentales. El grupo finalmente seleccionado incluyó 278 casos. Un total de 263 niños completaron el protocolo de estudio (edad media  $9.7 \pm 0.9$ ; rango 7.9-12.1). Otros casos fueron excluidos en base de criterios de calidad de imagen en cada análisis específico de resonancia magnética (*véase capítulo 4*).

La muestra de individuos con síndrome de Down incluía 68 participantes con síndrome de Down confirmado por cariotipo (edad media  $36.3 \pm 10.9$ ; rango 17-61). Los candidatos fueron reclutados por el Servicio Especializado en Salud Mental y Discapacidad Intelectual (SEMS-DI, Girona; TESIDAD, Barcelona) a través de organizaciones de padres. Los individuos con convulsiones o enfermedad neurológica (que no fuera síndrome de Down), trastorno psiquiátrico (incluyendo trastorno del espectro autista), condiciones médicas no estables, toma de medicamentos psicoactivos y que no reunían los requisitos para la evaluación de la RM fueron excluidos. Los participantes fueron seleccionados de un grupo grande de sujetos con síndrome de Down en base a tener >18 años, síndrome de Down confirmado por cariotipo, ningún tratamiento médico, QI leve a moderado, buena capacidad de entender las instrucciones de resonancia magnética y seguirlas, así como la actitud y la disposición óptima (participantes y padres) para participar (*véase capítulo 4*).

La muestra de pacientes con Prader-Willi comprendía 30 pacientes con síndrome de Prader-Willi (edad media  $27.4 \pm 8.0$ ; rango 18-47) reclutados del departamento de genética, pediatría y endocrinología del Parc Taulí de Sabadell, Barcelona (centro de referencia para el síndrome de Prader-Willi) y el servicio de salud mental y discapacidad intelectual del Parc Hospitalari Martí i Julià de Girona, Spain. Se descartaron del estudio pacientes menores de 18 años con condiciones médicas no estables e incapacidad para seguir las instrucciones dentro de la máquina de resonancia magnética. Como criterio de inclusión, a todos los participantes se les realizó un test genético para confirmar anomalías en el cromosoma 15 (véase capítulo 4).

### 7.3.2 Evaluaciones Cognitivas y Conductuales

Una evaluación cognitiva y/o conductual se realizó en todos los estudios (véase capítulo 4).

En la primera muestra (niños sanos), el desarrollo cognitivo se evaluó mediante el cambio a largo plazo en memoria de trabajo y atención. Desde enero de 2012 hasta marzo de 2013, los niños fueron evaluados cada 3 meses durante cuatro visitas, utilizando pruebas computarizadas de 40 minutos de duración. Se seleccionaron pruebas de memoria de trabajo y atención ya que maduran de manera constante durante la pre adolescencia (Anderson et al., 2002, Rueda et al., 2005). Las pruebas computarizadas elegidas (la tarea “N-back” en la memoria de trabajo (Anderson et al., 2002) y la prueba de red atencional [ANT]) (Rueda et al., 2004) (Figura 28) han sido validados estudios de resonancia magnética (Thomason et al., 2009; Rueda et al., 2004) y en la población general. Los niños fueron evaluados en grupos de 10-20 niños y había supervisión por un examinador entrenado cada 3-4 niños.

Para la prueba N-back, se examinaron diferentes cargas de N-back (hasta 3-back) y estímulos (colores, números, letras y palabras) (Figura 29). Los resultados de la prueba N-back se analizaron en base a la medida  $d'$ , una medida de detección que se obtiene restando a la tasa de aciertos la tasa de falsas alarmas:  $(Z \text{ tasa de aciertos} - Z \text{ tasa de falsas alarmas}) \times 100$ . A mayor  $d'$ , la actuación en la prueba ha sido más precisa. De la prueba ANT se escogieron como medidas la desviación estándar del tiempo de reacción (HRT-SE) (Connors et al., 2000): medición de la consistencia en velocidad de respuesta durante toda la prueba, ya que se mostró muy poco efecto aprendizaje y era la que más claramente crecía durante el período de estudio. Un mayor HRT-SE indicaba reacciones muy variables relacionadas con la falta de atención.



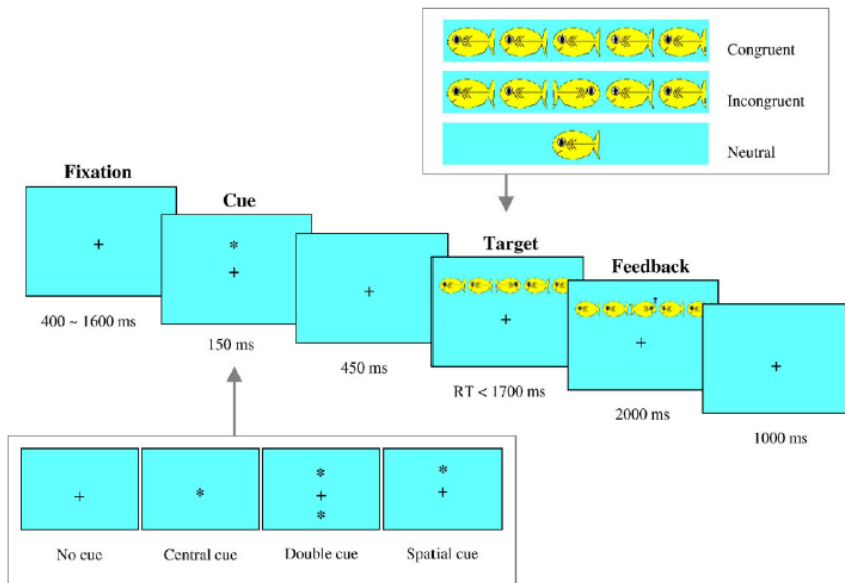


**Figura 28.** Descripción gráfica del Test de Red Atencional (ANT), en su versión infantil.

La segunda muestra (síndrome de Down) recibió una evaluación integral médica, psiquiátrica, neuropsicológica y de laboratorio. El estado cognitivo de los pacientes se evaluó mediante “Kaufman Brief Intelligent Test”, segunda edición (K-BIT) (Kaufman, 2004). Los candidatos fueron evaluados neuropsicológicamente a través del Wechsler Adult Intelligence Scale (WAIS), el Programa Integral Neuropsicológico para personas con Discapacidad Intelectual (PIEN-ID), Figura Compleja de Rey-Osterrieth (ROCF), Inventario Conductual sobre Función Ejecutiva (BRIEF), CAMDEX -DS, Torre de Londres (TOL), Color Trail Test (CTT), Lista de Conductas Aberrantes (ABC Escala) y la Escala de Comportamiento Adaptativo (ABS-RC2).



**Figura 29.** Descripción gráfica del Paradigma N-Back empleado en la evaluación cognitiva.

A la tercera muestra (síndrome de Prader-Willi) se le aplicaron unas pruebas selectivas para identificar la presencia y gravedad de los síntomas relacionados con el comportamiento obsesivo-compulsivo en el síndrome de Prader-Willi, incluida la Compulsive Behavior Checklist (Gedye et al., 1992) Para confirmar la presencia de varios síntomas compulsivos agrupados en varias categorías: orden, integridad, limpieza, control y conductas de aseo. Además, se utilizó la escala obsesiva compulsiva de Yale-Brown (Y-BOCS, Goodman et al., 1989) para proporcionar una evaluación complementaria de la gravedad de las compulsiones identificadas utilizando el cuestionario Compulsive Behavior Checklist. Para abordar el comportamiento compulsivo relacionado con la alimentación se utilizó el Cuestionario de Hiperfagia (Dykens et al., 2007), un instrumento de 13 ítems diseñado específicamente para medir los pensamientos relacionados con alimentos así como la gravedad de estos.

### **7.3.3 Neuroimagen**

Las adquisiciones de imágenes para todos los estudios se realizaron en la Sección de Neurorradiología, Servicio de Radiología del Hospital del Mar (Barcelona, España) de acuerdo con el protocolo de estudio específico.

En resumen, se utilizó un sistema Signa Excite 1,5 Teslas (General Electric, Milwaukee, WI) equipado con una bobina de ocho canales. El protocolo de estudio incluía imágenes de tensor de difusión (*para más detalles, véase capítulo 4*). El protocolo de procesado de imágenes para cada tipo de secuencia está especificado en cada estudio y en el *capítulo 3*.

### **7.3.4 Análisis Estadísticos**

Posteriormente, las imágenes anatómicas, el tensor de difusión y los mapas de conectividad funcional se incluyeron en análisis de segundo nivel (grupo). Los resultados se consideraron significativos con *clústers* de 1.032 ml y un umbral de  $P < 0.005$ .

## **7.4 Resultados**

---

***7.4.1 Estudio I: La Exposición al Cobre Ambiental en la Escuela está asociado con un peor Rendimiento Motor Y Alteraciones en los Ganglios de la Base***

Respecto a al efecto que tienen distintos contaminantes presentes en el aire sobre la cognición, se objetivó que la exposición a altos niveles de cobre (CU) correlacionaban con un peor rendimiento motor. En términos de toda la muestra ( $n = 2827$  después de las exclusiones), la correlación era significativa para la velocidad de respuesta motora (TR,  $r = 0.05$   $p=0.006$ ). Este efecto era incluso más robusto para la consistencia de la respuesta motora (Desviación Estándar del TR,  $r=0.09$   $p=0.0000008$ ).

En la muestra que participó en la adquisición del DTI mediante RM ( $n=253$ ), también apareció correlación positiva entre el TR y el CU ( $r = 0.14$   $p<0.05$ ). De manera que a más altos niveles de exposición al cobre, más se incrementa el tiempo de reacción de los niños.

A nivel de neuroimagen, el cobre se relacionó con altos niveles de concentración de sustancia gris en el estriado, específicamente el núcleo caudado, sin efecto sobre el volumen de sustancia gris.

En el análisis de resultados de DTI se relacionó el CU con un incremento del tejido cerebral anisotrópico (FA) en zonas específicas. Esta medida de DTI se puede expresar como el grado en que una estructura anatómica se compone de tractos de SB que presentan una dirección dominante. En las regiones del cerebro que contienen vías en una sola dirección, la FA aumenta como resultado de la maduración cerebral. Sin embargo, en estructuras complejas que poseen tractos que se cruzan en diferentes direcciones, una FA elevada puede denotar un tejido menos maduro o menos estructurado (Douaud et al., 2001; Jones et al., 2013). En nuestros análisis, altos niveles de cobre se asociaron con una FA alta en la SB cercana a los núcleos caudados (NC) o en los núcleos caudados en sí. Esta región está anatómicamente compuesta por fibras en dirección superior-inferior, posterior-anterior y lateral-medial (Kotz et al., 2013). Así que, en este contexto, una maduración deficitaria en la estructura, mostraba un alto nivel de FA.

Para entender el significado funcional de estos cambios en los núcleos caudados se llevaron a cabo análisis de conectividad funcional. Se generaron mapas de conectividad funcional usando coordenadas extraídas de anteriores trabajos y de los resultados de las anteriores pruebas de imagen. El resultado más relevante fue la asociación entre altos niveles de cobre y la reducción de la conectividad funcional entre el núcleo caudado y el opérculo del lóbulo frontal. Esta asociación era consistente con los resultados anatómicos y de DTI.

Además de los resultados de imagen, las correlaciones con las medidas neuropsicológicas ayudaron a establecer la naturaleza de los efectos del CU. El tiempo de reacción (TR) y la variabilidad del tiempo de reacción (Desviación Estándar del TR) mostraron una correlación significativa positiva con la FA adyacente a la sustancia blanca del núcleo caudado. Es decir, a mayor exposición a los efectos del CU, los niños tenían respuestas motoras más lentas, éstas eran

menos consistentes y mostraban mayor FA y una menor conectividad funcional en dicha región.

#### **7.4.2 Estudio II: La Exposición a la Contaminación producida por el Tráfico está asociada con Alteraciones de la Conectividad Funcional de los Niños en Edad Escolar**

La contaminación producida por el tráfico en las escuelas de los niños se determinó usando el promedio de dos indicadores de gases producidos por vehículos, llamados partículas de carbón elemental y dióxido de nitrógeno (NO<sub>2</sub>). Este indicador se correlacionó con mapas de todo el cerebro en desarrollo. No se encontraron correlaciones significativas entre la contaminación ambiental y las imágenes anatómicas estructurales, metabólicas y de DTI. Sin embargo, sí que se encontraron resultados consistentes en los análisis de imagen funcional.

La aproximación funcional de este estudio incluía la generación de mapas de conectividad funcional empleando coordenadas de estudios previos. El mapa de conectividad obtenido desde un *seed* en la corteza frontal (región de interés) nos proporcionó los resultados más ilustrativos. Se encontró que la contaminación producida por el tráfico estaba significativamente asociada con una conectividad funcional más débil entre las regiones que constituyen la “Default Mode Network” (DMN), indicando una integración baja entre las áreas que componen esta red (Fair et al., 2009).

El análisis de la correlación entre la edad de los niños y la conectividad funcional en la DMN fue útil para establecer la naturaleza perjudicial de los resultados. De hecho, el efecto de la edad sobre la conectividad funcional en esta red fue el contrario al efecto del contaminante. La edad se asoció significativamente con una conectividad funcional más fuerte dentro de los elementos de la DMN (integración) (Sherman et al., 2014) y con una conectividad funcional más débil con las regiones limítrofes (segregación) (Sherman et al., 2014).

Para probar si la contaminación medida se asociaba con el rendimiento cognitivo, se utilizó el rendimiento de los niños en una tarea de memoria de trabajo, velocidad de respuesta del motor y atención. El único resultado significativo apareció en las correlaciones con el tiempo de reacción. Índices de contaminación más altos predecían tiempos de reacción más lentos en 248 participantes analizados con resonancia magnética ( $\beta$ estandarizado = 0,154;  $p = 0,015$ ). Se realizó un análisis adicional para correlacionar TR de los niños con la conectividad funcional en el mapa DMN. Curiosamente, los tiempos de reacción más rápidos se asociaban con una mayor conectividad dentro de la DMN

(integración de la red) y una conectividad más débil en el opérculo frontal (segregación de red).

### **7.4.3 Estudio III: Videojuegos en Edad Escolar: ¿cuánto es suficiente?**

La muestra total del estudio comprendía 428 no jugadores y 2.014 jugadores (> 1 hora/semana). Como grupo, los jugadores jugaban una media de  $4,0 \pm 2,9$  horas por semana. Los chicos jugaban, en general, 1,7 hora/semana más que las mujeres (95% intervalo de confianza [IC] = 1,4-1,9 horas). Existía un efecto significativo de la edad, los niños mayores (por encima de la edad promedio de la muestra) jugaban 0,4 horas/semana más que los niños más jóvenes (IC del 95% = 0,2-0,7 horas). Todos los análisis estadísticos adicionales se ajustaron por edad y sexo (es decir, la edad y el sexo se incluyeron como covariables en comparaciones de grupos y correlaciones).

Los jugadores mostraron una respuesta motora más rápida ante la estimulación visual (es decir, menor tiempo de reacción) que los no jugadores, con una diferencia media de 65 milisegundos. Tal diferencia fue estadísticamente robusta ( $t = 8,1$ ,  $p = 6e^{-16}$ ) y era también significativa en la submuestra de MRI ( $t = 4,5$ ,  $p = 0,0001$ ). El uso de videojuegos también se asoció con una mayor coherencia de las respuestas motoras. Sin embargo, no hubo efectos sobre las funciones atencionales específicas o memoria de trabajo. Sorprendentemente, el mayor beneficio sobre la capacidad de respuesta motora se observó en los niños que jugaban 1 hora por semana (diferencia media de 52 milisegundos con respecto a los no jugadores), con cambio mínimos observados después de las 2 horas de juego por semana.

Por el contrario, en el grupo de jugadores, el tiempo de juego semanal se asoció de manera constante con puntuaciones altas en las valoraciones de los padres (SDQ), en particular en lo que respecta a los problemas de conducta, los conflictos entre padres y la reducción de las capacidades pro-sociales. En nuestro análisis post hoc, los niños que jugaban en el rango de 9-17 horas por semana mostraron significativamente más problemas de comportamiento que los no jugadores (por ejemplo, problemas de conducta;  $t = 3,3$ ,  $p = 0,001$ ).

Al examinar las diferencias entre no jugadores y jugadores de bajo y de alto uso en las mediciones de volumen de materia blanca (ANCOVA), se observaron resultados significativos en una región adyacente a la cara ventral y lateral del cuerpo estriado extendiéndose hasta el lóbulo temporal. Sin embargo, no se obtuvieron resultados significativos para el volumen de materia gris.

Respecto al DTI, el ANCOVA mostró diferencias significativas entre los grupos en una región adyacente a la cara lateral del cuerpo estriado. El conjunto de mediciones de FA reveló un aumento de FA significativo en el estriado izquierdo, pero sólo en el grupo de alto uso. La comparación directa de no jugadores con los jugadores de alto uso confirmó el aumento de FA en esta región y detectó cambios adicionales en la región estriatal ventral bilateral, así como en el tálamo derecho y en la sustancia blanca occipital izquierda.

En las imágenes funcionales, los videojuegos se asociaron con una mayor conectividad funcional en el putamen y mapas núcleo caudado. Específicamente en el mapa putamen, se identificó un aumento de la conectividad con la corteza motora izquierda y la corteza prefrontal en ambos grupos (bajo y alto uso). En el mapa del caudado ventral, el hallazgo más relevante involucraba la corteza cingulada anterior dorsal (ACC), que mostraba un fuerte efecto en el grupo de alto uso y un efecto intermedio en el grupo bajo en comparación con los no jugadores.

En relación con la edad, el volumen de materia blanca aumentaba en el sistema visual y proyecciones sensoriomotrices a nivel de los ganglios de la base y el tálamo. Con la edad, la FA aumentó significativamente principalmente en la cápsula interna y los ganglios basales. Por lo tanto, las asociaciones identificadas de los videojuegos y las mediciones de la sustancia blanca son consistentes con los efectos de la edad.

#### ***7.4.4 Estudio IV: Anormalías en la Sustancia Blanca Cerebral y el Efecto de la Edad en pacientes con Síndrome de Down***

Los pacientes con síndrome de Down mostraron una reducción generalizada de anisotropía fraccional respecto a los controles sanos. Enfatizándose está reducción en los lóbulos frontales, centros semiovais, cuerpo calloso, cápsula externa, cápsula interna, putamen, tálamo, vías piramidales y tronco del encéfalo. Por lo tanto, aunque las principales vías cerebrales están afectadas, las alteraciones más graves aparecen en los circuitos fronto-subcorticales. Por ejemplo, 21 de los 25 sub-clústers que mostraban las mayores diferencias entre grupos ( $t > 5$ ) involucraron los circuitos fronto-subcorticales ( $\chi^2 = 11,5$ ,  $p < 0,001$ ). En el contraste opuesto, se encontró una FA significativamente mayor en la unión temporo-parietal de los pacientes con síndrome de Down.

Respecto al rendimiento cognitivo, no se encontraron correlaciones significativas entre las mediciones de anisotropía fraccional y el rendimiento en las matrices (K-BIT) y de memoria de trabajo (Dígitos WAIS). Por el contrario, la FA reveló una correlación significativamente positiva con la fluidez semántica (es decir,

menores valores de FA, peor rendimiento) en una variedad de regiones que involucran los lóbulos frontales, el cuerpo caloso, los centros semiovais, el fascículo arqueado, el núcleo caudado, la cápsula externa, el tálamo y el hipocampo.

En relación al efecto de la edad, en ambos grupos la anisotropía fraccional disminuyó en función de la edad. Los controles sanos mostraron cambios en FA relacionados con la edad en los lóbulos frontales, el cuerpo caloso, los ganglios basales (caudado), el tálamo, centros semiovais y vías piramidales. En los pacientes con síndrome de Down, se encontraron correlaciones significativas con la edad en los lóbulos frontales, fascículo arqueado izquierdo, cápsula externa derecha e hipotálamo. No se encontraron diferencias significativas entre los grupos, es decir, no se obtuvo una correlación significativa de la interacción.

#### ***7.4.5 Estudio V: Estudio Longitudinal sobre los Cambios Anatómicos que preceden a la Demencia en el Síndrome de Down***

La duración media del estudio fue de 23 meses (desviación estándar, 2 meses) y el estado cognitivo de los pacientes varió a lo largo del estudio. Cinco pacientes cambiaron su estado clínico de estable a deterioro cognitivo leve (DCL) y dos más pasaron de un estado cognitivo estable a demencia tipo Alzheimer. Así pues, el 26% de los casos (N=7) mostraron evidencias clínicas de deterioro cognitivo progresivo en un período de 2 años aproximadamente.

Respecto a los resultados de neuroimagen, en el seguimiento se encontraron reducciones significativas del volumen de sustancia gris en una región del prosencéfalo basal y en la zona ventral de los ganglios basales que involucra la sustancia innominada, en la corteza orbitofrontal derecha y en la cara lateral del lóbulo temporal derecho. Además, se identificó una reducción significativa del volumen de la sustancia blanca en una región que compromete el hipocampo derecho y en el fascículo arqueado izquierdo.

Los pacientes con síndrome de Down que presentaban progresión del deterioro cognitivo mostraron una reducción significativa del volumen de sustancia gris en comparación con el resto de la muestra en la sustancia innominada y en el hipocampo izquierdo. Aunque menos extensa, la reducción de volumen en la región de la sustancia innominada se superponía notablemente a los otros cambios en la muestra completa.

En el análisis de las correlaciones entre los cambios anatómico y cognitivos, se observaron los siguientes resultados: una correlación entre la reducción de la puntuación en memoria y la reducción del volumen de la materia gris en una

pequeña porción del hipocampo izquierdo y la amígdala. Una correlación entre la reducción de la puntuación de la comprensión verbal y la reducción del volumen de la materia gris en el área de Wernicke (y la corteza auditiva) y la reducción del volumen en parte del fascículo arqueado izquierdo. Una correlación entre la reducción de la puntuación de la memoria prospectiva y la reducción del volumen de la materia gris y blanca en una porción extensa del lóbulo prefrontal bilateral, la reducción bilateral del volumen de la sustancia gris en el lóbulo paracentral y la reducción bilateral del volumen de la materia blanca que involucra la corteza temporal inferior y el hipocampo.

Todas estas asociaciones se observaron en la dirección positiva esperada (*ejemplo*: reducción del volumen de tejido en paralelo con la reducción de la puntuación cognitiva).

#### ***7.4.6 Estudio VI: Anomalías Hipotalámicas y en regiones relacionadas en el Síndrome de Prader-Willi evaluadas mediante Tensor de Difusión***

Se encontró una reducción significativa en los valores de FA en un número de regiones del cerebro determinadas en pacientes con síndrome de Prader-Willi que en los controles. La FA se redujo significativamente en el núcleo lenticular (bilateral), hipotálamo, amígdala y sub-genu. Las características de difusividad observadas indican anomalías de desarrollo en estas zonas de sustancia blanca, que son altamente consistentes con las características clínicas del síndrome de Prader-Willi.

## **7.5 Discusión**

---

La importancia del estado de la sustancia blanca en el correcto funcionamiento del cerebro y su influencia sobre diversos dominios cognitivos es innegable. Además, diversos estudios han revelado su susceptibilidad a ser modulada por factores genéticos y ambientales. Específicamente, los trastornos genéticos del neurodesarrollo alteran la trayectoria de crecimiento las vías de sustancia blanca y generan consecuencias cognitivas y neuropsiquiátricas irreversibles. Pero, aunque las principales características del desarrollo de la materia blanca están determinadas genéticamente, no están exentas de ser moduladas en respuesta a ciertas exposiciones ambientales. Los principales estudios sobre el tema apoyan que algunas experiencias/exposiciones pueden influir en la formación de la mielina y modificar la adquisición de ciertas habilidades.



Nuestros resultados sobre la influencia de diversos contaminantes en la infancia confirman nuestra hipótesis inicial, el cobre ambiental está significativamente asociado con un menor rendimiento motor y un daño detectable de la sustancia blanca en los ganglios basales. En concreto, en la dirección de los hallazgos de exposición al cobre, los niños que presentaron un tiempo de reacción más lento y una respuesta motora menos consistente tenían cambios en esta región. Estas alteraciones son altamente congruentes con las bien conocidas consecuencias del exceso de cobre sobre el cerebro, siendo los ganglios basales el target principal del cobre. Aunque una dieta normal contiene una cantidad considerable (~1 mg) de cobre (Morris et al., 2006), los datos sugieren que niveles relativamente bajos actuarían como neurotóxicos durante exposiciones crónicas. La exposición a largo plazo al cobre se ha relacionado con el aumento del riesgo de padecer enfermedad de Parkinson (Gorell et al., 2004, Caudle et al., 2015) y aumenta la tasa de conversión de deterioro cognitivo leve a enfermedad de Alzheimer (Squitti et al., 2014c; Squitti et al., 2014b). En este contexto, el cobre puede jugar un papel causal en los trastornos neurodegenerativos de aparición tardía (Bandmann et al., 2015). Es importante señalar que nuestras asociaciones se han demostrado con niveles dentro de los límites permitidos en áreas urbanas, lo que sugiere un riesgo para grandes poblaciones y tendría implicaciones potencialmente significativas para la salud pública en general. Los niños pueden ser particularmente vulnerables al cobre si entendemos éste como agente capaz de interferir con el desarrollo del cerebro durante las etapas críticas del desarrollo. De acuerdo con nuestros resultados, un estudio reciente ha informado de una asociación significativa entre altos niveles de cobre en sangre y menor rendimiento cognitivo en niños en edad escolar normal (Zhou et al., 2015). Nuestra conclusión es que el efecto del cobre en los ganglios basales es sutil, pero biológicamente significativo.

A pesar de los resultados tan claros obtenidos con el cobre, no hemos sido capaces de detectar el impacto de otros contaminantes sobre las vías de sustancia blanca. En nuestro caso, estudiamos la contaminación relacionada con el tráfico utilizando el promedio ponderado de dos indicadores de polución relacionados con el tráfico de vehículos, es decir, el carbono elemental y el NO<sub>2</sub> y no identificamos asociaciones significativas entre el índice de contaminación citado y nuestra medida de materia blanca (FA). Por el contrario, el análisis de imagen funcional sí que mostró resultados consistentes. La razón de los hallazgos negativos en DTI puede ser que la exposición a la contaminación atmosférica relacionada con el tráfico se asocia comúnmente a cambios funcionales en el cerebro, sin efecto evidente sobre la anatomía cerebral, la estructura o el metabolismo. Los niños de escuelas con mayores índices de contaminación relacionada con el tráfico mostraron menor integración funcional y segregación en las redes cerebrales. Lo que indica que una mayor exposición se asocia con una maduración cerebral más lenta. Se observaron efectos similares entre

diferentes redes funcionales y las áreas sensibles a la edad, éstas coincidieron notablemente con las áreas que muestran una correlación significativa con la contaminación. Afortunadamente, a pesar del evidente efecto de la contaminación sobre la conectividad funcional, la repercusión global del cerebro puede, hasta cierto punto, ser considerada sutil, ya que los cambios no implican ninguna medición estructural. Por lo tanto, podemos especular sobre la reversibilidad del daño cerebral y la eficacia potencial de las acciones dirigidas a reducir la contaminación. Sin embargo, el efecto de la contaminación atmosférica puede ser mucho más dramático de lo que se esperaría cuando la exposición implica períodos de desarrollo tempranos y exposiciones a largo plazo. Estudios recientes han revelado que la exposición a largo plazo a la contaminación ambiental puede afectar, en última instancia, al volumen del tejido cerebral en las personas mayores (Chen et al., 2015).

Por otro lado, nuestros hallazgos relacionados con el uso de videojuegos demostraron que el uso de videojuegos está asociado con una respuesta motora más rápida a la estimulación visual. A nivel neuronal, los cambios estructurales de la sustancia blanca asociados con el uso del juego son más evidentes en los ganglios basales. Hubo diferencias significativas entre los grupos en una región adyacente a la cara lateral del estriado. Las medidas de FA de esta región revelaban un aumento de FA significativo, pero sólo en el grupo de que jugaba intensivamente (<2 horas/semana). La comparación directa de no jugadores con jugadores de alto rendimiento confirmó el aumento de FA en esta región y detectó cambios adicionales significativos en la región ventral del estriado, en el tálamo derecho y en áreas occipitales izquierdas. Las asociaciones observadas entre el uso de videojuegos y los cambios en la conectividad estructural de los ganglios basales confirman la idea de que algunas habilidades son más entrenables que otras. Es bien sabido que los circuitos de los ganglios basales son esenciales para el aprendizaje procedimental basado en la adquisición de nuevas habilidades a través de la práctica (Doyon et al., 2003).

Por tanto, nuestros resultados son generalmente consistentes con otros estudios de imagen que informan de los efectos de determinados videojuegos sobre la estructura y función de los ganglios basales. Específicamente, autores como Erickson et al. (2010) ya mostraron que la adquisición de determinadas habilidades estimuladas por el uso de videojuegos puede predecirse mediante cambios en el volumen del cuerpo estriado. Tradicionalmente, los niños adquieren habilidades de procedimentales a través de las acciones, por ejemplo, en relación con la práctica de determinados deportes y juegos al aire libre. Los recientes estudios basados en neuroimagen sugieren que el entrenamiento en los ambientes virtuales también es capaz de modular ciertos sistemas del cerebro relacionados con la materia blanca que es la base biológica del aprendizaje procedimental.

En resumen, al estudiar estos dos ejemplos de moduladores de ambientales hemos confirmado que el desarrollo de la sustancia blanca es un proceso activo influenciado por distintos factores ambientales activos y pasivos. Sin embargo, no todos los efectos moduladores de la sustancia blanca son predecibles o incluso reversibles. Es bien sabido que las enfermedades genéticas del neurodesarrollo producen una organización de la materia blanca anómala desde el nacimiento, cuyas consecuencias se hacen más evidentes en la edad adulta.

Nuestros resultados con la muestra del síndrome de Down indican que la sustancia blanca en los pacientes con síndrome de Down muestra una FA más baja de forma generalizada en comparación con sujetos sanos, lo que sugiere la existencia de un subdesarrollo de los tractos de sustancia blanca.

En nuestro caso, las estructuras más afectadas fueron los lóbulos frontales, la sustancia blanca subcortical y algunas partes del tronco encefálico. Esta FA baja en síndrome de Down se asoció, además, con una fluidez semántica más pobre, lo que muestra un grado de correspondencia entre la integridad de la sustancia blanca y el rendimiento cognitivo de estos pacientes. Por otro lado, la FA de la sustancia blanca disminuyó con la edad tanto en el síndrome de Down como en los controles sanos, pero no encontramos el esperado efecto acelerado de la edad sobre el grupo de síndrome de Down. Nuestros resultados son consistentes con los estudios anatómicos que muestran de forma generalizada volúmenes reducidos de sustancia blanca en el síndrome de Down en comparación con controles sanos (Weis et al., 1991; White et al., 2003). Además, nuestros datos pueden contribuir aún más a la caracterización de las alteraciones de la sustancia blanca en el síndrome de Down, ya que indican que los cambios no se limitan a reducciones generales de volumen, sino que también pueden implicar un patrón de conectividad estructural menos desarrollado.

Aunque las anomalías de FA involucraban las principales vías cerebrales, los circuitos frontero-subcorticales mostraron las alteraciones más severas. Como tendencia general, los resultados son consistentes con el perfil de los déficits cognitivos del síndrome de Down progresando hacia un deterioro profundo en la producción de lenguaje y funciones ejecutivas, dominios cognitivos dependientes en gran medida de los lóbulos frontales (Lott et al., 2010).

Un problema relevante en la evaluación de las capacidades cognitivas en el síndrome de Down es la notable falta de reproducibilidad de las puntuaciones en algunas pruebas neuropsicológicas. Nosotros utilizamos una evaluación neuropsicológica extensa, pero sólo la fluidez verbal se pudo asociar con alteraciones de FA en el síndrome de Down, lo que indica un cierto paralelismo entre el patrón identificado de alteraciones de la materia blanca y el rendimiento cognitivo. Sin embargo, no encontramos asociaciones similares con el

rendimiento IQ y la memoria de trabajo. Consideramos que estas pruebas no son las más adecuadas para predecir las alteraciones cognitivas en el síndrome de Down. El desarrollo de herramientas más sensibles y específicas para este tipo de pacientes podría ser de gran utilidad en futuros estudios. Por otro lado, no se encontraron resultados significativos entre los distintos grupos en lo referente al efecto de la edad relacionada con cambios en la sustancia blanca. Esto significa que, aunque ambos grupos sufrieron una variación de la estructura de la sustancia blanca con la edad, no hubo diferencias entre grupos. En nuestro grupo de síndrome de Down, no había ningún participante diagnosticado de enfermedad de Alzheimer y sólo 3 pacientes tenían DCL según criterios clínicos. Por tanto, no pudimos demostrar los efectos anticipados del envejecimiento prematuro sobre la sustancia blanca usando mediciones FA, lo que contrasta con los hallazgos positivos en estudios sobre la enfermedad de Alzheimer familiar. Probablemente, el enfoque DTI adoptado no era lo suficientemente sensible como para detectar alteraciones relacionadas con el proceso de demencia en estadios subclínicos de la enfermedad de Alzheimer.

A pesar de los desafíos son inherentes a las evaluaciones longitudinales y más en individuos con discapacidad intelectual, nuestro estudio longitudinal en el ejemplo de que se pueden identificar cambios anatómicos cerebrales que preceden a la demencia en pacientes con este tipo de patologías. Nuestros resultados se centraron en las reducciones de volumen después de dos años en la sustancia innominada del prosencéfalo basal, hipocampo, corteza temporal lateral y fascículo arqueado izquierdo. Sin embargo, no encontramos cambios significativos en FA en estas regiones específicas.

Los cambios de volumen identificados en nuestro estudio longitudinal y sus asociaciones con la progresión del deterioro cognitivo son, en general, notablemente coherentes con los cambios anatómicos bien descritos sobre la progresión de la demencia en la enfermedad de Alzheimer. Por lo tanto, la involución del cerebro en individuos mayores con síndrome de Down parece acercarse al proceso degenerativo de la enfermedad de Alzheimer, a pesar de tener lugar en una situación compleja con una patología de base. Los sistemas cerebrales que se afectan tempranamente en la enfermedad de Alzheimer como el prosencéfalo basal, el hipocampo y el lóbulo prefrontal también se encuentran selectivamente afectados en el síndrome de Down antes de la demencia, según nuestro estudio. Finalmente, es importante destacar las implicaciones bidireccionales de nuestros hallazgos, en primer lugar dando soporte al valor potencial del síndrome de Down como modelo genético de la neurodegeneración en la enfermedad de Alzheimer, y en segundo lugar, afirmando que los pacientes con síndrome de Down en riesgo de desarrollar demencia son candidatos a beneficiarse del tratamiento propiamente indicado para la enfermedad de Alzheimer.

Una de las principales críticas que se podría hacer a esta investigación es por qué no describimos los cambios en los tractos de sustancia blanca medidos con DTI si hemos demostrado la existencia de reducciones de volumen en sustancia blanca analizadas con VBM. En realidad, encontramos reducciones significativas de FA después de dos años en giro temporal derecho y tractos de proyección frontal, regiones que no coinciden con nuestros resultados de VBM. A pesar de esto, nuestros resultados de FA coinciden con un estudio anterior de VBM basado en sujetos con deterioro cognitivo leve y sujetos sanos (Wang et al., 2010) que mostraron reducciones significativas de volumen de sustancia blanca en pacientes con deterioro cognitivo leve en relación con los controles en giro temporal bilateral, corteza cingulada anterior derecha, giro superior bilateral, giro frontal medial y angular parietal derecho.

En la actualidad, la patogénesis de la sustancia blanca en la enfermedad de Alzheimer y especialmente en población con síndrome de Down sigue sin estar clara. Estudios recientes postularon que la descomposición de la mielina es el proceso principal que conduce a la enfermedad de Alzheimer (Bartzokis et al., 2003). Como todos sabemos, la deposición de  $\beta$ -amiloide extracelular ( $A\beta$ ) es un acontecimiento temprano importante en la patogénesis de la enfermedad de Alzheimer. La literatura científica indica que la mielina puede ser dañada directamente por el  $A\beta$  (Marnier et al., 2003). Además, las respuestas homeostáticas a esta descomposición de mielina aumentan la toxicidad intracortical y podrían explicar el daño neuronal progresivo de la enfermedad de Alzheimer. Sin embargo, la distribución de la degradación de la mielina no es global. Más bien, progresa de regiones más susceptibles a la neurodegeneración como son las áreas de asociación cortical que mielinizan tarde en la vida a otras áreas menos complejas (Braak et al., 2000; Bartzokis et al., 2004).

En nuestros resultados de DTI, la distribución de las anomalías de la sustancia blanca en el cerebro apoya la hipótesis de descomposición de la mielina. En primer lugar, según la teoría, las regiones de mielinización tardía, tales como los lóbulos temporales y las áreas de asociación neocortical, serían el foco de los primeros depósitos de  $A\beta$  y por tanto de la descomposición de mielina. En segundo lugar, los lóbulos frontales y los lóbulos parietales que mielinizan tarde en la vida serían más susceptibles a la desmielinización que los lóbulos occipitales. Nuestros hallazgos de la distribución de anomalías de la sustancia blanca proporcionan evidencia de un patrón de daño en la mielina que parece ser el opuesto al de la mielinización. Los resultados de Wang et al. (2010) son consistentes con algunos estudios previos de la enfermedad de Alzheimer o deterioro cognitivo leve usando el método DTI, los cuales han reportado cambios en la sustancia blanca mediante la medición del valor de FA (Medina et al., 2006; Huang et al., 2007; Stahl et al., 2007). Otros estudios han utilizado métodos basados en VBM para analizar las diferencias halladas en sustancia blanca en

pacientes con enfermedad de Alzheimer, deterioro cognitivo leve y controles sanos (Xie et al., 2006). Muchos de ellos han encontrado alteraciones de la integridad de la sustancia blanca en el temporal medial, esplenium del cuerpo calloso, lóbulo parietal y cíngulo. Nuestros resultados longitudinales basados en FA incluyen giro temporal y proyecciones frontales que serían consistentes con los anteriores estudios sobre deterioro cognitivo leve en población sana. Lamentablemente, hasta la fecha estos hallazgos no han sido podrido ser replicados en pacientes con síndrome de Down con deterioro cognitivo leve o demencia tipo Alzheimer.

Hemos estado hablando de síndrome de Down durante la mayor parte de este discusión, pero esta patología tiene una tasa mayor de incidencia que otras enfermedades genéticas no es la única enfermedad del neurodesarrollo que muestra alteraciones cognitivas y conductuales, sugiriendo un desarrollo cerebral anormal. Nuestros resultados preliminares basados en una muestra de pacientes con síndrome de Prader-Willi confirman la presencia de anomalías estructurales extensas en la sustancia blanca que conectan el hipotálamo con las estructuras cerebrales relacionadas que pueden estar debajo los trastornos endocrinológicos y la hiperfagia en estos pacientes. Estos hallazgos y los anteriores sobre la muestra de síndrome de Down confirman el efecto innegable de diversas enfermedades del neurodesarrollo en el crecimiento y maduración de la materia blanca.

## **Limitaciones**

Una de las principales limitaciones al evaluar poblaciones especiales como son niños o personas con discapacidad intelectual es controlar el movimiento de cabeza excesivo durante la adquisición de las imágenes. Específicamente en la muestra de síndrome de Down, se usaron sesiones de práctica diseñadas para minimizar es problema y habituar a los sujetos al sonido y procedimiento de la resonancia.

Además, decidimos excluir casos que presentaban una degradación de imagen detectable, ya que ningún procedimiento de corrección a posteriori es totalmente eficiente a la hora de corregir el movimiento. Aunque el control preciso de los efectos de movimiento de la cabeza puede ser un punto fuerte del estudio, la selección estricta de los participantes también es una limitación, ya que nos obligaba a excluir de los distintos estudios a bastantes sujetos.

Por otro lado, nuestros resultados DTI en la muestra de síndrome de Down no se pueden generalizar a todos los pacientes con síndrome de Down, ya que utilizamos individuos con capacidad intelectual levemente afectada o normal. Por

lo tanto, nuestras conclusiones deben limitarse a las personas con síndrome de Down con rendimiento cognitivo relativamente alto.

Y por último, aunque teníamos la opción de emplear una máquina de resonancia de 3 Teslas, los estudios se desarrollaron con una máquina de 1.5 Teslas siguiendo las recomendaciones del Comité de Revisión de Ética del 7PM-ERC para limitar el impacto del campo magnético en niños.

## 7.6 Conclusiones

---

Las conclusiones de esta tesis derivadas de los estudios realizados son:

- I. El cobre presente en el aire se asocia con un menor rendimiento motor y alteraciones de los ganglios basales en niños en período de desarrollo.
- II. La exposición a contaminación atmosférica relacionada con los gases de los vehículos se asocia con cambios cerebrales funcionales, sin ningún efecto evidente sobre la anatomía cerebral.
- III. Jugar a videojuegos se asocia con una respuesta motora más rápida ante estimulación visual y cambios en los circuitos de los ganglios basales. Un exceso de juego está asociado con problemas de conducta.
- IV. Los pacientes con síndrome de Down muestran en general una FA más baja, lo que sugiere un infradesarrollo de los tractos de la sustancia blanca.
- V. Los cambios en volúmenes cerebrales regionales, pero no en FA, en el síndrome de Down son concordantes con los cambios anatómicos que indican la progresión hacia la demencia en la enfermedad de Alzheimer.
- VI. Los pacientes con síndrome de Prader-Willi muestran anomalías estructurales extensas en la sustancia blanca que conecta el hipotálamo con estructuras cerebrales adyacentes.

# 8. REFERENCES





## 8. References

Adluru N, Destiche DJ, Lu SY, Doran ST, Birdsill AC, Melah KE, et al. White matter microstructure in late middle-age: effects of apolipoprotein E4 and parental family history of Alzheimer's disease. *Neuroimage Clin* 2014; 2: 730-742.

Amato F, Rivas I, Viana M, et al. Sources of indoor and outdoor PM2.5 concentrations in primary schools. *Sci Total Environ* 2014; 490: 757-765.

American Psychiatric Association. *Diagnostic and Statistical Manual-Text Revision (DSM-IV-TR)*. American Psychiatric Association, 2000. Washington, DC.

Anderson P. Assessment and development of executive function (EF) during childhood. *Child Neuropsychol* 2002; 8: 71-82.

Anderson AF, Kludt R, Bavelier D. Verbal versus visual working memory skills in action video game players. Poster presented at the *Psychonomics Soc Meet Seattle* 2011.

Anderson CA, Shibuya A, Ithori N, et al. Violent video game effects on aggression, empathy, and prosocial behavior in Eastern and Western countries: a meta-analytic review. *Psychol Bull* 2010; 136: 151-173.

Assaf Y, Pasternak O. Diffusion tensor imaging (DTI) based white matter mapping in brain research: a review. *J Mol Neurosci* 2008; 34: 51-61.

Aylward EH, Li Q, et al. MRI volumes of the hippocampus and amygdala in adults with Down's syndrome with and without dementia. *Am J Psychiatry* 1999; 156(4): 564-568.

Ball SL, Holland AJ, Huppert F, Treppner P, Dodd K. The Cambridge Examination for Mental Disorders of Older People with Down's syndrome and others with Intellectual Disabilities (CAMDEX-DS). Cambridge: Cambridge University, 2006.

Ballard C, Mobley W, Hardy J, Williams G, Corbett A. Dementia in Down's syndrome. *Lancet Neurol* 2016; 15: 622-636.

Bandmann O, Weiss KH, Kaler SG. Wilson's disease and other neurological copper disorders. *Lancet Neurol* 2015; 14: 103-113.

Bartzokis G, Cummings JL, Sultzer D, Henderson VW, Nuechterlein KH, Mintz J. Whitematter structural integrity in aging and Alzheimer's disease: a magnetic resonance imaging study. *Arch Neurol* 2003; 60: 393–398.

Bartzokis G, Sultzer D, Lu PH, et al. Heterogenous age related breakdown of white matter structural integrity: implications for cortical “disconnection” in aging and Alzheimer's disease. *Neurobiol Aging* 2004; 25: 843–851.

Bavelier D, Green CS, Han DH, et al. Brains on video games. *Nat Rev Neurosci* 2011; 12: 763–768.

Bavelier D, Green CS, Pouget A, Schrater P. Brain plasticity through the life span: learning to learn and action video games. *Annu Rev Neurosci* 2012; 35: 391–416.

Beacher F, Daly E, Simmons A, Prasher V, Morris R, et al. Alzheimer's disease and Down's syndrome: an in vivo MRI study. *Psychol Med* 2009; 39(4):675-684.

Beacher F, Daly E, Simmons A, Prasher V, Morris R, et al. Brain anatomy and ageing in non-demented adults with Down's syndrome: an in vivo MRI study. *Psychol Med* 2010;40(4):611-9.

Bellgrove MA, Hester R, and Garavan H. The functional neuroanatomical correlates of response variability: Evidence from a response inhibition task. *Neuropsychologia* 2004; 42: 1910–1916.

Benzinger TL1, Blazey T, Jack CR Jr, Koeppe RA, Su Y, Xiong C, et al. Regional variability of imaging biomarkers in autosomal dominant Alzheimer's disease. *Proc Natl Acad Sci USA*. 2013;110(47):E4502-9.

Blacker KJ, Curby KM, Klobusicky E, Chein JM. Effects of action video game training on visual working memory. *J Exp Psychol Hum Percept Perform* 2014; 40: 1992–2004.

Block ML, Calderón-Garcidueñas L. Air pollution: mechanisms of neuroinflammation and CNS disease. *Trends Neurosci* 2009; 32: 506–516.

Blüml S, Wisnowski JL, Nelson Jr. MD, et al. Metabolic maturation of the human brain from birth through adolescence: insights from in vivo magnetic resonance spectroscopy. *Cereb Cortex* 2013; 23: 2944–2955.

Boot WR, Kramer AF, Simons DJ, et al. The effects of video game playing on attention, memory, and executive control. *Acta Psychol (Amst)* 2008; 129: 387–398.

Bora E, Harrison BJ, Fornito A, Cocchi L, Pujol K, Fontenelle LF, et al. White matter microstructure in patients with obsessive-compulsive disorder. *J Psychiatry Neurosci* 2011; 36(1): 42-46.

Boyle CA, Decoufle P, Yeargin-Allsopp M. Prevalence and health impact of developmental disabilities in US children. *Pediatrics* 1994; 93: 399-403.

Braak H, Braak E. Development of Alzheimer-related neurofibrillary changes in the neocortex inversely recapitulate cortical myelogenesis. *Acta Neuropathol* 1996; 92: 197-201.

Brett M, Valabregue R, Poline J. Region of interest analysis using an SPM toolbox. *NeuroImage* 2003; 16: S497.

Brines M, Dall'osto M, Beddows DCS, et al. Traffic and nucleation events as main sources of ultrafine particles in high insolation developed world cities. *Atmos Chem Phys* 2015; 15: 5929-5945.

Burman P, Ritzen EM, Lindgren AC. Endocrine dysfunction in Prader Willi syndrome: a review with special reference to GH. *Endocr Rev* 2001; 22: 787-799.

Bush AI. The metallobiology of Alzheimer's disease. *Trends Neurosci.* 2003; 26: 207-214.

Caudle, WM. Occupational exposures and parkinsonism. *Handb Clin Neurol* 2015; 131: 225-239.

Calderón-Garcidueñas L. White matter hyperintensities, systemic inflammation, brain growth, and cognitive functions in children exposed to air pollution. *J Alzheimers Dis* 2012; 31: 183-191.

Capone GT. Down syndrome: advances in molecular biology and the neurosciences. *Journal of Developmental & Behavioral Pediatrics* 2001; 22: 40-59.

Carducci F, Onorati P, Di Gennaro G, Quarato PP, Pierallini A, Sarà M, et al. Whole-brain voxel-based morphometry study of children and adolescents with Down syndrome. *Funct Neurol* 2013; 28: 19-28.

Casanova MF, Walker LC, Whitehouse PJ, Price DL. Abnormalities of the nucleus basalis in Down's syndrome. *Ann Neurol* 1985; 18(3):310-313.

Cassidy SB, Schwartz S, Miller JL, et al. Prader Willi syndrome. *Genet Med* 2012; 14: 10-26.

Caudle WM. Occupational exposures and parkinsonism. *Handb Clin Neurol* 2015; 131: 225-239.

Chai XJ, Ofen N, Gabrieli JD, Whitfield-Gabrieli S. Selective development of anticorrelated networks in the intrinsic functional organization of the human brain. *J Cogn Neurosci* 2014; 26: 501-513.

Chapman RS, Hesketh LJ. Behavioral phenotype of individuals with Down syndrome. *Ment Retard Dev Disabil Res Rev* 2000; 6: 84-95.

Chen JC, Wang X, Wellenius GA, et al. Ambient air pollution and neurotoxicity on brain structure: Evidence from Women's Health Initiative Memory Study. *Ann Neurol* 2015; 78: 466-476.

Clark C, Crombie R, Head J, van Kamp I, van Kempen E, et al. Does traffic-related air pollution explain associations of aircraft and road traffic noise exposure on children health and cognition? A secondary analysis of the United Kingdom sample from the RANCH project. *Am J Epidemiol* 2012; 176: 327-337.

Compston A. Progressive lenticular degeneration: a familial nervous disease associated with cirrhosis of the liver, by S. A. Kinnier Wilson, (from the National Hospital, and the Laboratory of the National Hospital, Queen Square, London) *Brain* 2009; 132: 1997-2001.

Cyrus J, Eeftens MR, Heinrich J., et al. Variation of NO<sub>2</sub> and NO<sub>x</sub> concentrations between and within 36 European study areas: results from the ESCAPE study. *Atmos Environ* 2012; 62: 374-390.

Dekker AD, Strydom A, Coppus AM, Nizetic D, Vermeiren Y, et al. Behavioural and psychological symptoms of dementia in Down syndrome: Early indicators of clinical Alzheimer's disease? *Cortex* 2015; 73:36-61.

De la Torre R, de Sola S, Farré M, Pujol J, Dierssen M and the TESDAD Study Group. Safety and efficacy of the combination of cognitive training and epigallocatechin-3-gallate for cognitive improvement in young adults with Down syndrome: a double-blind randomised controlled trial. *Lancet Neurol* 2016; 15: 801-810.

De Onis M, Garza C, Onyango AW, Rolland-Cachera MF. WHO development standards for infants and young children. *Arch Pediatr* 2009; 16: 47-53.

De Sola S, de la Torre R, Sánchez-Benavides G, Benejam B, Cuenca-Royo A, Del Hoyo L, et al. A new cognitive evaluation battery for Down syndrome and its relevance for clinical trials. *Front Psychology* 2015; 6: 708.

Del Hoyo L, Xicota L, Sánchez-Benavides G, Cuenca-Royo A, de Sola S, et al. Semantic verbal fluency pattern, dementia rating scores and adaptive behavior correlate with plasma A $\beta$ 42 concentrations in Down syndrome young adults. *Front Behav Neurosci* 2015; 9: 301.

Di Martino A, Fair DA, Kelly C, et al. Unravelling the miswired connectome: a developmental perspective. *Neuron* 2014; 83: 1335– 1353.

Dickerson BC, Bakkour A, Salat DH, Feczko E, Pacheco J, et al. The cortical signature of Alzheimer's disease: regionally specific cortical thinning relates to symptom severity in very mild to mild AD dementia and is detectable in asymptomatic amyloid-positive individuals. *Cereb Cortex* 2009; 19(3):497-510.

Dickerson BC, Stoub TR, Shah RC, Sperling RA, Killiany RJ, et al. Alzheimer-signature MRI biomarker predicts AD dementia in cognitively normal adults. *Neurology* 2011; 76(16):1395-1402.

Dobbing J. Vulnerable periods in developing brain, in: Davison AN, (Ed) *Applied Neurochemistry*. Philadelphia: Davis 1968, 287–316.

Dong Q, Welsh RC, Chenevert TL, Carlos RC, Maly-Sundgren P, Gómez-Hassan DM, et al. Clinical applications of diffusion tensor imaging. *Journal of Magnetic Resonance Imaging* 2004; 19: 6-18.

Douaud G, Jbabdi S, Behrens TE, Menke RA, Gass A, Monsch AU, et al. DTI measures in crossing-fibre areas: increased diffusion anisotropy reveals early white matter alteration in MCI and mild Alzheimer's disease. *NeuroImage* 2011; 55: 880–890.

Doyon J, Penhune V, Ungerleider LG. Distinct contribution of the cortico-striatal and cortico-cerebellar systems to motor skill learning. *Neuropsychologia* 2003; 41: 252–262.

Dye MW, Green CS, Bavelier D. Increasing speed of processing with action video games. *Curr Dir Psychol Sci* 2009; 18: 321–326.

Dykens EM, Maxwell MA, Pantino E, Kossler R, Roof E. Assessment of hyperphagia in Prader-Willi syndrome. *Obesity* 2007; 15(7):1816-1826.

Emerson JF, Kesslak JP, Chen PC, Lott IT. Magnetic resonance imaging of the aging brain in Down syndrome. *Prog Clin Biol Res* 1995; 393:123-138.

Erickson KI, Boot WR, Basak C, et al. Striatal volume predicts level of video game skill acquisition. *Cereb Cortex* 2010; 20: 2522–2530.

Eskici G, Axelse PH. Copper and oxidative stress in the pathogenesis of Alzheimer's disease. *Biochemistry* 2012; 51: 6289–6311.

Esteba-Castillo S, Dalmau-Bueno A, Ribas-Vidal N, Vilà-Alsina M, Novell-Alsina R, García-Alba J. Adaptation and validation of CAMDEX-DS (Cambridge Examination for Mental Disorders of Older People with Down's Syndrome and others with intellectual disabilities) in Spanish population with intellectual disabilities. *Rev Neurol* 2013; 57(8):337-346.

Esteba-Castillo S, Peña-Casanova J, García-Alba J, Castellanos MA, Torrents-Rodas D, et al. Test Barcelona para Discapacidad Intelectual (TB-DI): Un nuevo instrumento para la valoración neuropsicológica clínica de adultos con Discapacidad Intelectual. *Rev Neurol* 2017 (*under revision*)

Fair DA, Cohen AL, Power JD, et al. Functional brain networks develop from a “local to distributed” organization. *PLoS Comput Biol* 2009; 5: e1000381.

Fenoll R, Pujol J, Esteba-Castillo S, de Sola S, Ribas-Vidal N, García-Alba J, et al. Anomalous white matter structure and the effect of age in Down syndrome patients. *J Alzheimers Dis* 2017; 57(1): 175-184.

Ferguson CJ. Do angry birds make for angry children? A meta-analysis of video game influences on children's and adolescents' aggression, mental health, prosocial behavior, and academic performance. *Perspect Psychol Sci* 2015; 10: 646–666.

Fischl B, Sereno MI, Dale AM. Cortical surface-based analysis. II: inflation, flattening, and a surface-based coordinate system. *NeuroImage* 1999; 9: 195–207.

Fish J, Wilson BA, Manly T. The assessment and rehabilitation of prospective memory problems in people with neurological disorders: a review. *Neuropsychol Rehabil* 2010; 20(2):161-179.

Fisher S. Identifying video game addiction in children and adolescents. *Addict Behav* 1994; 19(5): 545–553.

Forns J, Esnaola M, López-Vicente M, et al. The n-back test and the attentional network task as measures of child neuropsychological development in epidemiological studies. *Neuropsychology* 2014; 28: 519–529.

Fortea J, Sala-Llonch R, Bartrés-Faz D, Bosch B, Lladó A, et al. Increased cortical thickness and caudate volume precede atrophy in PSEN1 mutation carriers. *J Alzheimers Dis* 2010;22(3):909-922.

Fox MD, Snyder AZ, Vincent JL, et al. The human brain is intrinsically organized into dynamic, anticorrelated functional networks. *Proc Natl Acad Sci USA* 2005; 102: 9673–9678.

Gedye, A. Recognizing obsessive-compulsive disorder in clients with developmental disabilities. The *Habilitative Mental Healthcare Newsletter* 1992; 11: 73-77.

Geffen G, Moar KJ, O'Hanlon AP, Clark CR, Geffen LB. Performance measures of 16- to 86-year old males and females on the Auditory Verbal Learning Test. *Clin Neuropsychol* 1990;4:45–63.

Gens S, Steward CE, Malpas CB, Velakoulis D, O'Brien TJ, Desmond PM. Short-term white matter alterations in Alzheimer's disease characterized by diffusion tensor imaging. *J Magn Reson Imaging* 2006; 43: 627-634.

Gentile DA, Choo H, Liau A, et al. Pathological video game use among youths: a two-year longitudinal study. *Pediatrics* 2011; 127: e319–e329.

Ginsberg G, Hattis D, Sonawane B. Incorporating pharmacokinetic differences between children and adults in assessing children's risks to environmental toxicants. *Toxicol Appl Pharmacol* 2004; 198: 164–83.

Gogtay N, Giedd JN, Lusk L, et al. Dynamic mapping of human cortical development during childhood through early adulthood. *Proc Natl Acad Sci USA* 2004; 101: 8174–8179.

Goodman R. Psychometric properties of the strengths and difficulties questionnaire. *J Am Acad Child Adolesc Psychiatry* 2001; 40: 1337–1345.

Goodman WK, Price LH, Rasmussen SA, Mazure C et al. The Yale-Brown obsessive-compulsive scale. Development, use and reliability. *Arch Gen Psychiatry* 1989; 46(11): 1006-1011.



Gorell JM, Peterson EL, Rybicki BA, Johnson CC. Multiple risk factors for Parkinson's disease. *J Neurol Sci* 2004; 217:169–174.

Grandjean P, Landrigan PJ. Neurobehavioural effects of developmental toxicity. *Lancet Neurol* 2014; 13: 330–338.

Grandjean P, White RF. Developmental effects of environmental neurotoxicants, in: Tamburlini G, von Ehrenstein O, Bertollini R. (Ed) *Children's health and environment*. Environmental issue report Copenhagen: European Environment Agency 2002; 29: 66–78.

Graybiel AM. Habits, rituals, and the evaluative brain. *Annu Rev Neurosci* 2008; 31: 359–387.

Greenfield PM. Technology and informal education: What is taught, what is learned. *Science* 2009; 323: 69–71.

Grice S, Stedman J, Kent A, et al. Recent trends and projections of primary NO<sub>2</sub> emissions in Europe. *Atmos Environ* 2009; 43: 2154–2167.

Grieco J, Pulsifer M, Seligsohn K, Skotko B, Schwartz A. Down syndrome: Cognitive and behavioral functioning across the lifespan. *Am J Med Genet C Semin Med Genet* 2015; 169: 135-149.

Grugni G, Marzullo P. Diagnosis and treatment of GH deficiency in Prader Willi syndrome. *Best Pract & Research: Clin Endocr & Metab* 2016; 30: 785-794.

Guxens M, Sunyer J. A review of epidemiological studies on neuropsychological effects of air pollution. *Swiss Med Wkly* 2012; 141: pw13322.

Haier RJ, Head K, Head E, Lott IT. Neuroimaging of individuals with Down's syndrome at-risk for dementia: evidence for possible compensatory events. *Neuroimage* 2008; 39(3):1324-1332.

Harrison BJ, Pujol J, Cardoner N, et al. Brain corticostriatal systems and the major clinical symptom dimensions of obsessive compulsive disorder. *Biol Psychiatry* 2013; 73: 321–328.

Harrison BJ, Pujol J, López-Solà M, et al. Consistency and functional specialization in the default mode brain network. *Proc Natl Acad Sci USA* 2008; 105: 9781–9786.

Harrison BJ, Soriano-Màs C, Pujol J, et al. Altered corticostriatal functional connectivity in obsessive-compulsive disorder. *Arch Gen Psychiatry* 2009; 66: 1189–1200.

Hartley D, Blumenthal T, Carrillo M, DiPaolo G, Esralew L, Gardiner K, et al. Down syndrome and Alzheimer Disease: common pathways, common goals. *Alzheimer & Dementia* 2014; 11(6): 700-709.

Head E, Lott IT, Wilcock DM, Lemere CA. Aging in Down syndrome and the development of Alzheimer's disease Neuropathology. *Current Alzheimer Research* 2016; 13: 18-29.

Hermann W. Morphological and functional imaging in neurological and non-neurological Wilson's patients. *Ann NY Acad Sci* 2014; 1315: 24–29.

Huang J, Friedland RP, Auchus AP. Diffusion tensor imaging of normal-appearing white matter in mild cognitive impairment and early Alzheimer disease: preliminary evidence of axonal degeneration in the temporal lobe. *Am J Neuroradiol* 2007; 28: 1943-1948.

Hulskotte JH, Van der Gon HA, Visschedijk AJ, and Schaap M. Brake wear from vehicles as an important source of diffuse copper pollution. *Water Sci Technol* 2007; 56: 223–231.

Hunt, E. What makes nations intelligent? *Perspectives on Psychological Science*, 2012; 7: 284–306.

Ikeda M, Arai Y. Longitudinal changes in brain CT scans and development of dementia in Down's syndrome. *Eur Neurol* 2002; 47(4): 205–208.

Jack CR, Wiste HJ, Vemuri P, Weigand SD, Senjem ML, Zeng G, et al. Alzheimer's Disease Neuroimaging Initiative. Brain beta-amyloid measures and magnetic resonance imaging atrophy both predict time-to-progression from mild cognitive impairment to Alzheimer's disease. *Brain* 2010; 133(11):3336-3348.

Jones DK, Knösche TR, Turner R. White matter integrity, fiber count, and other fallacies: the do's and don'ts of diffusion MRI. *NeuroImage* 2013; 73: 239–254.

Kaufman A, Kaufman, N. Kaufman Brief Intelligence Test, Second Edition (KBIT-2). Bloomington: Pearson, 2004.

Kelly AM, Uddin LQ, Biswal BB, et al. Competition between functional brain networks mediates behavioral variability. *NeuroImage* 2008; 39: 527–537.

Kesslak JP, Nagata SF, Lott I, Nalcioglu O. Magnetic resonance imaging analysis of age-related changes in the brains of individuals with Down's syndrome. *Neurology* 1994; 44(6): 1039–1045.

Kim YH, Kang DW, Kim D, et al. Real-time strategy video game experience and visual perceptual learning. *J Neurosci* 2015; 35: 10485–10492.

Kim CH, Yoo DC, Kwon YM, Han WS, Kim GS, Park MJ, et al. A study on characteristics of atmospheric heavy metals in subway station. *Toxicol Res* 2010; 26: 157–162.

Koepp MJ, Gunn RN, Lawrence AD, et al. Evidence for striatal dopamine release during a video game. *Nature* 1998; 393(6682): 266–267.

Korkman, M., Kirk, U., & Kemp, S. NEPSY: A developmental neuropsychological assessment. San Antonio, TX: The Psychological Corporation, 1998.

Kotz SA, Anwender A, Axer H, and Knösche TR. Beyond cytoarchitectonics: the internal and external connectivity structure of the caudate nucleus. *PLoS One* 2013; 8: e70141.

Krasuski JS, Alexander GE, et al. Relation of medial temporal lobe volumes to age and memory function in non-demented adults with Down's syndrome: implications for the prodromal phase of Alzheimer's disease. *Am J Psychiatry* 2002; 159(1): 74–81.

Krinsky-McHale SJ, Silverman W. Dementia and mild cognitive impairment in adults with intellectual disability: issues of diagnosis. *Dev Disabil Res Rev* 2013; 18: 31-42.

Kühn S, Gallinat J. Amount of lifetime video gaming is positively associated with entorhinal, hippocampal and occipital volume. *Mol Psychiatry* 2014c; 19: 842–847.

Kühn S, Gleich T, Lorenz RC, et al. Playing Super Mario induces structural brain plasticity: gray matter changes resulting from training with a commercial video game. *Mol Psychiatry* 2014b; 19: 265–271.

Kühn S, Lorenz R, Banaschewski T, et al. Positive association of video game playing with left frontal cortical thickness in adolescents. *PLoS One* 2014a; 9: e91506.

Kühn S, Romanowski A, Schilling C, et al. The neural basis of video gaming. *Transl Psychiatry* 2011; 1: e53.

Landrigan PJ, Whitworth RH, Baloh RW, Staehling NW, Barthel WF, Rosenblum BF. Neuropsychological dysfunction in children with chronic low-level lead absorption. *Lancet* 1975; 1: 708–712.

Lanfranchi S, Jerman O, Vianello R. Working memory and cognitive skills in individuals with Down syndrome. *Child Neuropsychol* 2009; 15: 397-416.

Langley J, Huddleston DE, Merritt M, Chen X, McMurray R, Silver M, Factor SA, Hu X. Diffusion tensor imaging of the substantia nigra in Parkinson's disease revisited. *Hum Brain Mapp* 2016; 29, doi: 10.1002/hbm.23192.

Langner R, Eickhoff SB. Sustaining attention to simple tasks: a meta-analytic review of the neural mechanisms of vigilant attention. *Psychol Bull* 2013; 139: 870–900.

Latham AJ, Patston LL, Tippett LJ. The virtual brain: 30 years of video-game play and cognitive abilities. *Front Psychol* 2013; 4: 629.

Le Bihan D, Breton E. In vivo magnetic resonance imaging of diffusion I.C.R. *Academy of Sciences II* 1985; 301: 1109–1112.

Le Bihan D, Mangin JF, Poupon C, Clark CA, Pappata S, Molko N, et al. Diffusion tensor imaging: concepts and applications. *Journal of Magnetic Resonance Imaging* 2001; 13: 534-546.

Lerner A, Mogensen MA, Kim PE, Shirishi MS, Hwanf DH, Law M. Clinical Applications of diffusion tensor imaging. *World Neurosurgery* 2014; 82, 1/2: 96-109.

Lin AL, Powell D, Caban-Holt A, Jicha G, Robertson W, Gold BT, et al. H-MRS metabolites in adults with Down syndrome: Effects of dementia. *Neuroimage Clin* 2016; 11: 728-735.

Liu AK, Chang RC, Pearce RK, Gentleman SM. Nucleus basalis of Meynert revisited: anatomy, history and differential involvement in Alzheimer's and Parkinson's disease. *Acta Neuropathol* 2015; 129(4): 527-540.

Liu H, Yang Y, Xia Y, Zhu W, Leak RK, Wei Z, et al. Aging of cerebral white matter. *Ageing Research Reviews* 2017; 34: 64-76.

Lorenz RC, Gleich T, Gallinat J, Kühn S. Video game training and the reward system. *Front Hum Neurosci* 2015; 9: 40.

Lott IT, Dierssen M. Cognitive deficits and associated neurological complications in individuals with Down's syndrome. *Lancet Neurol* 2010; 9: 623-633.

Loxham M, Cooper MJ, Gerlofs-Nijland ME, Cassee FR, Davies DE, Palmer MR, et al. Physicochemical characterization of airborne particulate matter at a mainline underground railway station. *Environ Sci Technol* 2013; 47: 3614-3622.

MacDonald SW, Nyberg L, Bäckman L. Intraindividual variability in behavior: links to brain structure, neurotransmission and neuronal activity. *Trends Neurosci* 2006; 29: 474-480.

Madden DJ, Bennett IJ, Burzynska A, Potter GG, Chen NK, Song AW. Diffusion tensor imaging of cerebral white matter integrity in cognitive aging. *Biochim Biophys Acta* 2012; 1822: 386-400.

Madden DJ, Bennett IJ, Song AW. Cerebral white matter integrity and cognitive aging: contributions from diffusion tensor imaging. *Neuropsychology Review* 2009; 19: 415-435.

Madsen E, Gitlin JD. Copper and iron disorders of the brain. *Annu Rev Neurosci* 2007; 30: 317-337.

Mak E, Gabel S, Mirette H, Su L, Williams GB, Waldman A, Wells K, Ritchie K, Ritchie C, O'Brien G. Structural neuroimaging in preclinical dementia: From microstructural deficits and grey matter atrophy to macroscale connectomic changes. *Ageing Res Rev* 2016; pii: S1568-1637(16)30062-9.

Mann DM, Yates PO, Marcyniuk B. Alzheimer's presenile dementia, senile dementia of Alzheimer type and Down's syndrome in middle age form an age related continuum of pathological changes. *Neuropathol Appl Neurobiol*. 1984;10(3):185-207.

Mantoulan C, Payoux P, Diene G, Glattard M, Rogé B, Molinas C, et al. PET scan perfusion imaging in the Prader-Willi syndrome: new insights into the psychiatric and social disturbances. *Journal of Cerebral Blood Flow & Metabolism* 2011; 31: 275-282.

Marner L, Nyengaard JR, Tang Y, Pakkenberg B. Marked loss of myelinated nerve fibers in the human brain with age. *J Comp Neurol* 2003; 462: 144-152.

Medina D, De Toledo-Morrell L, Urresta F, et al. White matter changes in mild cognitive impairment and AD: a diffusion tensor imaging study. *Neurobiol Aging* 2006; 27: 663–72.

Melby-Lervåg M, Hulme C. Is working memory training effective? A meta-analytic review. *Dev Psychol* 2013; 49: 270–291.

Menon V. Developmental pathways to functional brain networks: emerging principles. *Trends Cogn Sci* 2013; 17: 627–640.

Mesulam MM. Cholinergic circuitry of the human nucleus basalis and its fate in Alzheimer's disease. *J Comp Neurol* 2013; 521(18): 4124-4144.

Mesulam M, Shaw P, Mash D, Weintraub S. Cholinergic nucleus basalis tauopathy emerges early in the aging-MCI-AD continuum. *Ann Neurol* 2004; 55(6): 815-828.

Mori S, Zhang J. Principles of diffusion tensor imaging and its applications to basic neuroscience research. *Neuron* 2006; 51: 527-539.

Morris MC, Evans DA, Tangney CC, Bienias JL, Schneider JA, Wilson RS, et al. Dietary copper and high saturated and trans fat intakes associated with cognitive decline. *Arch Neurol* 2006; 63: 1085–1088.

Nadel, L. Down syndrome in cognitive neuroscience perspective. In: Tager-Flusberg, H, Ed. *Neurodevelopmental Disorders*. Boston, MA: The MIT Press; 1999.

Oei AC, Patterson MD. Are videogame training gains specific or general? *Frontiers in Systems Neuroscience* 2014; 8(54): 1-9.

Oei AC, Patterson MD. Enhancing cognition with video games: a multiple game training study. *PLoS One* 2013; 8: e58546.

Ogura K, Fujii T, Abe N, Hosokai Y, Shinohara M, et al. Regional cerebral blood flow and abnormal eating behavior in Prader-Willi syndrome. *Brain & Development* 2013; 35: 427-434.

Ogura K, Fujii T, Abe N, Hosokai Y, Shinohara M, Takahashi S, Mori E. Small gray matter volume in orbitofrontal cortex in Prader-Willi syndrome: a voxel-based MRI study. *Human Brain Mapping* 2011; 32: 1059-1066.

Pal A, Prasad R. An overview of various mammalian models to study chronic copper intoxication associated Alzheimer's disease like pathology. *Biomaterials* 2015; 28: 1–9.

Paus T. Mapping brain maturation and cognitive development during adolescence. *Trends Cogn Sci* 2005; 9: 60–68.

Paus T. Population neuroscience: why and how. *Hum Brain Mapp* 2010; 31: 891–903.

Perera FP, Li Z, Whyatt, R, et al. Prenatal airborne polycyclic aromatic hydrocarbon exposure and child IQ at age 5 years. *Pediatrics* 2009; 124: e195–e202.

Peters A. The effects of normal aging on myelin and nerve fibers: a review. *J Neurocytol* 2002; 31: 581–593.

Petersen RC. Mild cognitive impairment. *N Engl J Med* 2011; 364: 2227–2234.

Peterson BS, Rauh VA, Bansal R. et al. Effects of prenatal exposure to air pollutants (polycyclic aromatic hydrocarbons) on the development of brain white matter, cognition, and behavior in later childhood. *JAMA Psychiatry* 2015; 72, 531–540.

Pfefferbaum A, Sullivan EV. Increased brain white matter diffusivity in normal adult aging: relationship to anisotropy and partial voluming. *Magnetic Resonance in Medicine* 2003; 49: 953–961.

Pierpaoli C, Jezzard P, Basser PJ, Barnett A, Di Chiro G. Diffusion tensor MR imaging of the human brain. *Radiology* 1996; 201: 637–648.

Pinter, JD, Eliez S, Schmitt JE, Capone GT, Reiss AL. Neuroanatomy of Down's syndrome: a high-resolution MRI study. *Am J Psychiatry* 2001; 158: 1659–1665.

Powell D, Caban-Holt A, Jicha G, Robertson W, Davis R, Gold BT, et al. Frontal white matter integrity in adults with Down syndrome with and without dementia. *Neurobiology of Aging* 2014; 35: 1562–1569.

Power JD, Mitra A, Laumann TO, et al. Methods to detect, characterize, and remove motion artifact in resting state fMRI. *NeuroImage* 2014; 84: 320–341.

Powers KL, Brooks PJ, Aldrich NJ, et al. Effects of video-game play on information processing: a meta-analytic investigation. *Psychon Bull Rev* 2013; 20: 1055–1079.

Pujol J, Batalla I, Contreras-Rodríguez O, et al. Breakdown in the brain network subserving moral judgment in criminal psychopathy. *Soc Cogn Affect Neurosci* 2012; 7: 917–923.

Pujol J, del Hoyo L, Blanco-Hinojo L, et al. Anomalous brain functional connectivity contributing to poor adaptive behavior in Down syndrome. *Cortex* 2014a; 64C: 148–156.

Pujol J, López-Sala A, Sebastián-Gallés N, Deus J, et al. Delayed myelination in children with developmental delay detected by volumetric MRI. *NeuroImage* 2004; 22: 897–903.

Pujol J, Macià D, Blanco-Hinojo L, et al. Does motion-related brain functional connectivity reflect both artifacts and genuine neural activity? *NeuroImage* 2014b; 101: 87–95.

Pujol J, Macià D, Garcia-Fontanals A, et al. The contribution of sensory system functional connectivity reduction to clinical pain in fibromyalgia. *Pain* 2014c; 155: 1492–1503.

Pujol J, Martínez-Vilavella G, Macià D, et al. Traffic pollution exposure is associated with altered brain connectivity in school children. *NeuroImage* 2016; 129: 175–184.

Pujol J, Soriano-Màs C, Ortiz H, et al. Myelination of language-related areas in the developing brain. *Neurology* 2006; 66: 339–343.

Pujol J, Vendrell P, Junqué C, Martí-Vilalta JL, Capdevila A. When does human brain development end? Evidence of corpus callosum growth up to adulthood. *Ann Neurol* 1993; 34: 71–75.

Przybylski AK. Electronic gaming and psychosocial adjustment. *Pediatrics* 2014; 134: e716–e722.

Racette BA, McGee-Minnich L, Moerlein SM, Mink JW, Videen TO, Perlmutter JS. Welding-related parkinsonism: clinical features, treatment, and pathophysiology. *Neurology* 2001; 6: 8–13.

Rafii MS, Wishnek H, Brewer JB, Donohue MC, Ness S, et al. The Down syndrome biomarker initiative (DSBI) pilot: proof of concept for deep phenotyping of Alzheimer's disease biomarkers in down syndrome. *Front Behav Neurosci* 2015; 9:239.

Raz, N, Torres IJ, Briggs SD, Spencer WM, Thornton AE, Loken WJ, et al. Selective neuroanatomic abnormalities in Down's syndrome and their cognitive correlates: evidence from MRI morphometry. *Neurology* 1995; 45(2): 356–366.



Reche C, Querol X, Alastuey A, et al. New considerations for PM, black carbon and particle number concentration for air quality monitoring across different European cities. *Atmos Chem Phys* 2011; 11, 6207–6227.

Rivas I, Viana M, Moreno T, et al. Child exposure to indoor and outdoor air pollutants in schools in Barcelona, Spain. *Environ Int* 2014; 69: 200–212.

Rueda MR, Fan J, McCandliss BD, et al. Development of attentional networks in childhood. *Neuropsychologia* 2004; 42: 1029– 1040.

Rueda MR, Rothbart MK, McCandliss BD, Saccomanno L, Posner MI. Training, maturation, and genetic influences on the development of executive attention. *Proc Natl Acad Sci USA* 2005; 102: 14931–14936.

Sabbagh MN, Chen K, Rogers J, Fleisher AS, Liebsack C, et al. Florbetapir PET, FDG PET, and MRI in Down syndrome individuals with and without Alzheimer's dementia. *Alzheimer's Dement* 2015;11(8):994-1004.

Sánchez-Valle R, Monté GC, Sala-Llonch R, Bosch B, Fortea J, Lladó A, et al. White Matter Abnormalities Track Disease Progression in PSEN1 Autosomal Dominant Alzheimer's Disease. *J Alzheimers Dis* 2016; 51: 827-35.

Schapiro MB, Luxenberg JS, Kaye JA, Haxby JV, Friendland RP, et al. Serial quantitative CT analysis of brain morphometrics in adult Down's syndrome at different ages. *Neurology* 1989; 39(10): 1349–1353.

Schapiro MB, Luxenberg JS, Kaye JA, Haxby JV, Friendland RP, Rapoport SI. Serial quantitative CT analysis of brain morphometrics in adult Down's syndrome at different ages. *Neurology* 1989; 39: 1349–1353.

Scheiber IF, Mercer JF, Dringen R. Metabolism and functions of copper in brain. *Prog Neurobiol* 2014; 116: 33–57.

Schmithorst VJ, Youan W. White matter development during adolescence as shown by diffusion MRI. *Brain and Cognition* 2010; 72: 16-25.

Sheehan R, Sinai A, Bass N, Blatchford P, Bohnen I, Bonell S, Courtenay K, et al. Dementia diagnostic criteria in Down syndrome. *Int J Geriatr Psychiatry* 2015; 30: 857-863.

Sherman LE, Rudie JD, Pfeifer JH., et al. Development of the default mode and central executive networks across early adolescence: a longitudinal study. *Dev Cogn Neurosci* 2014; 10: 148–159.

Shipstead ZI, Redick TS, Engle RW. Is working memory training effective? *Psychol Bull* 2012; 138: 628–654.

Silverman W, Mizejecki C, Ryan R, Zigman W, Krinsky-McHale S, Urv T. Stanford-Binet & WAIS IQ differences and their implications for adults with intellectual disability. *Intelligence* 2010; 38: 242-248.

Smith SM, Jenkinson M, Johansen-Berg H, et al. Tract-based spatial statistics: voxelwise analysis of multi-subject diffusion data. *NeuroImage* 2006; 31: 1487–1505.

Smith SM, Jenkinson M, Woolrich MW, et al. Advances in functional and structural MR image analysis and implementation as FSL. *NeuroImage* 2004; 23 (Suppl. 1): S208–S219.

Soriano-Mas C, Hernández-Ribas R, Pujol J, Urretvizcaya M, Deus J, et al. Cross-sectional and longitudinal assessment of structural brain alterations in melancholic depression. *Biol Psychiatry* 2011; 69: 318-325.

Squitti R. Copper subtype of Alzheimer's disease (AD): meta-analyses, genetic studies and predictive value of nonceruloplasmin copper in mild cognitive impairment conversion to full AD. *J Trace Elem Med Biol* 2014c; 28: 482–485.

Squitti R, Ghidoni R, Siotto M, Ventriglia M, Benussi L, Paterlini A, et al. Value of serum nonceruloplasmin copper for prediction of mild cognitive impairment conversion to Alzheimer disease. *Ann Neurol* 2014a; 75:574–580.

Squitti R, Simonelli I, Ventriglia M, Siotto M, Pasqualetti P, Rembach A, et al. Meta-analysis of serum non-ceruloplasmin copper in Alzheimer's disease. *J Alzheimers Dis* 2014b; 38: 809–822.

Stanton LR, Coetzee RH. Down's syndrome and dementia. *Advances Psych Treatment* 2004; 10: 50–58.

Stejskal EO, Tanner JE. Spin Diffusion measurements: spin echoes in the presence of a time-dependent field gradient. *J Chem Phys* 1965; 42: 288–292.

Straker L, Abbott R, Collins R, Campbell A. Evidence-based guidelines for wise use of electronic games by children. *Ergonomics* 2014; 57: 471–489.

Suglia SF, Gryparis A, Wright RO, et al. Association of black carbon with cognition among children in a prospective birth cohort study. *Am J Epidemiol* 2008; 167: 280–286.

Sunyer J, Esnaola M, Álvarez-Pedrerol M, et al. Traffic-related air pollution in schools impairs cognitive development in primary school children. *PLoS Med* 2015; 2: e1001792.

Stahl R, Dietrich O, Teipel SJ, et al. White matter damage in Alzheimer disease and mild cognitive impairment: assessment with diffusion-tensor MR imaging and parallel imaging techniques. *Radiology* 2007; 243: 483–492.

Tang T, Miller JL, Von Deneen KM, He G, Gold MS, Driscoll DJ, Liu Y. A DTI study of structural integrity of white matter in Prader-Willi syndrome. *Proc Intl Soc Mag Reson Med* 2009; 17.

Tang Y, Nyengaard JR, Pakkenberg B, Gundersen HJ. Age-induced white matter changes in the human brain: a stereological investigation. *Neurobiol Aging* 1997; 18: 609-615.

Teipel SJ, Alexander GE, Schapiro MC, Möller HJ, Papoport SI, Hampel H. Age-related cortical grey matter reductions in non-demented Down's syndrome adults determined by MRI with voxel-based morphometry. *Brain* 2004; 127: 811-824.

Teipel SJ, Hampel H. Neuroanatomy of Down syndrome in vivo: a model of preclinical Alzheimer's disease. *Behav Genet* 2006; 36(3):405-415.

Theofilas P, Dunlop S, Heinsen H, Grinberg LT. Turning on the Light Within: Subcortical Nuclei of the Isodentritic Core and their Role in Alzheimer's Disease Pathogenesis. *J Alzheimers Dis* 2015; 46(1):17-34.

Toga AW, Thompson PM, Sowell ER. Mapping brain maturation. *Trends Neurosci* 2006; 29: 148–159.

Uddin LQ, Supekar K, Menon V. Typical and atypical development of functional human brain networks: insights from resting-state FMRI. *Front Syst Neurosci* 2010; 4: 21.

Van Kempen E, Fischer P, Janssen N, Houthuijs D, van Kamp I, et al. Neurobehavioral effects of exposure to traffic-related air pollution and transportation noise in primary schoolchildren. *Environ Res* 2012; 115: 18–25.

Verfaillie SC, Tijms B, Versteeg A, Benedictus MR, et al. Thinner temporal and parietal cortex is related to incident clinical progression to dementia in patients with subjective cognitive decline. *Alzheimer's Dement (Amst)* 2016; 5:43-52.

Via E, Zalesky A, Sánchez I, Forcano L, Harrison BJ, et al. Disruption of brain white matter microstructure in women with anorexia nervosa. *J Psychiatry Neurosci* 2014; 39(6): 367-375.

Wang Z, Guo X, Qi Z, Yao L, Li K. Whole-brain voxel-based morphometry of white matter in mild cognitive impairment. *European Journal of Radiology* 2010; 75: 129-133.

Wang S, Zhang J, Zeng X, et al. Association of traffic-related air pollution with children's neurobehavioral functions in Quanzhou, China. *Environ. Health Perspect* 2009; 117: 1612-1618.

Weis S, Weber G, Neuhold A, Rett A. Down syndrome: MR quantification of brain structures and comparison with normal control subjects. *American Journal of Neuroradiology* 1991; 12(6): 1207-1211.

White NS, Alkire MT, Haier RJ. A voxel-based morphometric study of non demented adults with Down syndrome. *NeuroImage* 2003; 20: 393-403.

Wilker EH, Preis SR, Beiser AS, et al. Long-term exposure to fine particulate matter, residential proximity to major roads and measures of brain structure. *Stroke* 2015; 46: 1161-1166.

Wilson, BA, Cockburn, J, Baddeley, AD. The Rivermead Behavioural Memory Test. Bury St Edmunds, UK: Thames Valley Test Company, 1985.

Wiseman FK, Al-Janabi T, Hardy J, Karmiloff-Smith A, Nizetic D, et al. A genetic cause of Alzheimer disease: mechanistic insights from Down syndrome. *Nat Rev Neurosci* 2015; 16: 564-574.

Wisniewski KE, Dalton AJ, et al. Alzheimer's disease in Down's syndrome: clinicopathologic studies. *Neurology* 1985; 35(7): 957- 961.

World Health Organisation ICD-10: International Statistical Classification of Diseases and Related Health Problems. *World Health Organisation*; Geneva 1992; 20: 3-9.

Xie S, Xiao JX, Gong GL, et al. Voxel-based detection of white matter abnormalities in mild Alzheimer disease. *Neurology* 2006; 66: 1845-1849.

Yakovlev PI, Lecours AR. The myelogenetic cycles of regional maturation of the brain. In Regional development of the brain in early life, 1961. Minkowski A, Ed. *Blackwell Scientific*, Oxford, pp 3-10.

Yamada K, Matsuzawa H, Uchiyama M, Kwee IL, Nakada T. Brain developmental abnormalities in Prader-Willi syndrome detected by diffusion tensor imaging. *Pediatrics* 2006; 118: 442-448.

Yap QJ, Teh I, Fusar-Poli P, Sum MY, Kuswanto C, Sim K. Tracking cerebral white matter changes across the lifespan: insights from diffusion tensor imaging studies. *J Neural Transm* 2013; 120: 1369-1395.

Yin HH, Knowlton BJ. The role of the basal ganglia in habit formation. *Nat Rev Neurosci* 2006; 7: 464-476.

Yoshida S, Oishi K, Faria AV, Mori S. Diffusion tensor imaging of normal brain development. *Pediatr Radiol* 2013; 43: 15-27.

Zhang K, Sejnowski TJ. A universal scaling law between gray matter and white matter cerebral cortex. *Proc Natl Sci USA* 2000; 97: 5621-5626.

Zheng W, Monnot AD. Regulation of brain iron and copper homeostasis by brain barrier systems: implication in neurodegenerative diseases. *Pharmacol Ther* 2012; 133: 177-188.

Zhou G, Ji X, Cui N, Cao S, Liu C, Liu J. Association between serum copper status and working memory in school children. *Nutrients* 2015; 7: 7185-7196.

# 9. PUBLICATIONS

